USING SMALL MOLECULE PROBES TO STUDY THE BIOLOGICAL FUNCTIONS OF CD38

A Dissertation

Presented to the Faculty of the Graduate School

of Cornell University

in Partial Fulfillment of the Requirements for the Degree of

Doctor of Philosophy

by

Jonathan Harold Shrimp

January 2015

USING SMALL MOLECULE PROBES TO STUDY THE BIOLOGICAL FUNCTIONS OF CD38

Jonathan Harold Shrimp, Ph.D.

Cornell University 2015

CD38 gene knockout studies in mice have identified physiological functions including insulin secretion, susceptibility to bacterial infection caused by loss of neutrophil chemotaxis, and social behavior through modulating neuronal oxytocin secretion. These physiological functions are explained by its NAD-degrading enzymatic activity and transmembrane signaling activity. Despite the large amount of literature on CD38, there still exists fundamental questions. Developing chemical tools to address these questions is the goal of my thesis research.

Most notable is the previously reported link between CD38 robust hydrolysis of NAD and the intracellular localization that would cause regulation of intracellular NAD and affect other NAD-dependent enzymes. Consequently, whether CD38 is intracellular and regulating NAD deserves careful investigation. Development and usage of a cell permeable, fluorescent small molecule probe (SR101-F-araNMN) that covalently labels CD38 in cells and reveals CD38 intracellular localization indicated that CD38 is predominantly on the plasma membrane with very little intracellular present in Raji and retinoic acid treated HL-60 cell lines. The discovery in these two human cancer cell lines suggests the major enzymatic function of CD38 is to hydrolyze extracellular NAD rather than intracellular NAD.

Further, CD38 has a single transmembrane domain with a short cytoplasmic tail and has a role in activating mitogen activated protein kinase (MAPK) signaling that is important for

cellular differentiation induced by retinoic acid. However, the question remains as to how CD38 induces MAPK signaling. Development of dimeric small molecule probes that can dimerize two cell surface CD38 molecules allowed for investigation of whether dimerization of CD38 is sufficient to induce MAPK signaling.

Finally, since CD38 is highly expressed in hematologic cancers, a novel approach using an antibody-recruiting small molecule (ARM) that can covalently and specifically label CD38 was used to target CD38-overexpressing cancer cells. As part of an integral three-body complex – CD38, ARM and antibody – capable of enacting immune-effector cells for target cell cytotoxicity, the ARM molecule showed a 2.5 fold increase in target cell cytotoxicity.

Through employment of a chemical biology approach, my work contributed to elucidation of the mechanisms of CD38 function and increased knowledge of CD38 function in various normal and pathological conditions.

BIOGRAPHICAL SKETCH

Jonathan Shrimp was born in Lewisburg, Pennsylvania. He received his high school diploma upon graduation from Meadowbrook Christian School in Milton, Pennsylvania. He earned a Bachelor of Science degree in chemistry from Bloomsburg University of Pennsylvania. While there, he synthesized an N-heterocyclic carbene chloroform adduct and collected kinetic data that demonstrated an increased reaction rate using the N-heterocyclic carbene chloroform adduct to catalyze alcohol acetylation. This work was conducted under the guidance of Dr. John P. Morgan. In August of 2009, he began graduate study at Cornell University and joined Prof. Hening Lin and his group, where he investigated the molecular mechanisms underlying the physiological roles of CD38.

Dedicated to my loving parents, Fred and Joyce.
Thank you for always encouraging me throughout
my academic pursuits and for being a wonderful
example for me.

ACKNOWLEDGMENTS

I am extremely grateful to my advisor, Professor Hening Lin, for facilitating my development as a scientist. I have benefitted greatly from conversations with Dr. Lin regarding my research and other significant topics within the field of chemical biology. Additionally, I thank Dr. Lin for his patience with me while guiding me through experimental details and data analysis. I greatly appreciate his desire and willingness to see me develop as a scientist and help in matters beyond my time in the lab.

I would like to thank each Cornell University faculty member who has contributed to my academic and personal development. To my committee members, Prof. Andrew Yen and Prof. Bruce Ganem, I greatly appreciate your discussions with me and your valuable insight and advice, which have contributed to my research projects and my development as a scientist.

I would like to thank all of my fellow labmates. Specifically, I thank Dr. Hong Jiang for initiating the research on CD38 within our lab and for helping me continue the research on CD38. I appreciate your suggestions for experiments, critical analysis of my data and answers to my questions. I greatly appreciate assistance from Dr. Jin Hu in developing my skills and knowledge of organic synthesis. It was a great pleasure to learn from Dr. Hu because of her patience and willingness to assist me in experiments and data analysis. A special thank you to Dr. Colleen Kuemmel who was helpful within the lab and very encouraging. Dr. Kuemmel willingly guided me in the writing of my research proposal and gave me valuable suggestions on reading material to learn cell biology. I thank Brian Wang for helping me in the synthesis of the F-araNMN alkyne and ARM molecule. Finally, I greatly appreciate the rest of the Lin group members, present and past – Dr. Min Dong, Dr. Sushabhan Sadhukhan, Dr. Zhi Li, Dr. Ying-

Ling Chiang, Polly, Zhen, Zhewang, Xiaoyu, Hui, Ornella, Xiao, Seth, Nicole, Xuan, Dr. Bin He, Dr. Qingjie Zhao, Yoon Ha, Anita, Xiaoyang, Saba and Xuling – for all your help, playing sports and eating delicious food with me that I did not make. To all the past and present Lin lab members, I thank you for not only the valuable help I received towards my research projects but also for the fun memories of times spent together.

I want to thank all those who I have directly collaborated with on my research projects, including: Prof. Andrew Yen and Robert MacDonald where the cell biology analysis of the dimeric small molecule CD38 probes has been done; Prof. Andrew Yen and Dr. Rodica Petruta Bunaciu for assisting me in obtaining and analysis of flow cytometry data for the ARM molecule project; Prof. Quan Hao for providing purified CD38 protein.

I would like to thank Carol Bayles from the Cornell University Imaging Facility for her assistance in training, data analysis and suggestions for confocal cell imaging. Thank you to Jeff Roberts for use of their Typhoon and Storm imagers.

Finally, I owe so much gratitude to my loving family. To my parents – Fred and Joyce – I thank you for being a wonderful life example for me. I appreciate the sacrifices you have made financially and with your time, prayers, support and encouragement that you willingly give to me. To my peerless brothers – Frederick and David – I appreciate the care and encouragement that you have given me. To Fred, thank you for giving me my first experience in a chemistry lab while you were a student at Bucknell University. I found my interest in chemistry as I saw you go through the learning process to become a chemist. To David, I appreciate your patience and willingness to deal with my computer problems and fix them. I greatly appreciate the love and support from my family.

"In all your ways acknowledge Him, and He shall direct your paths" – Proverbs 3:6

TABLE OF CONTENTS

LIST OF FIGURES

Chapter 1

Early Studies and Background on Cluster Designation 38 (CD38) Protein

1.1. Early Studies of CD38

During the 1970's, the hybridoma technology developed by Kohler and Milstein for production of monoclonal antibodies led to the discovery of CD38. Kohler and Milstein developed hybridoma cells between malignant myeloma cells and select antibody-producing B cells in order to produce antibodies of interest (*1*). This technique allowed for several murine monoclonal antibodies (mAbs) to become readily available. Subsequently, studies were conducted to probe the cell surface of human leukocytes with mAbs. Two or more mAbs binding to the same target were said to form a cluster at their target. This concept was called cluster designation (CD), and those targets that formed clusters were assigned a number. Thus in 1980, cluster designation 38 (CD38) was identified while defining the stages of human T-cell differentiation (*2*). CD38 was first called T10 but later became solely known as cluster designation 38. From there, CD38 was identified on the cell surface of normal lymphocytes and in a few leukemias and myelomas (*3*). Also, CD38 was identified in an array of both lymphoid and non-lymphoid tissues, such as prostate (*4*), brain (*5*), pancreas (*6*) and heart (*7*).

Beyond functioning as a cell surface marker for T-cell differentiation, CD38 most likely acts as both a transmembrane receptor and as an enzyme (*8*). Following isolation, sequencing and expression of the full length cDNA clone that encodes for CD38, CD38 was shown to be a type II, 45-kDa transmembrane glycoprotein that consists of 20 intracellular amino acids, 23 transmembrane amino acids, and 257 extracellular amino acids (*9*). CD38 has 69% overall homology to a cyclase enzyme found in *Aplysia*, whose enzymatic function is conversion of

nicotinamide adenine dinucleotide (NAD) to cyclic adenosine diphosphate-ribose (cADPR), a molecule that is reported to be a calcium mobilizing messenger (*10*). Thus, CD38 is considered to have a similar enzymatic function (*10*). However, the soluble extracellular portion of CD38 catalyzes the formation of mainly adenosine diphosphate ribose (ADPR) and only a minute amount of cADPR (*11-14*). Under acidic conditions and in the presence of high amounts of nicotinic acid (NA), CD38 can also catalyze a base-exchange reaction converting nicotinamide adenine dinucleotide phosphate (NADP) to nicotinic acid adenine dinucleotide phosphate (NAADP), which is also a calcium mobilizing messenger (*15*). As a receptor, in response to the putative non-substrate ligand CD31, cell adhesion events are initiated between $CD38^+$ lymphocytes and endothelial cells (*16*). Through activation by agonist antibodies, CD38 transmits a signal to within the cell by phosphorylating extracellular signal-regulated protein kinase (ERK) and c-Cbl (*17, 18*).

1.2. Enzymatic Function of CD38

Research on the enzymatic function of CD38 has revealed it to be a multifunctional enzyme, which may explain its role in human physiology and pathology (*19*). Before any studies were conducted, the enzyme function of CD38 was thought to be similar to the ADP-ribosyl cyclase enzyme found in the *Aplysia* ovotestis due to amino acid sequence similarity (*10*). The *Aplysia* is a genus of sea slugs, and the first identified ADP-ribosyl cyclase enzyme was found in the *Aplysia*. The ADP-ribosyl cyclase in *Aplysia* is a 30 kDa protein that converts its single substrate, NAD, to almost entirely cADPR (*20*). CD38 is the corresponding mammalian homologue with a catalytic domain facing the exterior environment of the cell, classified as an ectoenzyme. However, once the enzyme function was studied in CD38, it was revealed that NAD, cADPR, NAADP and NADP with nicotinic acid could all be substrates for CD38. The

corresponding products are cADPR, ADPR, adenosine diphosphosphate ribose phosphate (ADPRP) and NAADP, respectively (*11, 21-27*). In catalyzing these reactions, CD38 displays enzymatic function under both neutral and acidic pH; more specifically, acidic pH is required for two of the catalyzed conversions. At neutral pH, NAD is predominantly hydrolyzed to ADPR with minute formation of the cyclization product, cADPR. Also, at neutral pH, cADPR can be converted to the linear ADPR molecule. Under acidic pH, NADP with NA is converted to NAADP. Also, at acidic pH, NAADP can be converted to ADPRP, as shown in Figure 1.1 (*26*). Though these enzymatic activities can be identified using purified CD38 protein, careful investigation of enzyme kinetics and cellular localization is required to determine whether these activities are physiologically relevant.

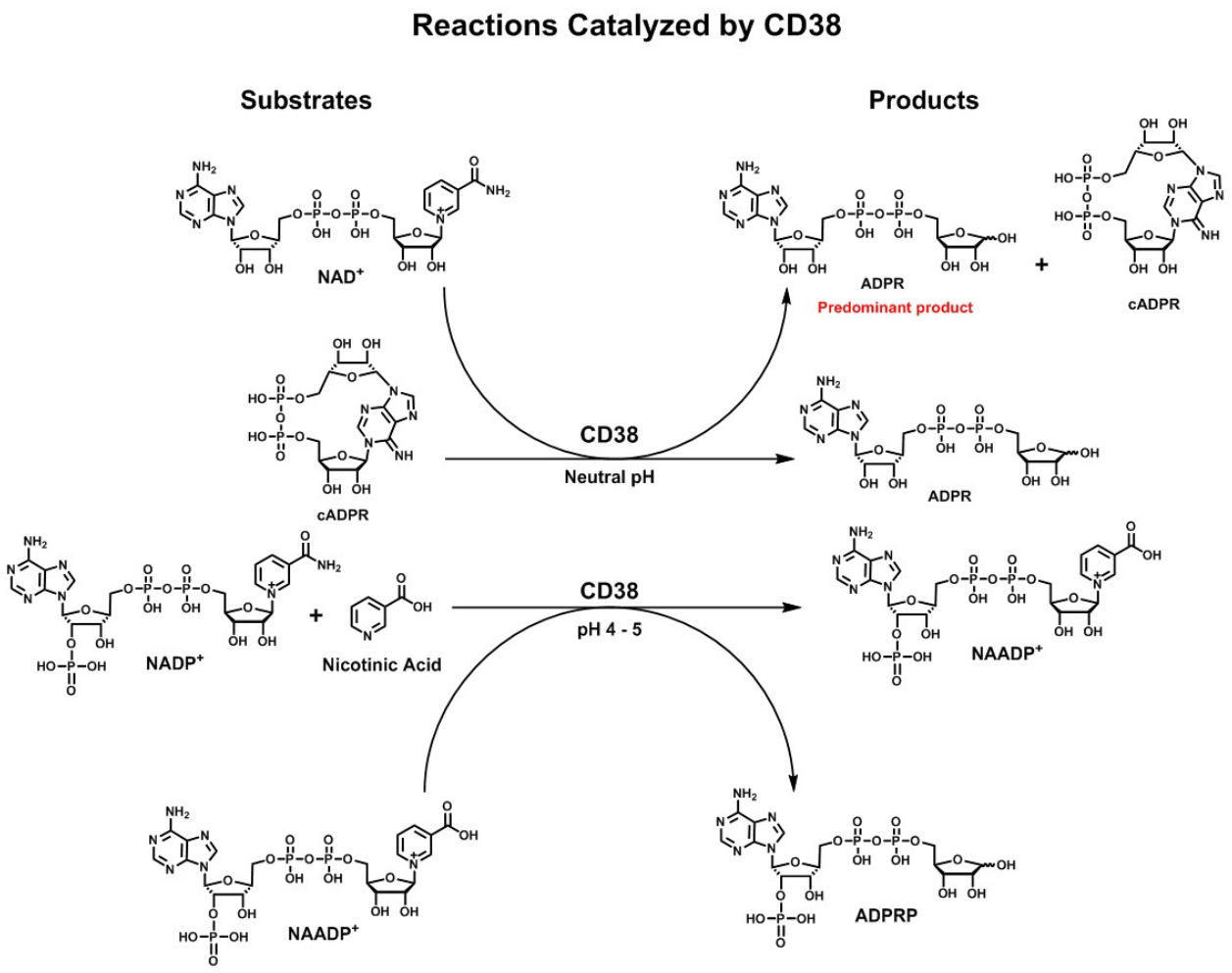

Figure 1.1. CD38 catalyzes the formation of two Ca^{2+} messengers, cADPR and NAADP. Additionally, CD38 catalyzes the hydrolysis of NAD/cADPR and NADP/NAADP.

The most significant of the CD38 substrates is NAD, which is most familiar for its capability as a small molecule cofactor able to be a two electron donor/acceptor and used in many metabolic reactions. As a redox cofactor, NAD can be reduced via a two electron hydride transfer resulting in NADH formation, which can then be oxidized back to form NAD (Figure 1.2A). Within these redox reactions the total amount of NAD and NADH is not altered (*28*).

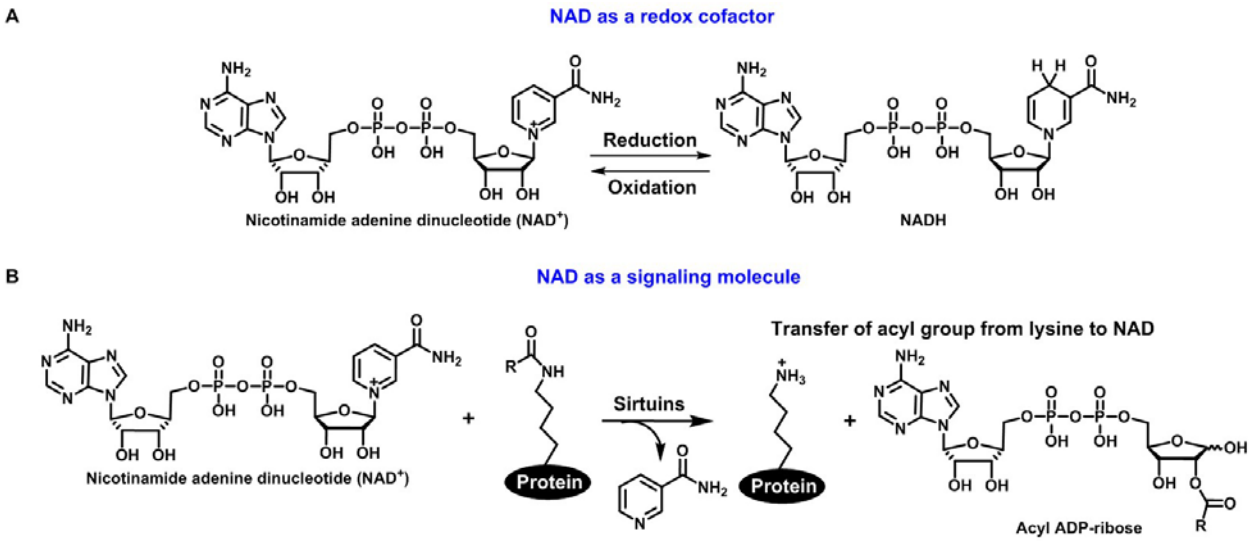

Figure 1.2. Cellular roles for NAD. (A) NAD as a redox cofactor. (B) NAD as a signaling molecule by being a part of the sirtuin catalyzed de-acylation reaction.

However, NAD is increasingly recognized as being an important signaling molecule by effecting protein posttranslational modifications, such as NAD-dependent deacylation (Figure 1.2B) and ADP-ribosylation (*28*). These NAD-consuming enzymes include 17 poly(ADP-ribose) polymerases (PARPs) (*29*), 4 mono(ADP-ribosyl) transferases (*30*), and 7 human deacylases (sirtuins) (*31*). These enzymes use NAD as a co-substrate to modify the functions of various substrate proteins that affects important biological functions, such as DNA repair, transcription regulation and mitosis. Additionally, the availability of NAD can modulate these proteins activity (*28, 32*). Consequently, an enzyme such as CD38 that has been reported to be intracellular and has the ability to quickly degrade NAD levels can affect the other NAD-dependent enzymes by regulating NAD concentrations (*32-34*). CD38 actively hydrolyzes NAD, and when measured using purified CD38 protein, it has a k_{cat} of $96s^{-1}$ and K_m of 16 μM (*35*). Unless there is a mechanism within the cell to modulate the robust NAD hydrolysis activity, CD38 may deplete intracellular NAD. As a result, multiple studies have shown that CD38 does

affect intracellular NAD levels, and in some cases may affect other protein activity through modulation of NAD levels (*32, 34, 36-39*). In particular, one study supporting this hypothesis found that CD38 may regulate availability of NAD to the SIRT1 enzyme; thus, indicating that CD38 may regulate SIRT1 enzymatic activity. It was observed in CD38 knockout mice that tissue levels of NAD are significantly increased and that the *in vivo* deacetylation of the SIRT1 substrate p53 is increased (*32*). In addition, a report demonstrates that CD38 indirectly affects cell surface ADP-ribosylation of cell surface proteins by limiting the availability of NAD, which is the substrate for ADP-ribosyltransferase-2 (ART-2) – an ADP-ribosylating ectoenzyme (*33*).

Another substrate for CD38 is NADP, which goes through an exchange of the nicotinamide group with nicotinic acid to form NAADP. This activity occurs selectively at acidic pH. Consequently, the pH dependence has led to the suggestion of CD38 having a functional role for the endocytic pathway in cells where acidic pH is present (*24, 26*). However, to confirm the link between the acidic dependence of this particular enzymatic conversion to a role in the endocytic pathway, the cellular localization needs careful investigation to determine if CD38 is localized in the endocytic pathway. As for the role played by NADP within the cell, it performs similarly to NAD in being a molecule that can be reduced by a two electron hydride ion to form NADPH. Structurally, NADP only differs from NAD by having a phosphate on the 2' hydroxyl group of the adenosine. This extra phosphate has no effect on the electron-transfer properties for NADP compared to NAD, but it does give the molecule a different shape. Consequently, NADP and NAD bind as substrates to different sets of enzymes that correspond to two sets of electron-transfer reactions (*40*). Lastly, the ratio of NADP/NADPH is kept low within the cell; thus, the catalytic efficiency of CD38 for NADP would have to be carefully obtained in order to determine whether this activity is physiologically relevant. In addition, NADP conversion to

NAADP requires acidic pH and high concentrations of nicotinic acid, which are not present outside of the cell. Therefore, if this is a physiologically relevant activity, then CD38 must be located on acidic organelles in the presence of nicotinic acid (*28*).

Another critical feature of CD38 enzyme activity is affecting intracellular calcium signaling through its products, which include cADPR, NAADP and ADPR (*41*). Calcium ions impact nearly every aspect of cell physiology. Protein function is controlled by protein structure; thus, calcium with its positive charge can alter the electrostatics of the local environment and protein conformation upon binding. The concentration of free calcium within the cytoplasm is typically between 10 to 100 nM. In contrast, the extracellular calcium concentration is in the mM range. Consequently, the intracellular concentration of calcium is carefully regulated by calcium channels located both on the plasma membrane and intracellular organelles (*42*). A well-recognized pathway for the increase of cytoplasmic calcium is the phospholipase C pathway. Phospholipase C is a membrane bound enzyme that upon activation will hydrolyze the plasma membrane phospholipid – phosphatidylinositol 4,5-bisphosphate (PIP2) – that releases inositol 1,4,5-trisphosphate (IP_3) and diacylglycerol (DAG). Subsequently, DAG remains attached to the cell membrane and functions to activate protein kinase C (PKC). Whereas, IP3 enters into the cytoplasm and once binding to IP_3 receptors on the smooth endoplasmic reticulum (ER), calcium channels on the smooth ER are opened. This causes diffusion of calcium ions from the smooth ER into the cytoplasm; thus, raising cytoplasmic calcium concentration from ~0.1 μM to ~1 μM transiently (*42*). This transient increase in cytoplasmic calcium concentration is sufficient for activation of several calcium-binding proteins that mediate cellular effects of calcium due to high affinity binding of calcium. One such example of a calcium-binding protein is calmodulin (*43*). Additionally, other calcium signaling pathways are mediated by the CD38 enzyme products –

cADPR, NAADP and ADPR. When compared to IP3, the molecules cADPR, NAADP and ADPR have distinctly different molecular structures and protein targets. cADPR targets the ryanodine receptor (RyR) in the ER (*44, 45*). NAADP activates calcium release from two-pore channels (TPCs) in lysosomes (*46, 47*). ADPR, the predominate product from CD38 metabolism of NAD, has been shown to induce calcium entry through the transient receptor potential cation channel (TRPM2) upon an increase in cytosolic ADPR from concanavalin A (*48*). However, it appears that cADPR requires associate protein factors, calmodulin and FK506 binding protein in order to mediate its calcium release response, though the mechanism of this interaction remains to be elucidated (*49, 50*). Also, results using a photoaffinity labeling reagent suggest the actual binding receptor for NAADP may not be TPCs (*51*). Consequently, the mechanism of activation for calcium release along with the various cellular effects from having multiple calcium signaling molecules requires further research. Though it is generally accepted that CD38 enzyme activity plays a role in the physiological functions of CD38, the cellular localization and catalytic efficiency needs to be carefully investigated to understand the physiological significance of these enzyme activities found *in vitro*.

1.3. Relevance to human health

Cell physiological role: CD38 gene knockout studies have shown that CD38 is critical in a wide range of physiological roles such as insulin secretion (*52*), susceptibility to bacterial infection (*53*) and social behavior of mice through modulating neuronal oxytocin secretion (*54*). Additionally, in CD38 knockout mice, mouse embryonic fibroblasts (MEFs) were significantly resistant to oxidative stress such as H_2O_2 injury compared with wild-type MEFs, suggesting a role in protection against DNA damage from oxidative stress (*55*). CD38 is a cell surface protein that plays an important role in cell survival and is overexpressed on malignant cells (*56, 57*).

CD38 in cancer: Prior to normal cells conferring a full cancer phenotype, several genetic changes must occur that allow cells to evade normal growth and proliferation mechanisms of control. These six fundamental cellular changes include: proliferation without external inducing signal, evasion of apoptosis, sustained angiogenesis to obtain blood supply, tissue invasion by metastasis, limitless replicative potential, and insensitivity to antigrowth signals (*58*). The genetic alterations causing the cancer phenotype can be studied through altered protein expression and function; therefore, thorough investigation of protein expression and function allows for proper diagnosis and treatment.

Currently, CD38 has drawn attention from cancer researchers as being a promising drug target, because within various different types of cancer, both positive and negative growth regulatory roles have been attributed to CD38. In HeLa human cervical carcinoma cells, CD38 propels cell cycle progression (*59*). However, in myeloid leukemia cells, it provides both a growth promoting and inhibitory signal (*60, 61*). The cause for these apparently distinctive roles could arise from different availability of cell receptors associating with CD38 or different intracellular proteins within the various cancer cells, thus affecting CD38 signaling outcome. As a result, CD38 function within different cancers remains enigmatic making it difficult to use CD38 as a prognostic indicator in a wide range of applications.

CD38 expression is typically associated as a negative prognostic indicator in chronic lymphocytic leukemia (CLL) (*62*). CLL is a cancer originating from lymphocytes and begins in the bone marrow. In later stages of CLL growth and proliferation, it can invade other organs. Currently, for diagnosis of CLL growth rate, a measurement of protein expression for Zeta-chain-associated protein kinase 70 (ZAP-70) and CD38 indicates CLL to grow slower when expression of these two proteins is low or absent. Therefore, ZAP-70 and CD38 must have some

role to play in CLL growth and proliferation. Over the past decade studies investigating the role of CD38 in CLL have uncovered a role as an active signaling receptor when CD38 ligation from an agonistic mAb was followed by Ca^{2+} flux and distinctly increased proliferation (*63*). Beyond the role of being another negative prognostic indicator, ZAP-70 is a cytoplasmic protein tyrosine kinase that has a role in CLL growth and proliferation together with CD38. ZAP-70 experiences significant tyrosine phosphorylation upon CD38 agonist ligation, and ZAP-70 is a limiting factor for the CD38 signaling pathway affects (*64*). It is still left to be determined whether CD38 and ZAP-70 in CLL will be effective therapeutic target proteins (*63*).

CD38 in diabetes: Diabetes is characterized by increased serum blood glucose levels due either to the absence of pancreatic beta cells (type 1 diabetes), or pancreatic beta cells producing inadequate insulin for the body's increased needs, thus referred to as insulin resistance (type 2 diabetes). The main source of energy for the body is glucose, which is released and absorbed into the bloodstream following food intake. However, the glucose from the bloodstream must move into body tissue in order for the cells to receive the glucose to use it for energy. Insulin secretion from pancreatic beta cells into the blood, allows for glucose to move from the blood to the cells.

Initial studies suggested a possible role for CD38 – present in rat pancreatic islet cells – for insulin secretion through its enzymatic function of cyclizing NAD to cADPR (*6*). Both cADPR and Ca^{2+} increase led to induced insulin secretion in permeabilized pancreatic islet cells, and the Ca^{2+} release was inositol triphosphate (IP3) independent (*65*). Similarly, a CD38 gene knockout mouse study showed that CD38 is required for producing a glucose-induced increase in both cADPR, intracellular calcium concentration and insulin secretion (*52*). The data supporting these conclusions include the following: 1) no glucose-induced increase of intracellular cADPR and a much attenuated intracellular calcium increase were detected in $CD38^{-/-}$ islet homogenate,

2) a much attenuated increase in insulin secretion upon addition of 20 to 30 mM glucose occurred in $CD38^{-/-}$ isolated islet cells, and 3) an analysis of $CD38^{-/-}$ serum levels showed a much higher glucose level at 15 – 60 min after addition of glucose intraperitoneally to the mouse and a much lower serum insulin level at 15 min after the glucose injection. However, this observed phenotype was rescued upon addition of a pancreatic beta cell-specific expression of CD38 cDNA. Consequently, this data support the causal role for CD38 in insulin secretion through CD38 enzymatic formation of cADPR from NAD. In humans, it was found that 14% of the examined diabetic patients have autoantibodies against CD38 that impaired the cADPR formation. *In vitro* data obtained on cultured rat pancreatic islets revealed that upon addition of anti-CD38 antibodies, insulin secretion induced by glucose was inhibited (*66*). Therefore, multiple studies report a link between CD38 enzymatic function to insulin secretion and thereby having a role in diabetes.

CD38 in HIV: CD38 has been recognized as having prognostic value for determining the progression of human immunodeficiency (HIV) to acquired immunodeficiency syndrome (AIDS) through measuring the percentage of $CD8^+$ T cells that also have CD38 expression (*67*). A higher percentage of $CD8^+$ T cells with CD38 expression proved to be a marker for progression of HIV to AIDS (*67*). HIV is a retrovirus that causes AIDS, a condition causing the immune system to fail in protection against life threating infections or cancers. Evaluation of CD38 expression on $CD8^+$ T cells is a rapid and simple method in order to analyze the progression of HIV to AIDS (*68*). Subsequent studies have analyzed whether CD38 has a biological role in the progression of HIV to AIDS or whether it can simply remain a prognostic indicator (*69, 70*).

CD38 in cancer therapeutics: Currently, CD38 has drawn attention as a promising target for monoclonal antibody-based immunotherapy due to its increased cell surface expression on certain leukemia cancers compared to normal cell expression (*71*). Additionally, a vast majority of therapeutic strategies for cancer treatment target surface molecules expressed by the cancer. Targeted immunotherapy with other CD proteins has already been important in successful treatment of several cancers. For example, the monoclonal antibody drug rituximab is a chimeric CD20 antibody that attaches to CD20 on B-cells, which makes the cells more visible to the immune system for targeted cell killing. Rituximab has revolutionized the treatment of several B-cell malignancies such as follicular lymphoma (*72*, *73*). CD38 has a relatively high expression on all malignant cells in multiple myeloma, a malignant disorder of the B-cell lineage (*57*). Multiple myeloma remains an incurable disease with a median survival of 4.4 to 7.1 yrs (*74*). Therefore, CD38 is the target of a novel therapeutic monoclonal antibody known as daratumumab. Daratumumab has received Breakthrough Therapy Designation from the United States Food and Drug Administration based on phase 1 data showing a promising efficacy, with nearly 70% of patients responding to the highest dose (*75*). As reported by Genmab in March 2014, Janssen Biotech Inc. began a Phase III study in relapsed or refractory multiple myeloma patients. Consequently, elucidating the molecular mechanisms of CD38 will enhance our understanding of its function within cells and lead to more effective therapeutics.

REFERENCES

1. Kohler, G., and Milstein, C. (1975) Continuous cultures of fused cells secreting antibody of predefined specificity, *Nature 256*, 495-497.
2. Reinherz, E. L., Kung, P. C., Goldstein, G., Levey, R. H., and Schlossman, S. F. (1980) Discrete stages of human intrathymic differentiation: analysis of normal thymocytes and leukemic lymphoblasts of T-cell lineage, *Proc Natl Acad Sci U S A 77*, 1588-1592.
3. Terhorst, C., van Agthoven, A., LeClair, K., Snow, P., Reinherz, E., and Schlossman, S. (1981) Biochemical studies of the human thymocyte cell-surface antigens T6, T9 and T10, *Cell 23*, 771-780.
4. Kramer, G., Steiner, G., Fodinger, D., Fiebiger, E., Rappersberger, C., Binder, S., Hofbauer, J., and Marberger, M. (1995) High expression of a CD38-like molecule in normal prostatic epithelium and its differential loss in benign and malignant disease, *J Urol 154*, 1636-1641.
5. Yamada, M., Mizuguchi, M., Otsuka, N., Ikeda, K., and Takahashi, H. (1997) Ultrastructural localization of CD38 immunoreactivity in rat brain, *Brain Res 756*, 52-60.
6. Li, Q., Yamada, Y., Yasuda, K., Ihara, Y., Okamoto, Y., Kaisaki, P. J., Watanabe, R., Ikeda, H., Tsuda, K., and Seino, Y. (1994) A cloned rat CD38-homologous protein and its expression in pancreatic islets, *Biochem Biophys Res Commun 202*, 629-636.
7. Chidambaram, N., Wong, E. T., and Chang, C. F. (1998) Differential oligomerization of membrane-bound CD38/ADP-ribosyl cyclase in porcine heart microsomes, *Biochem Mol Biol Int 44*, 1225-1233.
8. Mehta, K., Shahid, U., and Malavasi, F. (1996) Human CD38, a cell-surface protein with multiple functions, *FASEB J 10*, 1408-1417.
9. Jackson, D. G., and Bell, J. I. (1990) Isolation of a cDNA encoding the human CD38 (T10) molecule, a cell surface glycoprotein with an unusual discontinuous pattern of expression during lymphocyte differentiation, *J Immunol 144*, 2811-2815.
10. States, D. J., Walseth, T. F., and Lee, H. C. (1992) Similarities in amino acid sequences of Aplysia ADP-ribosyl cyclase and human lymphocyte antigen CD38, *Trends Biochem Sci 17*, 495.
11. Howard, M., Grimaldi, J. C., Bazan, J. F., Lund, F. E., Santos-Argumedo, L., Parkhouse, R. M., Walseth, T. F., and Lee, H. C. (1993) Formation and hydrolysis of cyclic ADP-ribose catalyzed by lymphocyte antigen CD38, *Science 262*, 1056-1059.
12. Kim, H., Jacobson, E. L., and Jacobson, M. K. (1993) Synthesis and degradation of cyclic ADP-ribose by NAD glycohydrolases, *Science 261*, 1330-1333.
13. Lee, H. C., Zocchi, E., Guida, L., Franco, L., Benatti, U., and De Flora, A. (1993) Production and hydrolysis of cyclic ADP-ribose at the outer surface of human erythrocytes, *Biochem Biophys Res Commun 191*, 639-645.
14. Takasawa, S., Tohgo, A., Noguchi, N., Koguma, T., Nata, K., Sugimoto, T., Yonekura, H., and Okamoto, H. (1993) Synthesis and hydrolysis of cyclic ADP-ribose by human leukocyte antigen CD38 and inhibition of the hydrolysis by ATP, *J Biol Chem 268*, 26052-26054.
15. Lee, H. C., and Aarhus, R. (1995) A derivative of NADP mobilizes calcium stores insensitive to inositol trisphosphate and cyclic ADP-ribose, *J Biol Chem 270*, 2152-2157.

16. Dianzani, U., and Malavasi, F. (1995) Lymphocyte adhesion to endothelium, *Crit Rev Immunol 15*, 167-200.
17. Kontani, K., Kukimoto, I., Nishina, H., Hoshino, S., Hazeki, O., Kanaho, Y., and Katada, T. (1996) Tyrosine phosphorylation of the c-cbl proto-oncogene product mediated by cell surface antigen CD38 in HL-60 cells, *J Biol Chem 271*, 1534-1537.
18. Munoz, P., Navarro, M. D., Pavon, E. J., Salmeron, J., Malavasi, F., Sancho, J., and Zubiaur, M. (2003) CD38 signaling in T cells is initiated within a subset of membrane rafts containing Lck and the CD3-zeta subunit of the T cell antigen receptor, *J Biol Chem 278*, 50791-50802.
19. Quarona, V., Zaccarello, G., Chillemi, A., Brunetti, E., Singh, V. K., Ferrero, E., Funaro, A., Horenstein, A. L., and Malavasi, F. (2013) CD38 and CD157: a long journey from activation markers to multifunctional molecules, *Cytometry B Clin Cytom 84*, 207-217.
20. Lee, H. C., and Aarhus, R. (1991) ADP-ribosyl cyclase: an enzyme that cyclizes NAD+ into a calcium-mobilizing metabolite, *Cell Regul 2*, 203-209.
21. Zocchi, E., Franco, L., Guida, L., Benatti, U., Bargellesi, A., Malavasi, F., Lee, H. C., and De Flora, A. (1993) A single protein immunologically identified as CD38 displays NAD+ glycohydrolase, ADP-ribosyl cyclase and cyclic ADP-ribose hydrolase activities at the outer surface of human erythrocytes, *Biochem Biophys Res Commun 196*, 1459-1465.
22. Gelman, L., Deterre, P., Gouy, H., Boumsell, L., Debre, P., and Bismuth, G. (1993) The lymphocyte surface antigen CD38 acts as a nicotinamide adenine dinucleotide glycohydrolase in human T lymphocytes, *Eur J Immunol 23*, 3361-3364.
23. Summerhill, R. J., Jackson, D. G., and Galione, A. (1993) Human lymphocyte antigen CD38 catalyzes the production of cyclic ADP-ribose, *FEBS Lett 335*, 231-233.
24. Aarhus, R., Graeff, R. M., Dickey, D. M., Walseth, T. F., and Lee, H. C. (1995) ADP-ribosyl cyclase and CD38 catalyze the synthesis of a calcium-mobilizing metabolite from NADP, *J Biol Chem 270*, 30327-30333.
25. Santella, L. (2005) NAADP: a new second messenger comes of age, *Mol Interv 5*, 70-72.
26. Lee, H. C. (2006) Structure and enzymatic functions of human CD38, *Mol Med 12*, 317-323.
27. Chini, E. N., Chini, C. C., Kato, I., Takasawa, S., and Okamoto, H. (2002) CD38 is the major enzyme responsible for synthesis of nicotinic acid-adenine dinucleotide phosphate in mammalian tissues, *Biochem J 362*, 125-130.
28. Lin, H. (2007) Nicotinamide adenine dinucleotide: beyond a redox coenzyme, *Org Biomol Chem 5*, 2541-2554.
29. Schreiber, V., Dantzer, F., Ame, J. C., and de Murcia, G. (2006) Poly(ADP-ribose): novel functions for an old molecule, *Nat Rev Mol Cell Biol 7*, 517-528.
30. Corda, D., and Di Girolamo, M. (2003) Functional aspects of protein mono-ADP-ribosylation, *EMBO J 22*, 1953-1958.
31. Sauve, A. A., Wolberger, C., Schramm, V. L., and Boeke, J. D. (2006) The biochemistry of sirtuins, *Annu Rev Biochem 75*, 435-465.
32. Aksoy, P., Escande, C., White, T. A., Thompson, M., Soares, S., Benech, J. C., and Chini, E. N. (2006) Regulation of SIRT 1 mediated NAD dependent deacetylation: a novel role for the multifunctional enzyme CD38, *Biochem Biophys Res Commun 349*, 353-359.

33. Krebs, C., Adriouch, S., Braasch, F., Koestner, W., Leiter, E. H., Seman, M., Lund, F. E., Oppenheimer, N., Haag, F., and Koch-Nolte, F. (2005) CD38 controls ADP-ribosyltransferase-2-catalyzed ADP-ribosylation of T cell surface proteins, *J Immunol 174*, 3298-3305.
34. Barbosa, M. T., Soares, S. M., Novak, C. M., Sinclair, D., Levine, J. A., Aksoy, P., and Chini, E. N. (2007) The enzyme CD38 (a NAD glycohydrolase, EC 3.2.2.5) is necessary for the development of diet-induced obesity, *FASEB J 21*, 3629-3639.
35. Sauve, A. A., Munshi, C., Lee, H. C., and Schramm, V. L. (1998) The reaction mechanism for CD38. A single intermediate is responsible for cyclization, hydrolysis, and base-exchange chemistries, *Biochemistry 37*, 13239-13249.
36. Chini, E. N. (2009) CD38 as a regulator of cellular NAD: a novel potential pharmacological target for metabolic conditions, *Curr Pharm Des 15*, 57-63.
37. Escande, C., Nin, V., Price, N. L., Capellini, V., Gomes, A. P., Barbosa, M. T., O'Neil, L., White, T. A., Sinclair, D. A., and Chini, E. N. (2013) Flavonoid apigenin is an inhibitor of the NAD+ ase CD38: implications for cellular NAD+ metabolism, protein acetylation, and treatment of metabolic syndrome, *Diabetes 62*, 1084-1093.
38. Aksoy, P., White, T. A., Thompson, M., and Chini, E. N. (2006) Regulation of intracellular levels of NAD: a novel role for CD38, *Biochem Biophys Res Commun 345*, 1386-1392.
39. Al-Abady, Z. N., Durante, B., Moody, A. J., and Billington, R. A. (2013) Large changes in NAD levels associated with CD38 expression during HL-60 cell differentiation, *Biochem Biophys Res Commun 442*, 51-55.
40. Bruce Alberts, A. J., Julian Lewis, Martin Raff, Keith Roberts, Peter Walter (2007) *Molecular Biology of the Cell*, Garland Science; 5 edition.
41. Lee, H. C. (1997) Mechanisms of calcium signaling by cyclic ADP-ribose and NAADP, *Physiol Rev 77*, 1133-1164.
42. Clapham, D. E. (2007) Calcium signaling, *Cell 131*, 1047-1058.
43. Harvey Lodish, A. B., Chris Kaiser, Monty Krieger, Matthew Scott, Anthony Bretscher, Hidde Ploegh (2008) *Molecular Cell Biology, 6th edition*, 6 ed., W. H. Freeman and Company.
44. Galione, A., Lee, H. C., and Busa, W. B. (1991) Ca(2+)-induced Ca2+ release in sea urchin egg homogenates: modulation by cyclic ADP-ribose, *Science 253*, 1143-1146.
45. Lee, H. C., Aarhus, R., and Graeff, R. M. (1995) Sensitization of calcium-induced calcium release by cyclic ADP-ribose and calmodulin, *J Biol Chem 270*, 9060-9066.
46. Brailoiu, E., Churamani, D., Cai, X., Schrlau, M. G., Brailoiu, G. C., Gao, X., Hooper, R., Boulware, M. J., Dun, N. J., Marchant, J. S., and Patel, S. (2009) Essential requirement for two-pore channel 1 in NAADP-mediated calcium signaling, *J Cell Biol 186*, 201-209.
47. Calcraft, P. J., Ruas, M., Pan, Z., Cheng, X., Arredouani, A., Hao, X., Tang, J., Rietdorf, K., Teboul, L., Chuang, K. T., Lin, P., Xiao, R., Wang, C., Zhu, Y., Lin, Y., Wyatt, C. N., Parrington, J., Ma, J., Evans, A. M., Galione, A., and Zhu, M. X. (2009) NAADP mobilizes calcium from acidic organelles through two-pore channels, *Nature 459*, 596-600.
48. Gasser, A., Glassmeier, G., Fliegert, R., Langhorst, M. F., Meinke, S., Hein, D., Kruger, S., Weber, K., Heiner, I., Oppenheimer, N., Schwarz, J. R., and Guse, A. H. (2006)

Activation of T cell calcium influx by the second messenger ADP-ribose, *J Biol Chem 281*, 2489-2496.
49. Lee, H. C., Aarhus, R., Graeff, R., Gurnack, M. E., and Walseth, T. F. (1994) Cyclic ADP ribose activation of the ryanodine receptor is mediated by calmodulin, *Nature 370*, 307-309.
50. Noguchi, N., Takasawa, S., Nata, K., Tohgo, A., Kato, I., Ikehata, F., Yonekura, H., and Okamoto, H. (1997) Cyclic ADP-ribose binds to FK506-binding protein 12.6 to release Ca2+ from islet microsomes, *J Biol Chem 272*, 3133-3136.
51. Walseth, T. F., Lin-Moshier, Y., Jain, P., Ruas, M., Parrington, J., Galione, A., Marchant, J. S., and Slama, J. T. (2012) Photoaffinity labeling of high affinity nicotinic acid adenine dinucleotide phosphate (NAADP)-binding proteins in sea urchin egg, *J Biol Chem 287*, 2308-2315.
52. Kato, I., Yamamoto, Y., Fujimura, M., Noguchi, N., Takasawa, S., and Okamoto, H. (1999) CD38 disruption impairs glucose-induced increases in cyclic ADP-ribose, [Ca2+]i, and insulin secretion, *J Biol Chem 274*, 1869-1872.
53. Partida-Sanchez, S., Cockayne, D. A., Monard, S., Jacobson, E. L., Oppenheimer, N., Garvy, B., Kusser, K., Goodrich, S., Howard, M., Harmsen, A., Randall, T. D., and Lund, F. E. (2001) Cyclic ADP-ribose production by CD38 regulates intracellular calcium release, extracellular calcium influx and chemotaxis in neutrophils and is required for bacterial clearance in vivo, *Nat Med 7*, 1209-1216.
54. Jin, D., Liu, H. X., Hirai, H., Torashima, T., Nagai, T., Lopatina, O., Shnayder, N. A., Yamada, K., Noda, M., Seike, T., Fujita, K., Takasawa, S., Yokoyama, S., Koizumi, K., Shiraishi, Y., Tanaka, S., Hashii, M., Yoshihara, T., Higashida, K., Islam, M. S., Yamada, N., Hayashi, K., Noguchi, N., Kato, I., Okamoto, H., Matsushima, A., Salmina, A., Munesue, T., Shimizu, N., Mochida, S., Asano, M., and Higashida, H. (2007) CD38 is critical for social behaviour by regulating oxytocin secretion, *Nature 446*, 41-45.
55. Ge, Y., Jiang, W., Gan, L., Wang, L., Sun, C., Ni, P., Liu, Y., Wu, S., Gu, L., Zheng, W., Lund, F. E., and Xin, H. B. (2010) Mouse embryonic fibroblasts from CD38 knockout mice are resistant to oxidative stresses through inhibition of reactive oxygen species production and Ca(2+) overload, *Biochem Biophys Res Commun 399*, 167-172.
56. Kawano, M. M., Huang, N., Harada, H., Harada, Y., Sakai, A., Tanaka, H., Iwato, K., and Kuramoto, A. (1993) Identification of immature and mature myeloma cells in the bone marrow of human myelomas, *Blood 82*, 564-570.
57. Lin, P., Owens, R., Tricot, G., and Wilson, C. S. (2004) Flow cytometric immunophenotypic analysis of 306 cases of multiple myeloma, *Am J Clin Pathol 121*, 482-488.
58. Hanahan, D., and Weinberg, R. A. (2000) The hallmarks of cancer, *Cell 100*, 57-70.
59. Zocchi, E., Daga, A., Usai, C., Franco, L., Guida, L., Bruzzone, S., Costa, A., Marchetti, C., and De Flora, A. (1998) Expression of CD38 increases intracellular calcium concentration and reduces doubling time in HeLa and 3T3 cells, *J Biol Chem 273*, 8017-8024.
60. Konopleva, M., Estrov, Z., Zhao, S., Andreeff, M., and Mehta, K. (1998) Ligation of cell surface CD38 protein with agonistic monoclonal antibody induces a cell growth signal in myeloid leukemia cells, *J Immunol 161*, 4702-4708.

61. Todisco, E., Suzuki, T., Srivannaboon, K., Coustan-Smith, E., Raimondi, S. C., Behm, F. G., Kitanaka, A., and Campana, D. (2000) CD38 ligation inhibits normal and leukemic myelopoiesis, *Blood 95*, 535-542.
62. D'Arena, G., Musto, P., Cascavilla, N., Dell'Olio, M., Di Renzo, N., Perla, G., Savino, L., and Carotenuto, M. (2001) CD38 expression correlates with adverse biological features and predicts poor clinical outcome in B-cell chronic lymphocytic leukemia, *Leuk Lymphoma 42*, 109-114.
63. Malavasi, F., Deaglio, S., Damle, R., Cutrona, G., Ferrarini, M., and Chiorazzi, N. (2011) CD38 and chronic lymphocytic leukemia: a decade later, *Blood 118*, 3470-3478.
64. Deaglio, S., Vaisitti, T., Aydin, S., Bergui, L., D'Arena, G., Bonello, L., Omede, P., Scatolini, M., Jaksic, O., Chiorino, G., Efremov, D., and Malavasi, F. (2007) CD38 and ZAP-70 are functionally linked and mark CLL cells with high migratory potential, *Blood 110*, 4012-4021.
65. Takasawa, S., Nata, K., Yonekura, H., and Okamoto, H. (1993) Cyclic ADP-ribose in insulin secretion from pancreatic beta cells, *Science 259*, 370-373.
66. Ikehata, F., Satoh, J., Nata, K., Tohgo, A., Nakazawa, T., Kato, I., Kobayashi, S., Akiyama, T., Takasawa, S., Toyota, T., and Okamoto, H. (1998) Autoantibodies against CD38 (ADP-ribosyl cyclase/cyclic ADP-ribose hydrolase) that impair glucose-induced insulin secretion in noninsulin- dependent diabetes patients, *J Clin Invest 102*, 395-401.
67. Liu, Z., Hultin, L. E., Cumberland, W. G., Hultin, P., Schmid, I., Matud, J. L., Detels, R., and Giorgi, J. V. (1996) Elevated relative fluorescence intensity of CD38 antigen expression on CD8+ T cells is a marker of poor prognosis in HIV infection: results of 6 years of follow-up, *Cytometry 26*, 1-7.
68. Ondoa, P., Dieye, T. N., Vereecken, C., Camara, M., Diallo, A. A., Fransen, K., Litzroth, A., Mboup, S., and Kestens, L. (2006) Evaluation of HIV-1 p24 antigenemia and level of CD8+CD38+ T cells as surrogate markers of HIV-1 RNA viral load in HIV-1-infected patients in Dakar, Senegal, *J Acquir Immune Defic Syndr 41*, 416-424.
69. Bofill, M., Fairbanks, L. D., Ruckemann, K., Lipman, M., and Simmonds, H. A. (1995) T-lymphocytes from AIDS patients are unable to synthesize ribonucleotides de novo in response to mitogenic stimulation. Impaired pyrimidine responses are already evident at early stages of HIV-1 infection, *J Biol Chem 270*, 29690-29697.
70. Bofill, M., and Parkhouse, R. M. (1999) The increased CD38 expressed by lymphocytes infected with HIV-1 is a fully active NADase, *Eur J Immunol 29*, 3583-3587.
71. Chillemi, A., Zaccarello, G., Quarona, V., Ferracin, M., Ghimenti, C., Massaia, M., Horenstein, A. L., and Malavasi, F. (2013) Anti-CD38 antibody therapy: windows of opportunity yielded by the functional characteristics of the target molecule, *Mol Med 19*, 99-108.
72. Coiffier, B. (2003) Monoclonal antibodies in the management of newly diagnosed, aggressive B-cell lymphoma, *Curr Hematol Rep 2*, 23-29.
73. Maloney, D. G. (2003) Rituximab for follicular lymphoma, *Curr Hematol Rep 2*, 13-22.
74. Raab, M. S., Podar, K., Breitkreutz, I., Richardson, P. G., and Anderson, K. C. (2009) Multiple myeloma, *Lancet 374*, 324-339.
75. Aggarwal, S. R. (2014) A survey of breakthrough therapy designations, *Nat Biotechnol 32*, 323-330.

Chapter 2

Revealing CD38 Cellular Localization Using a Cell Permeable, Mechanism-Based Fluorescent Small Molecule Probe*

Abstract

Nicotinamide adenine dinucleotide (NAD) is increasingly recognized as an important signaling molecule that affects numerous biological pathways. Thus, enzymes that metabolize NAD can have important biological functions. One NAD-metabolizing enzyme in mammals is CD38, a type II transmembrane protein that converts NAD primarily to adenosine diphosphate ribose (ADPR) and a small amount of cyclic adenosine diphosphate ribose (cADPR). Localization of CD38 was originally thought to be only on the plasma membrane, but later reports showed either significant or solely, intracellular CD38. With the efficient NAD-hydrolysis activity, the intracellular CD38 may lead to depletion of cellular NAD, thus producing harmful effects. Therefore, the intracellular localization of CD38 needs to be carefully validated. Here, we report the synthesis and application of a cell permeable, fluorescent small molecule (SR101-F-araNMN) that can covalently label enzymatically active CD38 with minimal perturbation of live cells. Using this fluorescent probe, we revealed that CD38 is predominately on the plasma membrane of Raji and retinoic acid (RA)-treated HL-60 cells.

Reproduced with permission from Shrimp, J. H. et al. *J. Am. Chem. Soc.* **2014**, *136*, 5656−5663.

Additionally, the probe revealed no CD38 expression in K562 cells, which was previously reported to have solely intracellular CD38. The finding that very little intracellular CD38 exists in these cell lines suggests that the major enzymatic function of CD38 is to hydrolyze extracellular NAD rather than intracellular NAD. The fluorescent activity-based probes that we developed allow the localization of CD38 in different cells to be determined, thus enabling a better understanding of the physiological function.

Introduction

Nicotinamide adenine dinucleotide (NAD) is an important cofactor used in many metabolic reactions. Recently, it has been increasingly recognized that in addition to serving as a cofactor, it also serves as an important signaling molecule by affecting protein posttranslational modifications, such as NAD-dependent deacylation and ADP-ribosylation (*1, 2*). Thus, enzymes that metabolize NAD can have important biological functions. One mammalian enzyme that metabolizes NAD is cluster designation 38 (CD38). CD38, a type II membrane protein, has important physiological functions, demonstrated by the compromised immune response and social memory defect in CD38 knockout mice (*3, 4*). In addition, its expression is associated with a poor prognosis in chronic lymphocytic leukemia (*5*). However, the molecular mechanism underlying its physiological functions is still not well understood. It is reported to function as both an enzyme and a receptor. CD38 has 69% overall homology to an *Aplysia* cyclase, which converts NAD to cyclic adenosine diphosphate ribose (cADPR), a molecule that is reported to be a calcium mobilizing messenger (*6*). CD38 was thus considered to have a similar enzymatic function (*6*). However, CD38 catalyzes the formation of mainly adenosine diphosphate ribose

(ADPR) and only a minute amount of cADPR (*7-10*). Under certain conditions, CD38 can also catalyze a base-exchange reaction converting nicotinamide adenine dinucleotide phosphate (NADP) to nicotinic acid adenine dinucleotide phosphate (NAADP), which is also a calcium mobilizing messenger (*11*). As a receptor, it was reported that CD38 can initiate transmembrane signaling in response to antibody binding (*12*).

The cellular localization of CD38 has also been perplexing. CD38 was originally identified as a cell surface protein, but was later reported to be present in intracellular compartments, such as the mitochondria, Golgi and ER, with the highest levels of expression in the nuclear membranes (*13-20*). In addition, a recent report suggested the existence of type III CD38 on the plasma membrane with the catalytic domain facing the cytosol (*21*). However, conflicting results on CD38 cellular localization have been reported, with some showing only plasma membrane CD38 and others showing only nuclear localized CD38 (*15, 22*). Due to the efficient NAD-hydrolysis activity of CD38, the intracellular CD38 may lead to depletion of cellular NAD, thus producing detrimental effects. Therefore, the intracellular localization of CD38 merits careful investigation. Methods used to study cellular localization of CD38 include the use of antibodies for confocal immunofluorescence after cell fixation and permeabilization, subcellular fractionation, and less frequently, CD38-GFP fusion proteins (*13-20, 22*). To mitigate the possibility of artifacts from these methods, there is a need for new methods with minimal perturbation of live cells and minimal interference with CD38 signaling. In addition, previously used labeling methods are typically followed by a separate step of organelle isolation to check CD38 enzymatic activity. A method to both localize and demonstrate activity will be helpful. Previously, we developed a CD38 labeling method that uses a suicide substrate, 2'-deoxy-2'-fluoro arabinosyl NAD conjugated with tetramethylrhodamine, Rh-6-(F-araNAD) (Figure 2.1A).

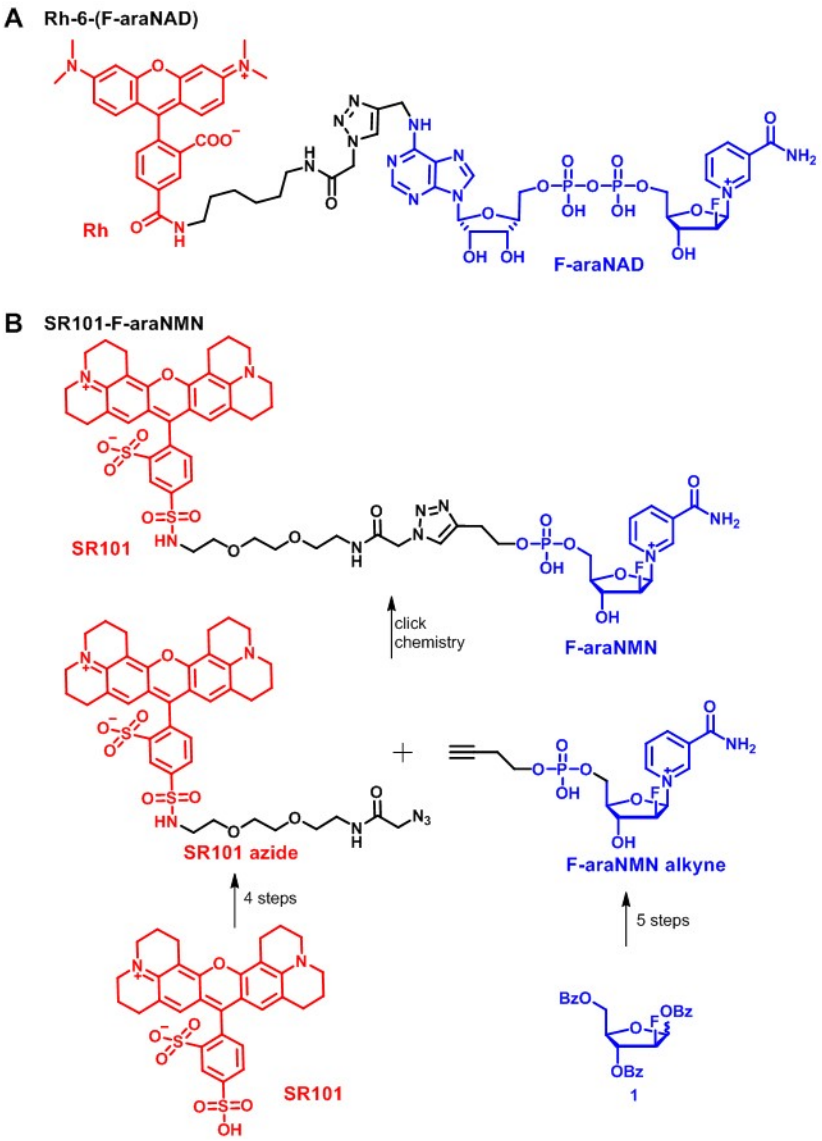

Figure 2.1. (A) Molecular Structure of Rh-6-(F-araNAD). (B) Synthesis of the Cell-Permeable Fluorescent CD38 Probe, SR101−F-araNMN

Rh-6-(F-araNAD) can covalently label CD38 on the key catalytic residue, Glu226, forming a stable covalent intermediate (*23*). This method was successful in labeling CD38 while not interfering with antibody-induced CD38 signaling events. It was mechanism-based labeling and thus only labeled catalytically active CD38. However, this molecule was not cell permeable; therefore, it cannot be used to label intracellular CD38. In the present study, we developed a cell

permeable fluorescent activity-based small molecule probe for labeling CD38 in live cells. This probe allowed detection of catalytically active CD38 both on the plasma membrane and inside the cells. Using this probe, we investigated the cellular distribution of CD38 in two leukemia (HL-60 and K562) and one lymphoma (Raji) cell lines that were previously reported to have intracellular CD38 (*15, 16*). Our results showed CD38 is localized mainly at the plasma membrane with very little intracellular CD38. In particular, our results showed no pronounced nuclear localization as previously reported, which may have been an artifact of the immunofluorescence method. The clarification of CD38 intracellular localization will facilitate the understanding of its physiological function.

Results

Design and Synthesis of a Cell-Permeable CD38 Probe

Our strategy for making a cell-permeable CD38 probe was to first choose a cell-permeable fluorophore and then conjugate it to F-araNMN instead of F-araNAD (Figure 2.1B). F-araNMN is smaller and has one fewer negative charges than F-araNAD, and thus may be more cell permeable. Among several fluorescent dyes that we checked, sulfurhodamine 101 (SR101) showed the desired cell permeability. This was interesting as SR101 has size, charge, and overall structure similar to those of tetramethylrhodamine, yet SR101 is more cell permeable. To conjugate SR101 to F-araNMN, we decided to use the copper-catalyzed Huisgen 1,3-dipolar cycloaddition between alkyne and azide, commonly known as click chemistry (Figure 2.1B) (*24*). We designed an alkyne-containing F-araNMN compound (F-araNMN alkyne) and an azide-containing SR101 compound (SR101 azide). To obtain F-araNMN alkyne, we began with a 2'-fluoroarabinoside (**1**) where all hydroxyl groups were protected with benzoyl groups. The

anomeric *O*-benzoyl group was first replaced with bromine and then by nicotinamide. The benzoyl groups were removed using potassium carbonate in methanol. Then in a one-pot reaction, the 5′-hydroxyl group was phosphorylated and then connected to 3-butyn-1-ol via a phosphodiester bond to give the desired F-araNMN alkyne compound. To make the SR101 azide compound, we first made the sulfonyl chloride derivative of SR101 and then attached a linker with an amino group and an azido group at opposite ends. Finally, the SR101 azide was conjugated to F-araNMN alkyne via click chemistry to obtain the desired SR101−F-araNMN (Figure 2.1B, full synthesis shown in Figure 2.13).

In Vitro Labeling of Purified CD38 by SR101−FaraNMN

To test whether SR101−F-araNMN can covalently label CD38 at the catalytic E226 residue, we used purified, wild-type, and catalytic mutants (E226Q and E226D) of CD38 extracellular catalytic domain. Both wild-type and mutants were incubated with SR101−F-araNMN for 10 min. The reaction mixtures were resolved by SDS-PAGE and visualized by fluorescence and then stained with Coomassie blue. Wild-type CD38 was fluorescently labeled by SR101−F araNMN, but the CD38 catalytic mutants were not (Figure 2.2).

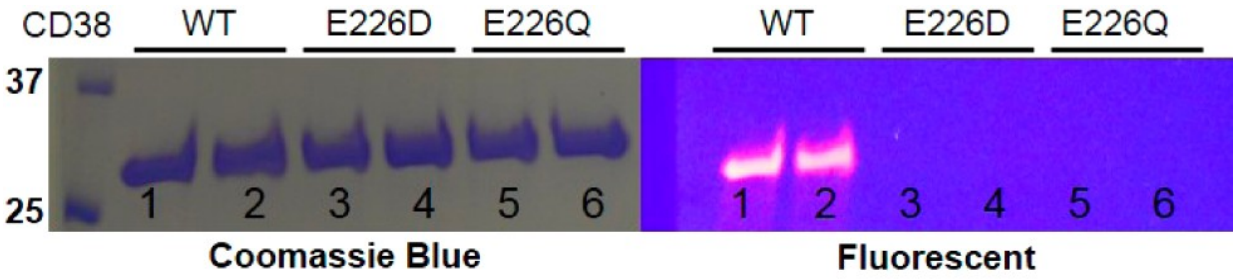

Figure 2.2. *In vitro* labeling of purified CD38 with SR101−F-araNMN. Lanes 1 and 2, CD38 wt; lanes 3 and 4, CD38 E226D; lanes 5 and 6, CD38 E226Q. Ladder is on the left, listed first.

These results demonstrated that SR101−F-araNMN is an activity-/mechanism-based probe for CD38. We compared the labeling efficiency of Rh-6-(F-araNAD) and SR101−F-araNMN. With CD38 at 1 μM and the probes at 10 μM, the labeling reactions were complete within 0.5 min for Rh-6-(F-araNAD) and within 5 min for SR101−F-araNMN (Figure 2.3A, D). Furthermore, the addition of NAD (1 mM) or nicotinamide (100 μM) to the labeling reaction had very little effect on SR101–F-araNMN labeling efficiency (Figure 2.3B, C). Thus, SR101−F-araNMN is slightly less efficient than Rh−F-araNAD, but still labels CD38 very efficiently.

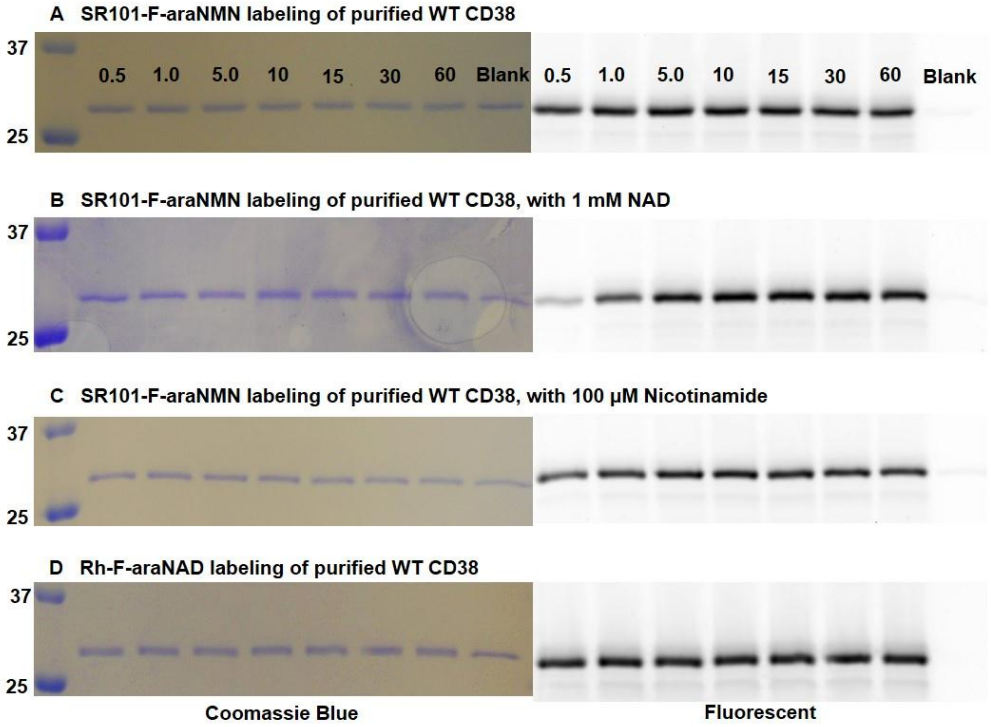

Figure 2.3. Time course of labeling wt CD38 with Rh-(6-F-araNAD) or SR101-F-araNMN. All time points are in minutes. (A) Labeling reaction with SR101-F-araNMN. (B) Labeling reaction with SR101-F-araNMN and 1 mM NAD. (C) Labeling reaction with SR101-F-araNMN and 100 μM nicotinamide. (D) Labeling reaction with Rh-F-araNAD. Protein ladder is on the left, listed first.

To confirm that this probe is specific for CD38 in cells, we used the human leukemia cell line, HL-60. HL-60 was chosen because these cells have a very low level of CD38 but could be

induced to express higher levels of CD38 with RA (*25*). Consequently, untreated HL-60 cells were used as the negative control. In one experiment, we labeled live cells, followed by collecting whole cell lysates and then resolved the whole cell lysates with SDS-PAGE (lanes 1, Figure 2.4). In another experiment, we collected the whole cell lysate, incubated with the probe, and then resolved the lysates by SDS-PAGE (lanes 2, Figure 2.4). In both cases, only one major fluorescent band, which corresponds to the size of CD38, was detected in RA-treated cells; while no major fluorescent bands were detected in untreated cells (Figure 2.4).

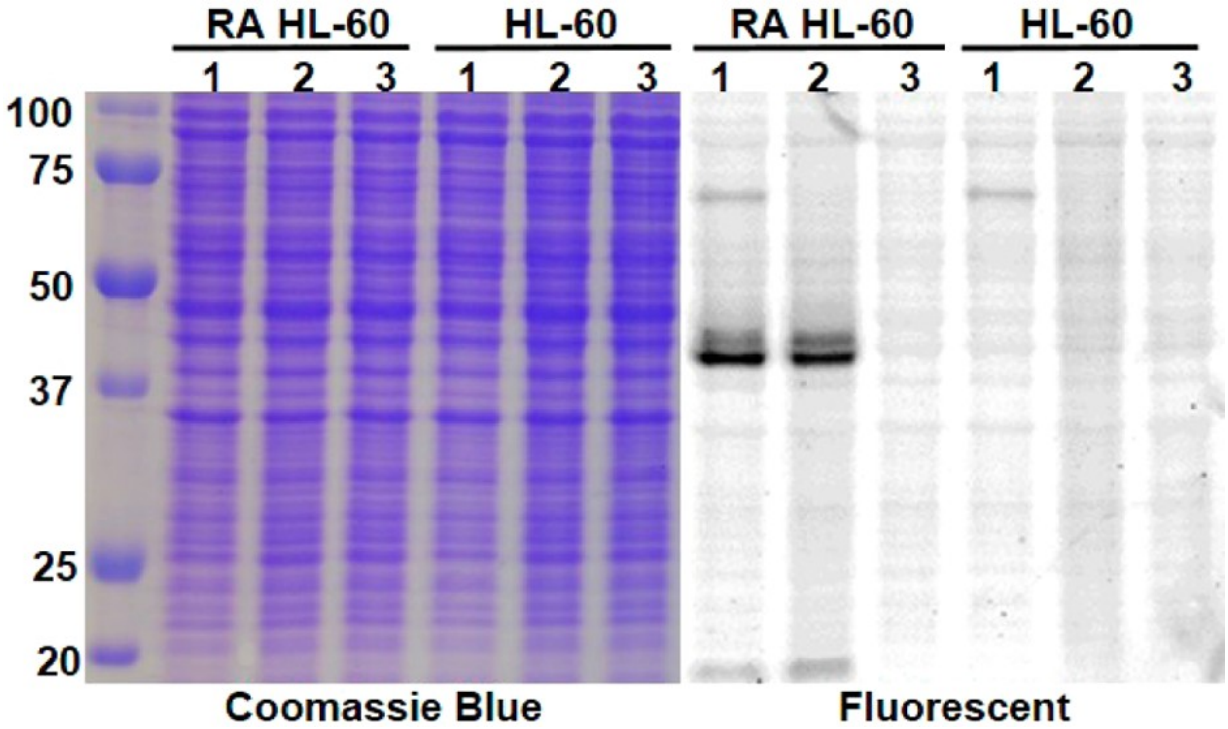

Figure 2.4. In-gel fluorescence analysis of CD38 in HL-60 cells (RA and untreated). Lanes 1, live-cell labeling with SR101−F-araNMN; lanes 2, whole cell lysate labeled with SR101−F-araNMN; lanes 3, whole cell lysate with no CD38 probe. Ladder is on the left, listed first.

The weak fluorescent band around 20 kD was shown to be from a cleaved form of CD38 (Figure 2.5). A weak fluorescent band at about 70 kD was also detected in both RA treated and untreated HL-60 cells in the live-cell labeling but not in the whole-cell lysate labeling (Figure 2.4). By optimizing the experimental conditions, we were able to partially or completely eliminate this

band (Figure 2.5). Altogether, this result demonstrated that SR101−FaraNMN is specific for CD38 in cells. The higher CD38 expression in RA-treated cells was also confirmed by Western blot using a monoclonal anti-CD38 antibody (see Figure 2.12C).

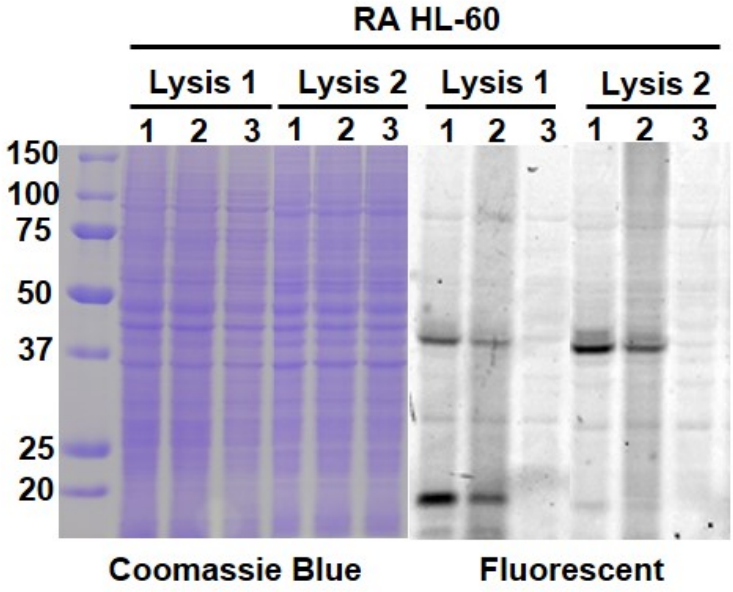

Figure 2.5. In-gel fluorescence analysis for labeling CD38 with SR101-F-araNMN in either live cells or whole cell lysate. Lysis 1 contained less protease inhibitors (contained only protease inhibitor cocktail or PIC used at 100x) than Lysis 2 (contained PIC at 20x, phosphatase inhibitor at 100x, PMSF at 1.0 mM, EDTA at 10 mM). Therefore, lysates from Lysis 2 showed a weaker fluorescent band around 20 kD than in Lysis 1, indicating that this 20 kD band was from CD38 cleavage. Lanes 1: live cell labeling then obtain whole cell lysate and resolve by SDS-PAGE; Lanes 2: obtain whole cell lysate then do probe labeling and resolve lysates by SDS-PAGE; Lanes 3: whole cell lysate resolved by SDS-PAGE, no CD38 probe. Protein ladder is on the left.

Confocal Microscopy Imaging for Labeling of CD38 in Live Cells with SR101−F-araNMN.

The ability of SR101−FaraNMN to enter live cells and label CD38 was next tested using HL-60 cells and visualized using confocal microscopy. We first incubated cells with either 10 μM SR101−F-araNMN or 10 μM Rh-6-(F-araNAD) for 8 min at RT followed by washing with PBS to remove excess unbound dye. The incubation time was determined to be sufficient to allow for the binding of the probe to CD38 as determined by an *in vitro* labeling experiment (Figure 2.3). We indeed found that SR101−F-araNMN was cell permeable as strong fluorescence

was observed inside HL60 cells (Figure 2.6A); conversely, HL-60 cells labeled with Rh-6-(F-araNAD) showed no fluorescence inside (Figure 2.6B). However, washing with PBS alone could not remove excess SR101−F-araNMN molecules in the cells (even HL-60 cells without RA treatment had strong fluorescence inside), making it difficult to differentiate free vs CD38-bound SR101−FaraNMN. To circumvent this problem, we used methanol to wash away the unbound SR101−F-araNMN as it was more soluble in methanol. This was proven successful as HL-60 cells treated with fluorescent molecule alone, SR101, then washed with methanol showed essentially no fluorescence (Figure 2.6C). In contrast, RA-treated HL-60 cells were strongly fluorescently labeled with SR101−F-araNMN (Figure 2.6D) on the plasma membrane and only weakly inside the cells.

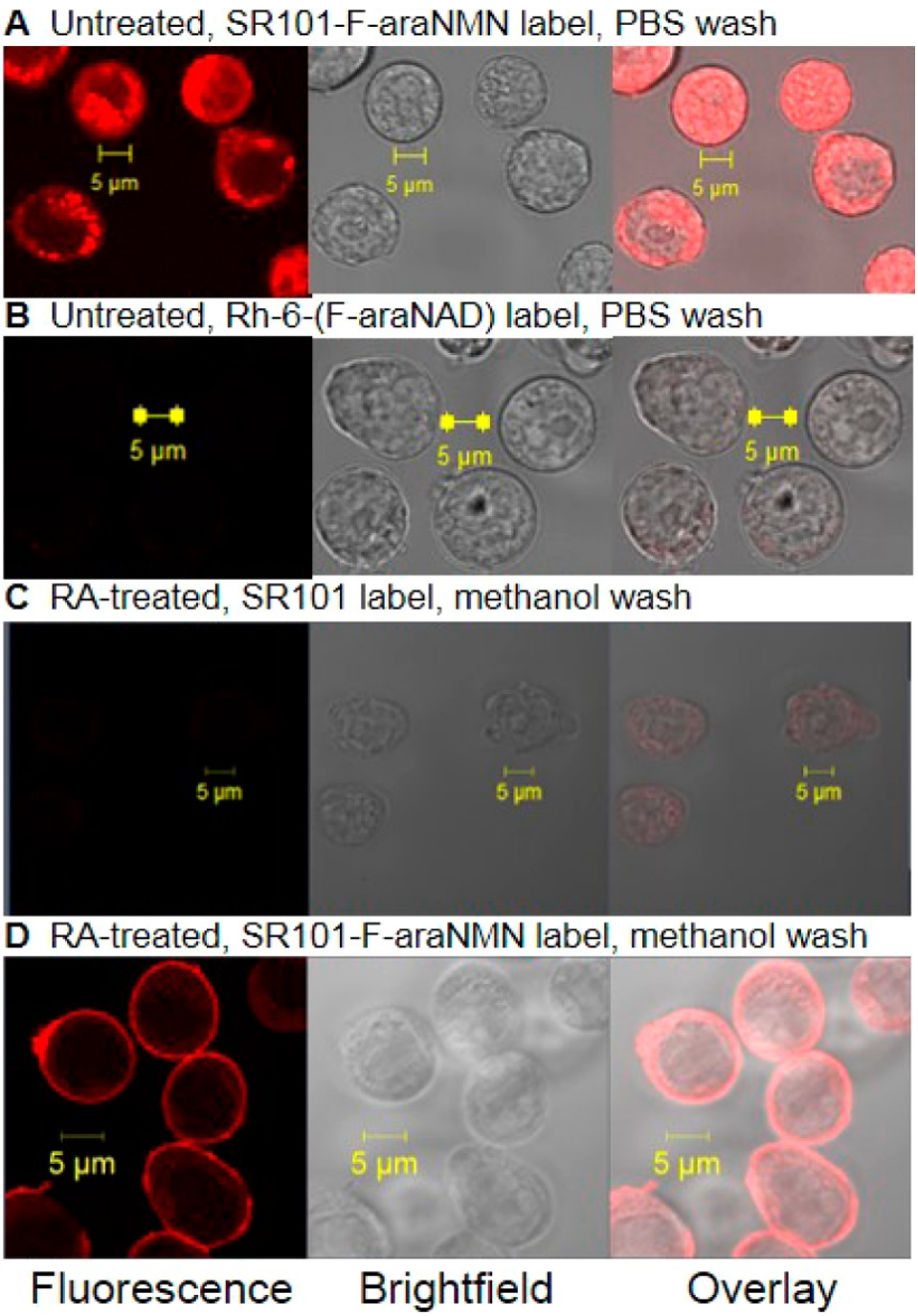

Figure 2.6. Confocal images of HL-60 cells (with or without RA- treatment): (A) Cells without RA-treatment labeled with SR101−F- araNMN and washed with PBS. (B) Cells without RA-treatment labeled with Rh-6-(F-araNAD) and washed with PBS. (C) RA-treated cells labeled with SR101 (negative control) and washed with methanol. (D) RA-treated cells labeled with SR101−F-araNMN and washed with methanol. Confocal microscope settings: laser power: 4.5 %, pinhole: 1.1 airy unit, master gain for PMT: 875.

Then, we turned our focus to locating the intracellular CD38 with SR101−F-araNMN. Although there was some weak fluorescence inside the RA-treated HL-60 cells, it was difficult to visualize the intracellular signal because the fluorescence on the plasma membrane was too strong. To overcome this, we used 6-alkyne-F-araNAD to first block plasma membrane CD38. The 6-alkyne-F-araNAD was not cell permeable and had no fluorescent molecule attached. HL-60 cells (RA treated and untreated) were first incubated with 6-alkyne-F-araNAD to block plasma membrane CD38, followed by incubation either with SR101 as negative control or SR101−F-araNMN to label intracellular CD38. This allowed us to clearly see the intracellular fluorescently labeled CD38, after optimizing the confocal microscope settings to maximize detection. HL-60 cells without RA treatment also showed very weak fluorescent signal. This represented the low levels of CD38 present, which was further confirmed by Western blot data shown later (see Figure 2.12C). Importantly, an increase in fluorescence (~2.5-fold) was observed in RA-treated cells compared to HL-60 cells without RA treatment, confirming that the probe was labeling CD38 (Figure 2.7).

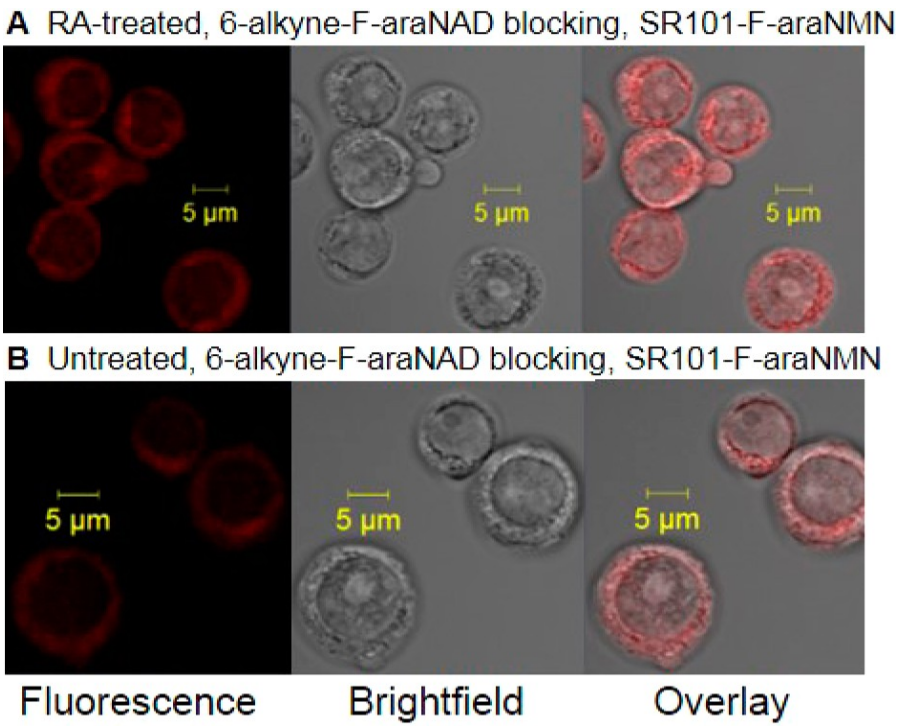

Figure 2.7. Confocal images of HL-60 cells (RA or untreated) blocked with 6-alkyne-(F-araNAD) followed by intracellular CD38 labeling with SR101−F-araNMN. (A) RA treated HL-60 cells. (B) Untreated HL-60 cells. Confocal microscope settings: laser power: 11.0%, pinhole: 1.3 airy units, Master gain for PMT: 940. With laser settings kept constant between the two images, higher fluorescence indicates higher amount of active CD38.

It has been reported that cell fixation with methanol alone can cause loss of cytosolic and nuclear proteins (*26*). To rule out that the low detection of intracellular CD38 was not due to the loss of CD38 during the methanol wash, we also used a combination of paraformaldehyde (PFA) fixation with methanol permeabilization after SR101−F-araNMN labeling of CD38 in RA-treated HL-60 cells (*26*). This method preserves both cell-surface and intracellular proteins (*26*). The data from this combined PFA fixation and methanol permeabilization led to the same conclusion that CD38 was mainly concentrated on the plasma membrane (data not shown). In addition, subcellular fractionation of RA-treated HL-60 cells was done to obtain nucleus, membrane, and cytosolic fractions (*27, 28*). Using a monoclonal anti-CD38 antibody that would presumably detect both catalytically active and inactive CD38, the Western blot data again showed that the

nucleus fraction contained very low levels of CD38, while the membrane fraction contain very high levels of CD38 (Figure 2.8).

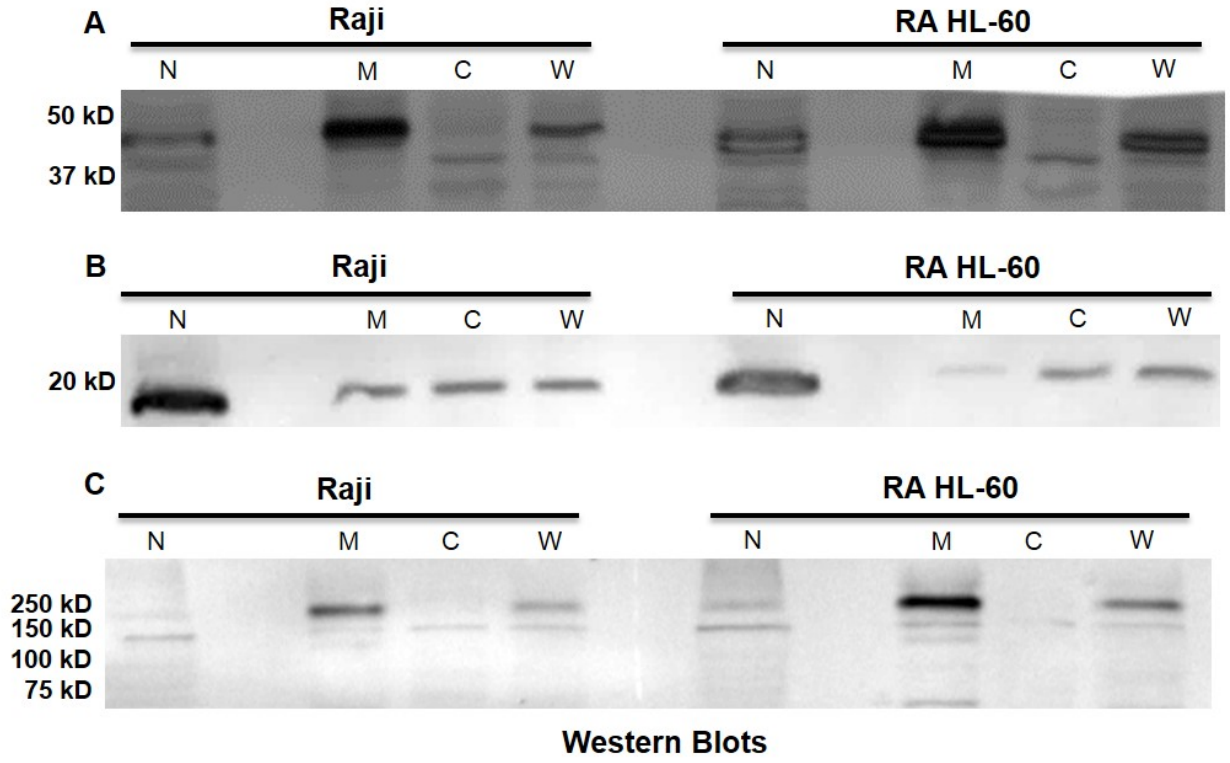

Figure 2.8. Western blot analysis following subcellular fractionation of Raji and RA treated HL-60 cells. Subcellular fractions were Nucleus (N), Membrane (M) and Cytosolic (C). Whole cell lysate (W) was run as a positive control. (**A**) Blotting for CD38. (**B**) Blotting for Histone 3 as a nucleus marker protein. (**C**) Blotting for Na+/K+ ATPase α1 as a plasma membrane marker protein. Image J quantification was done to analyze band intensity for CD38 and Na+/K+ ATPase α1 between nucleus and membrane fractions. Using ImageJ quantificiation of protein band intensity and relating CD38 band intensity to CD38 amount, showed the nucleus fraction for RA-treated HL-60 cells contained 22% of that present in the membrane fraction. CD38 amount in the nucleus fraction for Raji cells contained 23% of that present in the membrane fraction. However, the nucleus fraction for RA-treated HL-60 cells contained about 23% of the plasma membrane marker protein compared to that contained in the membrane fraction. Also, the nucleus fraction for Raji cells contained 21% of the plasma membrane marker protein compared to that in the membrane fraction. Therefore, the presence of CD38 in the nucleus fraction is mostly from contamination of the nucleus fraction from proteins that should have been collected in the membrane fraction alone.

Thus, SR101−F-araNMN was cell permeable and capable of labeling CD38 within live cells without perturbation of the cell before labeling. In addition, it signifies that the intracellular

CD38 is in fact catalytically active. Despite the intracellular presence, our results revealed that CD38 was mainly concentrated on the plasma membrane as the plasma membrane had the strongest fluorescence.

In-Gel Fluorescence of Whole Cell Lysate Using CD38 Probes to Label and Quantify Intracellular CD38

The weak intracellular labeling diverged from previous reports regarding pronounced intracellular CD38. We thus decided to quantify the relative amount of intracellular vs plasma membrane CD38. We split the cells from the same culture into two equal portions. One portion was treated with the impermeable Rh-6-(F-araNAD) and then the cells were lysed after washing away excess probes (live cell labeling). The other portion was lysed first and then the total cell lysate was incubated with Rh-6-(F-araNAD) (whole cell lysate labeling). The two batches of cell lysates were then resolved by SDSPAGE and analyzed by fluorescence and Coomassie blue staining. If a significant amount of CD38 is intracellular, then we expected that the live cell labeling intensity would be weaker than the whole cell lysate labeling intensity with the impermeable Rh-6-(F-araNAD). Contrary to this, we saw essentially the same labeling intensities with the live cell labeling and the whole cell lysate labeling (after correcting for protein loading using the Coomassie blue staining) with Rh-6-(F-araNAD) (Figure 2.9).

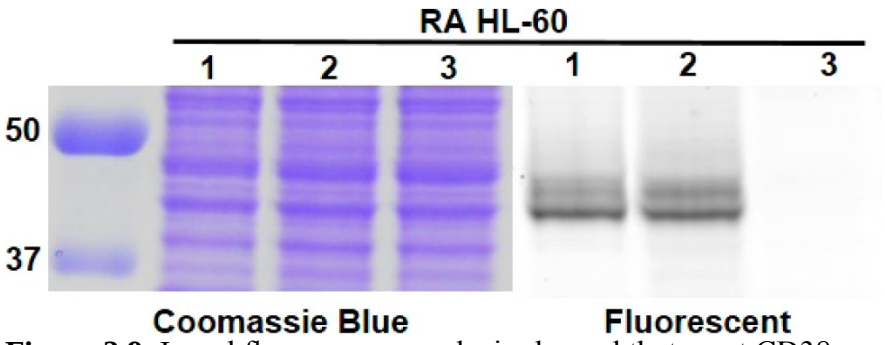

Figure 2.9. In-gel fluorescence analysis showed that most CD38 was present on plasma membrane. Lanes 1, live cell labeling with Rh-6-(F- araNAD) followed by in-gel fluorescence (labeling plasma membrane CD38 only); lanes 2, whole cell lysate was obtained first followed by labeling with Rh-6-(F-araNAD) (labeling all catalytically active CD38); lanes 3, whole cell lysate without CD38 probes. Protein ladder is on the left, listed first.

In addition, to more accurately quantify the percentage of intracellular CD38, we used another approach with the small-molecule probes. We first blocked cell surface CD38 with 6-alkyne-F-araNAD and then labeled intracellular CD38 with SR101−F-araNMN. In the control experiment, we labeled the total CD38 using SR101−FaraNMN without blocking of the cell surface CD38. We then collected the whole cell lysates and used in-gel fluorescence to quantify the intracellular CD38 vs total CD38 (Figure 2.10). Quantification using this method showed that about 6.5% of CD38 molecules were intracellular in RA-treated HL-60 cells. This result further supported the previous confocal imaging results with SR101−F-araNMN and suggested that the amount of intracellular and catalytically active CD38 was very little.

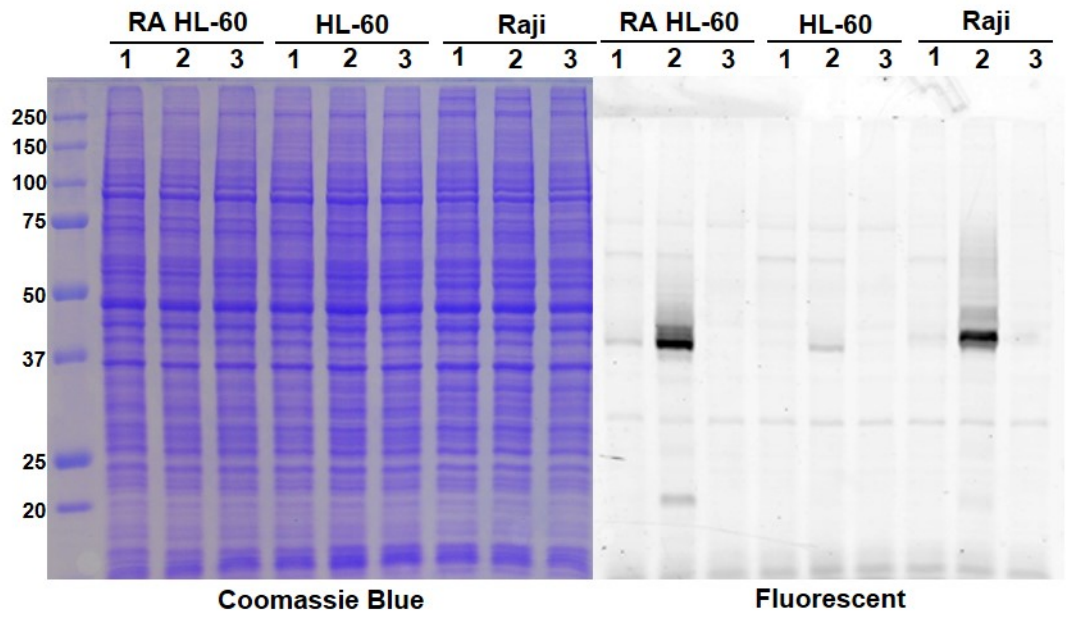

Figure 2.10. In-gel fluorescence analysis of CD38 in HL-60 (RA and untreated) and Raji cells to compare amount of intracellular versus cell surface CD38. Lanes 1, cell surface CD38 was blocked with 6-alkyne-F-araNAD then labeling intracellular CD38 with SR101-F-araNMN (fluorescence indicating intracellular CD38); Lanes 2, cells were only labeled with SR101-F-araNMN (fluorescence indicating all CD38); Lanes 3, No labeling molecules were added to the cells. Protein ladder is on the left.

CD38 Labeling in Raji and K562 Cells

Once cell permeability and CD38 specific labeling was confirmed for SR101−F-araNMN in HL-60 cells, we investigated the intracellular distribution of CD38 in Raji and K562, which are lymphoma and leukemia cell lines, respectively. Both types of cells were reported to have intracellular CD38 (*15*). In particular, in Raji cells, it was reported that CD38 was present in a special subnuclear location called the Cajal body. In K562 cells, it was reported that there was only intracellular CD38 and no plasma membrane CD38 (*15*). Raji cells showed strong plasma membrane fluorescent labeling by SR101−F-araNMN similar to RA-treated HL-60 cells (Figure 2.11A). To better visualize intracellular labeling, we first blocked plasma membrane CD38 with the nonfluorescent, cell impermeable probe, 6-alkyne-F-araNAD. Then, the cells were incubated

with SR101−F-araNMN. We also used DAPI to stain the nucleus. Very weak fluorescence was observed in the nucleus and most of the label localized in the cytoplasm when methanol was used to wash off the probe (Figure 2.11D). Similar results were obtained when we used PFA and methanol to treat cells (Figure 2.11B, C). We again used the in-gel fluorescence analysis, which showed essentially the same labeling intensities in the live cell labeling and the whole cell lysate labeling with Rh-6-(F-araNAD), after correcting for protein loading using the Coomassie blue staining (Figure 2.11E).

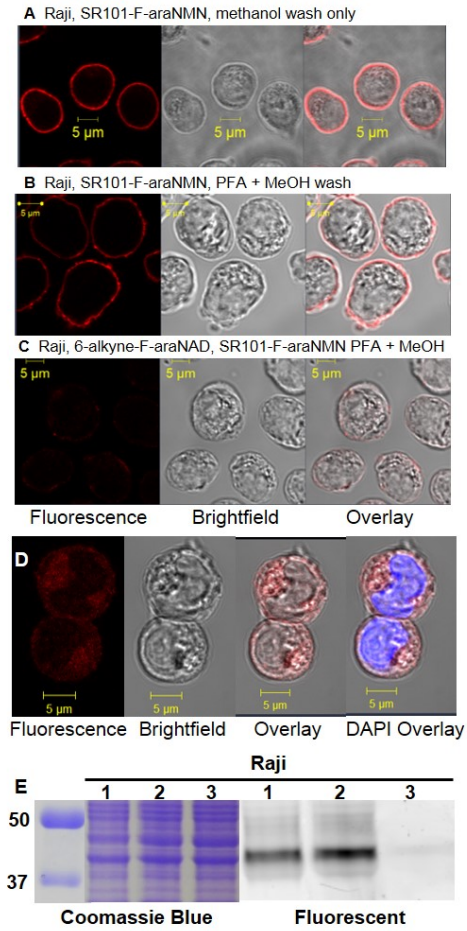

Figure 2.11. Labeling of CD38 in Raji cells. (A) Confocal image of Raji cells labeled with SR101−F-araNMN. Confocal microscope settings for (A): laser power: 5.5%, pinhole: 1.1 airy units, master gain for PMT: 866. (B) Confocal image of Raji cells labeled with SR101-F-araNMN, subsequently fixed and permeabilized with PFA and methanol after labeling of CD38 in live cells. Confocal microscope settings: laser power: 6.0%, pinhole: 1.1 airy units, master gain for PMT: 860. (C) First, labeling of plasma membrane CD38 with 6-Alkyne-F-araNAD followed by SR101-F-araNMN used to label intracellular CD38, subsequently fixed and permeabilized with PFA and methanol. Confocal microscope settings: laser power: 24%, pinhole: 1.1 airy units, master gain for PMT: 1060. (D) Confocal image of Raji cells blocked with 6-alkyne-(F- araNAD) then labeled with SR101−F-araNMN (visualization of intracellular CD38 only). DAPI (blue) staining dsDNA showing nucleus. Confocal microscope settings: laser power: 10%, pinhole: 1.1 airy units, master gain for PMT: 866. For detecting intracellular fluorescence emission, an increase in laser power and master gain was necessary; therefore, this indicates a low amount of active, intracellular CD38. (E) In-gel fluorescence analysis: lanes 1, live cell labeling with Rh-6-(F-araNAD) followed by in-gel fluorescence (labeling plasma membrane CD38 only); lanes 2, whole cell lysate was obtained first followed by labeling with Rh-6-(F-araNAD) (labeling all catalytically active CD38); lanes 3, whole cell lysate without CD38 probes. Ladder is on the left, listed first.

This result further supported the previous confocal imaging results with SR101−F-araNMN and suggested that the amount of intracellular CD38 was very little. Also, quantification using 6-alkyne-F-araNAD and SR101−F-araNMN as described above for RA-treated HL-60 cells, revealed that about 4.2% of catalytically active CD38 in Raji cells is intracellular (Figure 2.10). As for the K562 cells, no SR101−F-araNMN fluorescent labeling was detected from confocal imaging (Figure 2.12A). Consistent with this, labeling of cell lysate with SR101−F- araNMN also failed to detect the presence of CD38 (Figure 2.12B). This result was contrary to the reported result showing that K562 had only intracellular CD38. One possibility for the discrepancy was that intracellular CD38 was present but that it was not catalytically active for unknown reasons. To rule out this possibility, we further performed Western blot analysis on whole cell lysate to detect CD38. The Western blot again showed that K562 cells did not express CD38, while CD38 was detected in RA-treated HL-60 and Raji whole cell lysates, along with low expression in untreated HL-60 cells (Figure 2.12C). Therefore, our data collectively demonstrated that K562 cells did not express CD38.

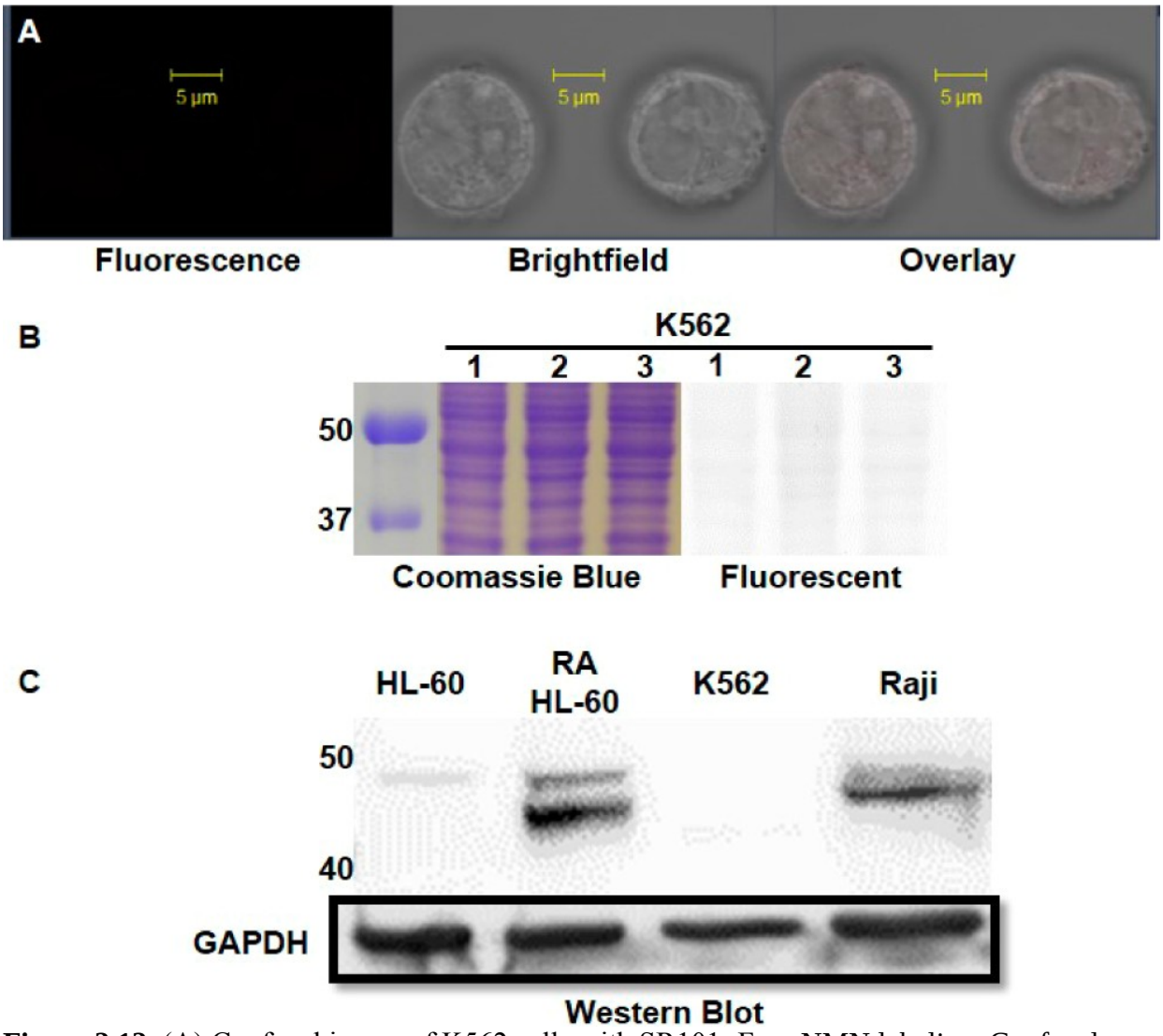

Figure 2.12. (A) Confocal image of K562 cells with SR101−F-araNMN labeling. Confocal microscope settings: laser power: 4.5%, pinhole: 1.1 airy units, master gain for PMT: 803. (B) K562 in-gel fluorescence analysis: lanes 1, live cell labeling with SR101−F-araNMN followed by in-gel fluorescence; lanes 2, obtained whole cell lysate then labeling with SR101−F-araNMN (labeling all catalytically active CD38); lanes 3, whole cell lysate without CD38 probe. Ladder is on the left, listed first. (C) Western blot analysis for detection of CD38 in all cell lines.

Discussion

We developed a cell-permeable CD38 probe, SR101−F-araNMN, by choosing a more cell-permeable fluorescent dye (SR101) and by using F-araNMN instead of F-araNAD. Using purified CD38, SR101−F-araNMN could label wild type CD38 but not the catalytic mutant of

CD38, confirming that it was an activity-based probe. Using three human blood cancer cell lines, we further confirmed that SR101−F-araNMN was cell permeable and was able to specifically label CD38. Combined with the previously developed impermeable CD38 probes, Rh- 6-(F-araNAD) and 6-alkyne-F-araNAD, we were able to better visualize intracellular CD38 in these cell lines and obtained CD38 localization information that could correct several misconceptions about the intracellular distribution, which are discussed below.

CD38 Is Highly Concentrated in the Plasma Membranes of Raji and RA-Treated HL-60 Cells

It was reported that CD38 was present mainly on the plasma membrane with the catalytic domain facing outside (*22*). Consistent with this, when we labeled CD38 in RA-treated HL-60 cells or untreated Raji cells with SR101−F-araNMN, the strongest fluorescence resided on the plasma membrane based on confocal imaging. When limiting the fluorescence detection to intracellular CD38, HL-60 cells showed nearly a 2.5-fold increase of intracellular CD38 level upon RA treatment. However, the CD38 expression on the plasma membrane had a much greater increase based upon fluorescence detected. Additionally, our probe was activity-based; therefore, the intracellular CD38 we detected in RA-treated HL-60 and untreated Raji cells should be catalytically active. As a consequence, if the intracellular CD38 had access to cellular NAD, it might lead to decreased intracellular NAD levels. On the basis of confocal imaging, intracellular CD38 was found to be present in punctate bodies in the cytosol, which were likely membrane organelles, such as ER, Golgi, or mitochondria. At this point, we do not know the exact identities of the intracellular organelles that contain CD38, nor do we know the topology of CD38 (facing the cytosol or the matrix) on these intracellular organelles.

Raji and RA-Treated HL-60 Cell Nuclei Have Little CD38.

A previous report on CD38 localization used confocal immunofluorescence to show the presence of CD38 primarily within the nucleus of Raji cells (*15*). In fact, it was shown that CD38 colocalized in nuclear Cajal bodies, which are small subnuclear membraneless organelles present either free in the nucleoplasm and/or physically associated to specific regions of chromatin. However, using the activity-based probes for CD38, we found very little CD38 labeled within the nucleus, and certainly no concentrated areas of fluorescence that would represent active CD38 in Cajal bodies. In fact, the nucleus had the weakest CD38 labeling in both Raji cells and RA-treated HL-60 cells. Although we could not rule out the presence of catalytic inactive CD38, the results obtained with the K562 cells suggested that this was unlikely (discussed below). Our results thus suggested that very little CD38 is present in the nuclei of Raji and RA-treated HL-60 cells.

K562 Cells Do Not Have Detectable CD38 Expression.

It was reported on the basis of confocal immunofluorescence that K562 cells express intracellular CD38 but no plasma membrane CD38 (*15*). When labeling K562 cells with SR101−F-araNMN, we saw no fluorescence from confocal microscopy imaging on either the plasma membrane or within the cell. To rule out that SR101−F-araNMN was not permeable to K562 cells, we also labeled K562 whole cell lysates with SR101−F-araNMN. No fluorescent CD38 band was observed on SDS-PAGE gel, consistent with the confocal imaging results. This result was contrary to the reported exclusive intracellular localization of CD38. To resolve the conflicting observations, we first considered the possibility that K562 cells had CD38 that was catalytically inactive; and thus, CD38 could not be labeled with our probe. However, a Western blot experiment using a monoclonal CD38 antibody showed that K562 cells had no detectable

CD38 expression. Therefore, the labeling result with SR101−F-araNMN in K562 cells was reliable and revealed the absence of CD38 in K562 cells.

Antibodies vs Activity-Based Probes for Detecting the Intracellular Localization of CD38

The most commonly used methods to detect CD38 cellular localization are confocal microscopy coupled with immunofluorescence or GFP fusion. Using GFP fusion proteins requires the overexpression of the fusion proteins, which may cause artifacts due to the overexpression or the fusion. Immunofluorescence has the advantages of detecting endogenous proteins, but it requires the use of antibodies. CD38 antibodies are convenient tools to use in most applications. However, for detecting the intracellular localization of CD38, antibodies have some limitations. First, antibodies are not cell permeable; thus, the cells have to be fixed and permeablized before labeling with antibodies. Second, washing conditions have to be controlled well to wash away unbound antibodies but not antibodies that bind to the protein target. The potential problems can be fixed but require extra efforts to optimize experimental conditions. The reported prominent nuclear CD38 in Raji and K562 cells is possibly a false positive caused by insufficient washing, which could have been avoided if proper negative and positive controls were used to help find the optimal washing conditions (*15*). When inspecting the data on the immunofluorescence detection of CD38 in Raji and K562 cells, we noticed that there were no negative or positive controls provided. Nuclear membrane localization was also reported in other cell types (*20*, *29*). Immunofluorescence was the major method used in these studies reporting the nuclear membrane localization of CD38. These studies may also suffer from similar problems. Compared with immunofluorescence, our permeable CD38 probe has certain advantages that can complement the use of antibodies. First, the probe identifies catalytically active CD38, because labeling proceeds in an activity-dependent way while immunofluorescence is used to reveal total

protein levels. Second, the probe is cell permeable and thus does not require detergent permeabilization of cells to get inside the cell. Consequently, the labeling can be done under less perturbing conditions. Unfortunately, we had to fix cells to wash away unbound probe molecule. Optimization of the probes to allow aqueous buffer wash will be required for live-cell imaging. Third, the probe forms a rather stable covalent linkage with CD38; therefore, the washing step can be done very extensively to make sure all unbound CD38 probes are washed away. This way, fewer false positives will be observed. This is probably an important feature that allowed us to conclude that there is very little intracellular CD38. The availability of both a permeable and impermeable CD38 probe greatly facilitated the quantification of intracellular versus cell surface CD38, which is otherwise not easy to accurately quantify.

Conclusion

NAD is increasingly recognized as an important signaling molecule that regulates many physiologically important processes. Understanding the function of NAD-metabolizing enzymes, such as CD38, is thus important and can impact a variety of different areas. Ensuring proper cellular function requires the spatial distribution of different proteins to be delicately regulated. In the case of CD38, localization is similarly important to its biological function. Investigating its correct cellular localization will help to understand several unaddressed questions about the function of CD38. Early studies on CD38 focused on its ability to make cADPR and NAADP, which are considered important second messengers capable of releasing intracellular stored calcium. However, *in vitro*, the most efficient activity of CD38 is the hydrolysis of NAD, with k_{cat} of 96 s^{-1} and K_m of 16 μM (*30*). If CD38 is present in the nucleus as previously reported, it will likely deplete nuclear NAD. Using the permeable and impermeable CD38 probes, we found

that the nucleus actually contained the least amount of fluorescence, which we interpreted as the lack of CD38 in the nucleus. Considering the efficient NAD hydrolysis activity, we think the lack of nuclear CD38 actually makes sense; otherwise, intracellular NAD may be depleted. CD38-catalyzed formation of cADPR accounted for less than 2% of the total product. If this activity is physiologically important, it is possible that a certain intracellular pool of CD38 may have higher cyclase activity. CD38-catalyzed formation of NAADP *in vitro* requires low pH and high concentration of nicotinic acid. The low pH condition is only possible in certain acidic organelles, such as the lysosome. Thus, investigating the exact intracellular localization of CD38 will likely provide insights into the physiological relevance of different enzymatic activities of CD38. The activity-based probes we developed will allow the determination of intracellular localization of CD38 in different cells and thus enable a better understanding of the physiological function of CD38.

Experimental

General Methods

Reagents, unless specified otherwise, were purchased from commercial suppliers in the highest purity available and used as supplied. Antibodies for detection of human CD38 (mouse) were bought from BD Biosciences (San Jose, California, USA, cat. #: 611114), while antibodies for detection of human GAPDH (rabbit), as well as horseradish peroxidase-linked anti-mouse and anti-rabbit antibodies were bought from Cell Signaling (Danvers, MA, USA). Mammalian protein extraction reagent (M-PER) was bought from Pierce (Rockford, IL, USA). All-trans retinoic acid (RA), protease and phosphatase inhibitors were bought from Sigma (St. Louis, MO, USA). ECL was bought from GE Healthcare (Pittsburgh, PA, USA).

Both sulforhodamine and tetramethylrhodamine fluorescence signals from protein gels were recorded by Typhoon 9400 Variable Mode Imager (GE Healthcare Life Sciences). For visualization of tetramethylrhodamine, a green laser at 532 nm was used for excitation and a collection filter of 580 nm with band-pass of 30 nm was used for emission collection. For visualization of sulforhodamine, the 532 nm laser was used for excitation and 610BP30 filter for emission collection. Detection of fluorescence was done using a PMT at 650 V and normal sensitivity. Images collected were analyzed by ImageQuant TL v2005. ^{1}H NMR was performed on INOVA 400/500/600 spectrometers, ^{13}C NMR was performed on INOVA 400 spectrometer, and 2D NMR was performed on INOVA 500/600 spectrometers. NMR data was analyzed by MestReNova (version 8.1.1). ^{1}H NMR chemical shifts are reported in units of ppm relative to tetramethylsilane. ^{1}H NMR data are reported in the following manner: chemical shift (multiplicity, integration). LC-MS experiments were carried out on a Shimadzu HPLC LC20-AD and Thermo Scientific LCQ Fleet with a Sprite TARGA C18 column (40 × 2.1 mm, 5 μm, Higgins Analytical, Inc.) monitoring at 215 and 260 nm with positive mode for mass detection. Solvents for LC-MS were water with 0.1% acetic acid (solvent A) and acetonitrile with 0.1% acetic acid (solvent B). Compounds were eluted at a flow rate of 0.3 mL/min with 0% solvent B for 2 min, followed by a linear gradient of 0% to 10% solvent B over 2 min, followed by a linear gradient of 10% to 100% solvent B over 5 min, and finally 100% solvent B for 1 min before equilibrating the column back to 0% solvent B over 1 min. Preparative HPLC experiments were done on a Beckman Coulter System Gold 125p Solvent Module & 168 Detector with a TARGA C18 column (250 × 20 mm, 10 μm, Higgins Analytical, Inc.) monitoring at 215 and 260 nm. Solvents for prep HPLC were water with 0.1% trifluoroacetic acid (solvent A) and acetonitrile with 0.1% trifluoroacetic acid (solvent B). Compounds were eluted at a flow rate of 8.0 mL/min

with 0% solvent B for 10 min, followed by first a linear gradient of 0% to X% (X depends on different compounds) solvent B over X min, then a linear gradient of X% to 100% solvent B over 5 min, and finally 100% solvent B for 5 min before equilibrating the column back to 0% solvent B over 5 min.

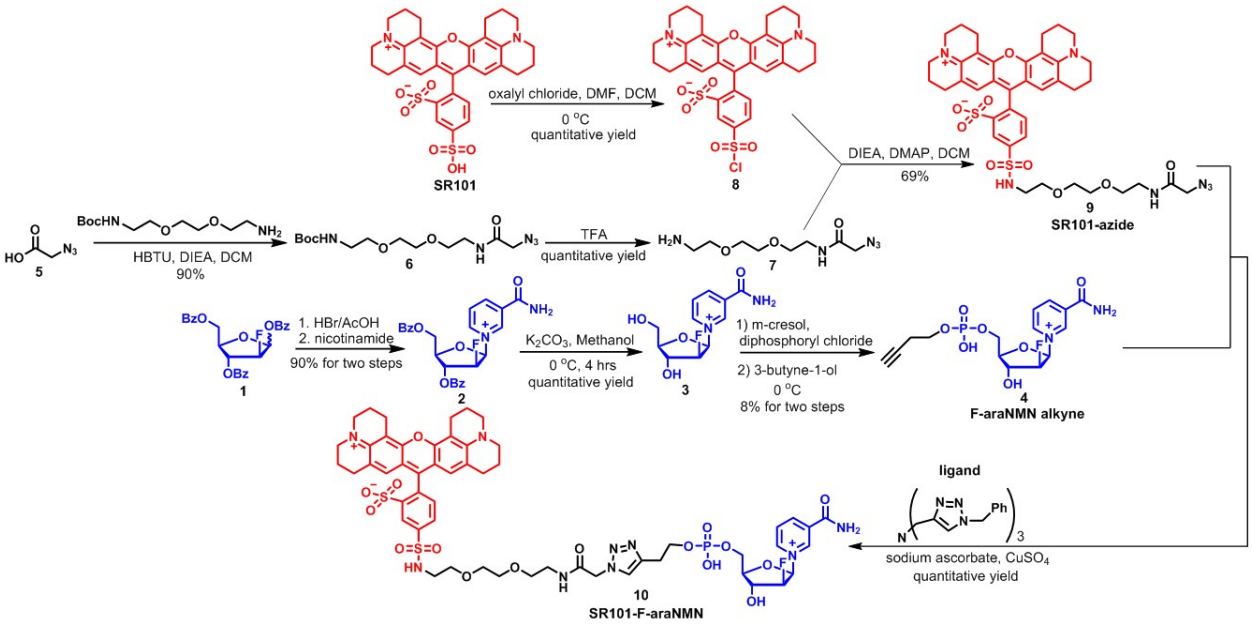

Figure 2.13. Detailed synthesis of SR101-F-araNMN.

1-((2R,3S,4R,5R)-4-(benzoyloxy)-5-((benzoyloxy)methyl)-3-fluorotetrahydrofuran-2-yl)-3-carbamoylpyridin-1-ium (2)

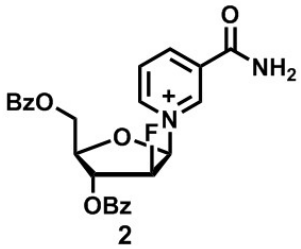

To a rt solution of (3S,4R,5R)-5-((benzoyloxy)methyl)-3-fluorotetrahydrofuran-2,4-diyl dibenzoate (**1**) (1.396 g, 3.0 mmol, 1.0 eq) in 10 mL of anhydrous DCM in a round-bottom flask fitted with a stir bar was added 33% HBr in acetic acid (2.2 mL, 37.1 mmol, 12.4 eq), whereupon the solution turned yellow. The reaction was stirred at rt overnight by which time the starting material had disappeared by TLC (5:1 EtOAc:hexanes). The homogeneous solution was washed using ice cold satd. $NaHCO_3$ (2 x 100 mL) and ice cold water (2 x 100 mL). The organic

layer was dried over anhydrous Na_2SO_4, filtered, then concentrated on a rotary evaporator and further dried under high vacuum. The resulting glycosyl bromide was used without further purification.

In a separate round bottom flask, nicotinamide (0.724 g, 5.93 mmol, 2.1 eq) was dissolved in 19.5 mL anhydrous acetonitrile by refluxing for 5 min under nitrogen. Once the solution cooled to rt, it was immediately transferred to the neat glycosyl bromide (1.17 g, 2.76 mmol). NOTE: the nicotinamide solution may begin to crystallize if not transferred immediately. The resulting heterogeneous mixture was stirred at rt overnight and became a homogeneous solution as the formation of product occurred. The solvent was evaporated on a rotary evaporator, and the product was purified by silica gel column chromatography (EtOAc to elute side product, 20:1 DCM: MeOH to elute nicotinamide, 10:1 DCM:MeOH to elute desired product). Compound 2 was obtained as a white solid (1.256 g, 90% yield). R_f was 0.3 in 10:1 CH_2Cl_2:CH_3OH. ^{1}H NMR (400 MHz, Methanol-d_4) δ 9.71 (s, 1H), 9.40 (dd, J = 6.4, 1.1 Hz, 1H), 9.12 (dt, J = 8.1, 1.5 Hz, 1H), 8.34 (dd, J = 8.1, 6.3 Hz, 1H), 8.21 – 8.13 (m, 2H), 8.13 – 8.03 (m, 2H), 7.72 – 7.66 (m, 1H), 7.65 – 7.57 (m, 1H), 7.58 – 7.51 (m, 2H), 7.47 (tt, J = 7.6, 1.5 Hz, 2H), 7.09 (dd, J = 18.0, 3.2 Hz, 1H), 6.00 (dd, J = 3.2, 1.3 Hz, 1H), 5.91 – 5.81 (m, 1H), 5.06 – 4.97 (m, 2H), 4.92 – 4.88 (m, 1H). LC-MS (ESI) calcd. for $C_{25}H_{22}FN_2O_6^+$ [M^+] 465.15, obsd. 465.08.

3-carbamoyl-1-((2R,3S,4R,5R)-3-fluoro-4-hydroxy-5-(hydroxymethyl)tetrahydrofuran-2 yl)pyridin-1-ium (3)

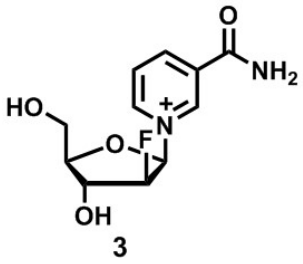

3

To a solution of **2** (415 mg, 0.89 mmol, 1.0 eq) in 9 mL anhydrous methanol in a round-bottom flask fitted with a stir bar was added K_2CO_3 (497 mg, 3.56 mmol, 4.0 eq) while under nitrogen and on ice. The resulting heterogeneous mixture was stirred for 5 h while kept on ice. The reaction mixture remained heterogeneous throughout the reaction time, but did change from colorless to yellow as the desired product (**3**) formed. The reaction was confirmed to be complete by detection of product and no detected starting material by LC-MS (260 nm). The undissolved K_2CO_3 was separated from the reaction mixture via vacuum filtration. The filtrate was concentrated on a rotary evaporator to afford an orange product, which was dissolved in water for purification by prep HPLC. Fractions collected were checked by LC-MS, and those that contained the desired product were pooled and lyophilized to afford **3** as a yellow solid (327 mg, 85% yield). Preparative HPLC: retention time t_R = 11 min with 0% solvent B until 18 min followed by a linear gradient of 0% - 10% solvent B over 11 min, then from 10% - 100% solvent B over 10 min. ^{1}H NMR (400 MHz, methanol-d_4) δ 9.78 (s, 1H), 9.44 (dd, *J* = 6.3, 1.2 Hz, 1H), 9.04 (dt, *J* = 8.0, 1.5 Hz, 1H), 8.28 (dd, *J* = 8.0, 6.3 Hz, 1H), 6.70 (dd, *J* = 8.1, 5.0 Hz, 1H), 5.48 (dt, *J* = 52.0, 5.0 Hz, 1H), 4.51 (ddd, *J* = 18.2, 6.2, 5.2 Hz, 1H), 4.21 (dt, *J* = 7.1, 3.5 Hz, 1H), 4.01 (ddd, *J* = 12.5, 3.3, 2.2 Hz, 1H), 3.88 (dd, *J* = 12.6, 3.7 Hz, 1H). LC-MS (ESI) calcd. for $C_{11}H_{14}FN_2O_4^+$ [M^+] 257.09, obsd. 257.00.

F-araNMN alkyne (4)

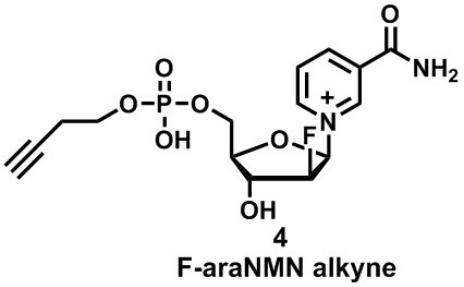

4
F-araNMN alkyne

A round-bottom flask fitted with a stir bar and containing compound **3** (39 mg, 0.15 mmol, 1.0 eq) was purged with nitrogen and put on ice. To it was added 1.5 mL *m*-cresol to dissolve compound **3**. While stirring the solution, diphosphoryl chloride (0.093 mL, 0.675 mmol, 4.5 eq) was added via pipettor to the flask. The reaction was stirred and kept on ice for 5 h while product formation was monitored by LC-MS (260 nm). After 5 h, compound **3** was not entirely consumed, based upon LC-MS mass detection. However, longer reaction times causes increased side product formation. Therefore, the cresol solution of crude phosphorylation product was immediately used for the next step in the synthesis.

3-Butyne-1-ol (2 mL) was added to a separate round-bottom flask that was purged with nitrogen and put on a mix of ice and sodium chloride to keep the temperature around -15 °C. The phosphorylation reaction mixture described above was slowly transferred via syringe to the round-bottom flask containing 3-butyne-1-ol while keeping the reaction temperature at -15 °C. Subsequently, the solution was kept on ice and was stirred for 4 h. **F-araNMN alkyne** formation was monitored by LC-MS (260 nm). After 4 hr, the reaction was quenched with cold water (10 mL), washed with ether (3 x 20 mL), and then purified by prep HPLC. Fractions collected from prep HPLC purification were checked by LC-MS and those containing the desired product were pooled and lyophilized to give the product as a white solid (3.77 mg, 8.0% yield). Preparative HPLC: t_R = 13.8 min with 0% solvent B until 20 min. Followed by a linear gradient of 0% - 100% solvent B over 10 min. ^{1}H NMR (599 MHz, Deuterium Oxide) δ 9.28 (s, 1H), 9.12 (d, *J* = 6.3 Hz, 1H), 8.83 (dt, *J* = 8.1, 1.4 Hz, 1H), 8.13 (dd, *J* = 8.0, 6.4 Hz, 1H), 6.58 (dd, *J* = 10.6, 4.5

Hz, 1H), 5.37 (dt, *J* = 51.2, 4.4 Hz, 1H), 4.47 (dt, *J* = 17.1, 4.9 Hz, 1H), 4.31 – 4.26 (m, 1H), 4.20 – 4.14 (m, 1H), 4.08 – 4.01 (m, 1H), 3.85 – 3.74 (m, 2H), 2.40 – 2.31 (m, 2H), 2.12 (t, 1H). ^{13}C NMR (151 MHz, Deuterium Oxide) δ 146.31, 143.50, 141.30, 128.18, 95.19, 94.00, 93.87, 84.00, 71.34, 63.88, 63.18, 63.17, 20.00. LC-MS (ESI) calcd. for $C_{15}H_{19}FN_2O_7P^+$ [M^+] 389.09, obsd. 389.08.

2-azidoacetic acid (5)

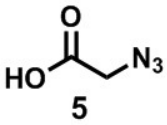

5

To a solution of sodium azide (4.677 g, 72 mmol, 2.0 eq) in 40 mL water in a round-bottom flask fitted with a stir bar at 0 °C was added 2-bromoacetic acid (5.0 g, 36 mmol, 1.0 eq). The reaction was stirred overnight at rt. The solution was acidified to pH 2 with 1 M HCl and then extracted with ether (3 x 75 mL). The combined ether extracts were dried using Na_2SO_4. The ether was evaporated, and product was obtained in quantitative yield. Compound **5** was used without further purification. ^{1}H NMR (300 MHz, Chloroform-*d*) δ 9.61 (s, 1H), 3.97 (s, 2H).

N-(2-(2-(2-aminoethoxy)ethoxy)ethyl)-2-azidoacetamide (6)

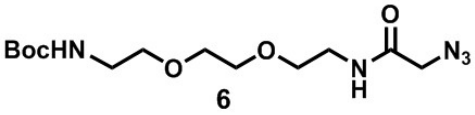

6

To a solution of **5** (202.12 mg, 2.0 mmol, 2.0 eq) in 15 mL DCM in a round-bottom flask fitted with a stir bar was added HBTU (758.5 mg, 2.0 mmol, 2.0 eq), DIEA (348 µL, 2.0 mmol, 2.0 eq) and the amine (*tert*-butyl (2-(2-(2-azidoacetamido)ethoxy)ethoxy)ethyl)carbamate (248.32 mg, 1.0 mmol, 1.0 eq, synthesized according to a reported method (*31*)). The homogeneous solution was stirred overnight at rt and monitored by TLC (DCM:MeOH 10:1, visualized using iodine). The reaction was quenched by adding water and the product was extracted with DCM (2 x 30 mL). The combined extracts were dried (Na_2SO_4), concentrated on a rotary evaporator and purified by

silica gel flash chromatography (DCM:MeOH 20:1). Compound **6** was obtained in 90% yield (298 mg). R_f was 0.4 in 10:1 DCM:MeOH.

N-(2-(2-(2-aminoethoxy)ethoxy)ethyl)-2-azidoacetamide (7)

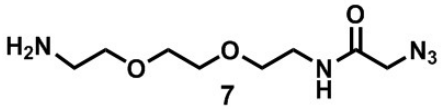

7

Compound **6** (200 mg, 0.60 mmol, 1.0 eq) was dissolved in 5 mL trifluoroacetic acid in a round-bottom flask fitted with a stir bar. The solution was stirred at room temperature for 1 h. The reaction was concentrated to yield product **7**, and **7** was used without further purification. LC-MS (ESI) calcd. for $C_8H_{18}N_5O_3$ $[(M+H)^+]$ 232.13, obsd. 232.08

SR101-chloride (8)

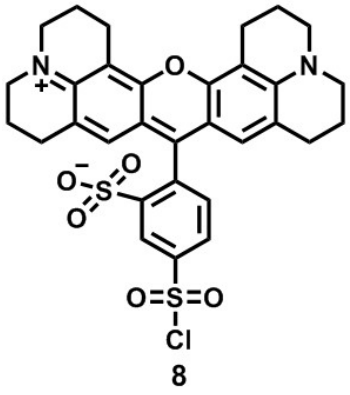

8

To a solution of **SR101** (50 mg, 0.082 mmol, 1.0eq) in 2 mL anhydrous DCM was added oxalyl chloride (0.031 mL, 0.412 mmol, 5 eq) and dimethylformamide (a few drops) in a flame-dried, round-bottom flask fitted with a stir bar while at 0 °C. The reaction was stirred overnight in a cold room (reaction kept cold in order to minimize double chloride substitution). Product formation was monitored using LC-MS (260 nm). The reaction was concentrated on a rotary evaporator and dried further using high vacuum to ensure removal of oxalyl choride. Product obtained was violet and used without any further purification.

SR101-azide (9)

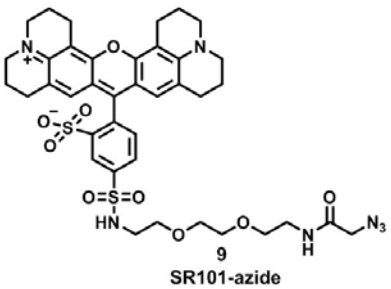

9
SR101-azide

To a solution of **7** (20 mg, 0.08 mmol, 1.0 eq) in 1 mL anhydrous DCM in a round-bottom flask fitted with a stir bar was added diisopropylethylamine (0.028 mL, 0.16 mmol, 2.0 eq)

with stirring. The resulting solution was then added to compound **8** (50 mg, 0.08 mmol, 1.0 eq) in a round-bottom flask fitted with a stir bar, followed by addition of DMAP (2 mg, 0.016 mmol). The solution was stirred overnight at rt. Product formation was monitored using LC-MS (260 nm). The reaction was concentrated on a rotary evaporator and purified by silica gel flash chromatography (DCM:MeOH 20:1). R_f was 0.45 in DCM:MeOH 20:1. Compound **9** (45 mg) was obtained in 69% yield as a violet solid. ^{1}H NMR (400 MHz, Chloroform-*d*) δ 8.83 (d, *J* = 1.9 Hz, 1H), 8.01 (dd, *J* = 7.9, 1.9 Hz, 1H), 7.88 – 7.74 (m, 1H), 7.19 (d, *J* = 7.9 Hz, 1H), 6.75 (s, 2H), 6.19 (t, *J* = 5.6 Hz, 1H), 3.75 (s, 2H), 3.62 (ddt, *J* = 13.8, 10.2, 5.2 Hz, 8H), 3.54 – 3.37 (m, 10H), 3.32 (q, *J* = 5.3 Hz, 2H), 3.08 – 2.93 (m, 4H), 2.84 – 2.56 (m, 4H), 2.16 – 2.02 (m, 4H), 2.02 – 1.86 (m, 4H). ^{13}C NMR (101 MHz, Chloroform-*d*) δ 168.01, 161.75, 161.41, 154.70, 152.07, 151.06, 146.85, 141.88, 134.51, 130.68, 127.65, 127.45, 126.89, 123.03, 113.43, 104.68, 77.36, 70.18, 70.08, 69.52, 69.21, 53.82, 51.83, 50.84, 50.35, 50.09, 43.05, 42.14, 39.14, 27.38, 20.56, 19.86, 19.72, 18.49, 18.46, 17.23, 17.21, 12.05, 12.02. LC-MS (ESI) calcd. for $C_{39}H_{46}N_7O_9S_2$ [$(M+H)^+$] 820.28, obsd. 820.64.

SR101-F-araNMN (10)

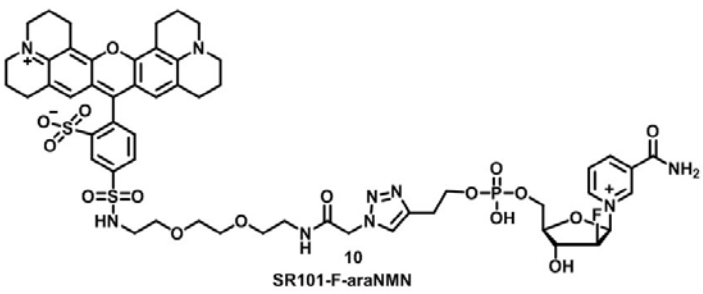

F-araNMN alkyne (101.6 µL of a 74.3 mM aqueous solution, 7.6 µmol), **SR101 azide** (2.0 mL of a 3.35 mM DMF solution, 6.7 µmol), Tris[(1-benzyl-1*H*-1,2,3-triazol-4-yl)methyl]amine (as ligand, 215.9 µL of an 100 mM DMF solution, 21.6 µmol), copper sulfate (1.080 mL of a 20 mM aqueous solution, 21.6 µmol), sodium ascorbate (1.727 mL of a 20 mM aqueous solution, 34.5 µmol) were added to DMF (500 µL) and water (500 µL) in that order in a

round-bottom flask fitted with a stir bar. The solution was stirred at rt overnight. Quantitative yield was determined from HPLC (260 nm) followed by purification by prep HPLC. Preparative HPLC: t_R = 43 min with a linear gradient of 0% - 35% solvent B from 10 – 25 min, then 35% - 50% solvent B from 25 – 50 min and 50% - 95% solvent B from 50 – 55 min. ^{1}H NMR (500 MHz, Methanol-d_4) δ 9.64 (s, 1H), 9.37 (s, 1H), 9.06 (d, *J* = 7.4 Hz, 1H), 8.66 (s, 1H), 8.40 – 8.16 (m, 2H), 8.16 – 8.01 (m, 1H), 7.44 (d, *J* = 7.9 Hz, 1H), 6.69 (dd, *J* = 10.2, 4.2 Hz, 1H), 6.63 (s, 2H), 5.42 (d, *J* = 51.7 Hz, 1H), 5.07 (s, 2H), 4.58 – 3.98 (m, 7H), 3.77 – 3.43 (m, 16H), 3.39 (t, *J* = 5.4 Hz, 2H), 3.26 (t, *J* = 5.2 Hz, 2H), 3.13 – 2.94 (m, 5H), 2.77 – 2.46 (m, 4H), 2.19 – 2.00 (m, 4H), 1.98 – 1.77 (m, 4H). LC-MS (ESI) calcd. for $C_{54}H_{64}FN_9O_{16}PS_2^+$ (M^+) 1208.36 and [(M^+)/2] 604.68, obsd. 604.92, 1208.42

***In Vitro* Labeling with Purified CD38 (wt and E226D, E226Q mutants) and SR101−F-araNMN**

CD38 (wt or E226D and E226Q mutants, 8 μM, expressed and purified as reported earlier (*32*, *33*)) and SR101−F-araNMN (20 μM) in 10 μL reaction buffer (25 mM HEPES, 50 mM NaCl, pH 7.4) were incubated at 37 °C for 30 min, then mixed with 2 μL 6× protein loading buffer. The samples were heated at 100 °C for 7 min and then resolved by SDS-PAGE. Before staining with Coomassie blue, the gel was irradiated under UV light (Transillum, Fisher Scientific, model DLT-A), and the fluorescence image was recorded with a digital camera (Nikon Coolpix L22).

Labeling of CD38 in Live Cells

HL-60 cells were treated with 1 μM RA in cell culture media (GIBCO RPMI Medium 1640 with 10% GIBCO Heat-inactivated Fetal Bovine Serum) for 24 h in a 5% CO_2 incubator at 37 °C. Untreated HL-60, Raji, and K562 cells were cultured using the same media without RA.

Then the cells were harvested from 4 mL cell culture (1×10^6 cells/mL) by centrifugation at 25 °C, 1200 rpm for 5 min. The cells were initially washed once using 500 μL PBS. Cells were resuspended in 100 μL PBS (reaction volume). In one experimental procedure, these cells were directly labeled with SR101−F-araNMN as detailed below to label all the CD38 molecules. In another experimental procedure, the cells were first treated with a nonfluorescent, cell-impermeable probe, 6-alkyne-F- araNAD, to block the cell surface CD38 before labeling intracellular CD38 with SR101−F-araNMN. 6-Alkyne-F-araNAD was added to a final concentration of 10 μM. After incubation at RT for 8 min, the cells were washed once with 500 μL PBS. Cells were resuspended in 100 μL PBS (reaction volume), and SR101−F-araNMN was added to a final concentration of 10 μM and allowed to incubate at RT for 8 min. The cells were then washed once with 500 μL cold PBS (PBS at 4 °C), followed by resuspending the cells in 1 mL cold methanol (methanol stored in −20 °C for at least 1 h prior to use), and samples were held at −20 °C for 10 min. Methanol was removed after centrifugation at 4 °C, 2000 rpm to pellet the cells. Cells were then resuspended in a fresh 1 mL of cold methanol (methanol at −20 °C) and incubated on ice for 40 min. Again, methanol was removed and cells were washed once with 500 μL fresh, cold PBS (PBS at 4 °C) to ensure removal of methanol. Finally, cells were resuspended in 100 μL of PBS. Then, 10 μL PBS containing the cell suspension was applied onto a microscope slide and covered with a micro cover glass. Confocal images (8 line average) of cells were acquired with a Zeiss LSM 710 confocal microscope with a 63×/1.4 oil immersion objective. Green 561 nm (15mW DPSS laser, laser power percentage given in the figure captions) was used for sulforhodamine (SR) fluorescence. Emission signal in the range of 566−717 nm (SR emission) was detected.

In-Gel Fluorescence Analysis of CD38 Intracellular Localization

Lysis buffer recipe: Tris-HCl pH 7.9 (25 mM), NaCl (150 mM), glycerol (10%), Igepal (1%), 25 μL protease inhibitor cocktail (PIC, Sigma-Aldrich, #P8340)/500 uL, PMSF (0.5 mM), EDTA pH 8.0 (5 mM).

HL-60 cells were treated with 1 μM RA in cell culture media for 24 h in a 5% CO_2 incubator at 37 °C. Raji and K562 cells were not treated with RA. Untreated HL-60, Raji, and K562 cells were cultured using the same media except for being used without any added treatment. A similar number of cells were used for both live cell and whole cell lysate in-gel fluorescent labeling by first counting the cells before harvesting the cells by centrifugation at 25 °C, 1200 rpm, for 5 min. Cells were washed twice with 1 mL PBS. From this point, one batch of cells was lysed to obtain whole cell lysate followed by fluorescent labeling, and to the other batch of cells fluorescent labeling was done first, followed by obtaining the whole cell lysate. To label live cells, the cells were first suspended in 100 μL PBS (reaction volume) and fluorescent molecule – either SR101−F-araNMN or Rh-6-(F-araNAD) – was added to a final concentration of 10 μM. Then the sample was kept at RT for about 8 min, followed by centrifugation at 4 °C, 1500 rpm, for 3 min. Cells were washed twice using 500 μL cold PBS (PBS at 4 °C). PBS was removed prior to addition of about 30 μL lysis buffer followed by freeze/thaw lysis (the samples were frozen at −80 °C and then removed from −80 °C and thawed on ice for ∼30 min while vortexing briefly every 5 min). Once samples were fully thawed on ice, they were centrifuged at 4 °C, 14,000 rpm, for 6 min to collect the supernatant (proteins solubilized by detergent in lysis buffer). Protein concentration in the cell lysate was determined using the Bradford assay, and 25 μg of lysate was resolved by SDS-PAGE. In the case of collecting whole cell lysate followed by fluorescent labeling, the cells were washed with PBS and resuspended in 30 μL lysis buffer, and

then the whole cell lysates were collected as described above. Protein concentration in the cell lysate was determined using the Bradford assay. Once protein concentration was determined, stock lysate was diluted to 2.5 μg/μL, and 10 μL of the diluted lysates was mixed with the fluorescent molecule to give a final 10 μM labeling concentration. The fluorescent labeling reaction was quenched using 2 μL of 6× SDS containing protein loading buffer. The samples were heated at 100 °C for 7 min and then resolved by SDS-PAGE. Before staining with Coomassie blue, the fluorescence image of the gel was recorded by a Typhoon 9400 Variable Mode Imager with settings of green laser at 532 nm and emission collection filter of 580BP30 (rhodamine) and 610BP30 (sulforhodamine). Detection was done using PMT650 V (normal sensitivity), and data was analyzed by ImageQuant TL v2005.

Western Blot Analysis

Cell cultures were seeded at 0.2×10^6 cells/mL, and those that received RA were treated at a concentration of 1 μM. After 48 h, cells were washed twice with PBS before being lysed by adding 400 μL of a lysis buffer consisting of M-PER with 1:100 (v/v) dilutions of protease inhibitors and phosphatase inhibitors, and the cells were placed on ice for 30 min. The lysate was then spun at 4 °C, 13,000 rpm, for 30 min, and supernatant was saved and used for analysis. Then, 25 μg of protein lysate was loaded per lane and resolved by SDS-PAGE analysis and transferred to PVDF membrane. Membranes were then blocked for 1 h in a solution of 5% dry nonfat milk in PBS-Tween before probing with 1:1000 (v/v) dilutions of antibody in 5% BSA in PBS-Tween overnight at 4 °C. Membranes were probed with 1:1000 (v/v) dilutions of secondary antibody in 5% BSA in PBS-Tween for 1 h at RT before visualizing with ECL. Blots shown are representative of at least three independent repeats.

Fluorescent labeling of purified CD38 with SR101-F-araNMN *in vitro*

CD38 (1 μM) and fluorescent probe (either SR101-F-araNMN or Rh-F-araNAD, at 10 μM) in 10 μL reaction buffer (25 mM HEPES, 50 mM NaCl, pH 7.4) were incubated at room temperature. To determine whether NAD or nicotinamide affected fluorescent labeling efficiency, NAD (1 mM) or nicotinamide (100 μM) was added simultaneously with SR101-F-araNMN to the reaction mixture. Then, samples were mixed with 2 μL 6x protein loading buffer to quench the reaction at specific time points. The samples were heated at 100°C for 10 min and then resolved by SDS-PAGE. Before staining with Coomassie blue, the fluorescence image of the gel was recorded using a Typhoon 9400 Variable Mode Imager with settings of Green laser at 532 nm and emission collection filter of 610BP30. Detection was done using an approximate PMT650V (normal sensitivity), and data was analyzed by ImageQuant TL v2005.

In-gel fluorescence analysis of intracellular CD38 using 6-alkyne-F-araNAD and SR101-F-araNMN

Lysis buffer recipe: Tris-HCl pH 7.9 (25 mM), NaCl (150 mM), Glycerol (10%), Igepal (1%), 25 uL protease inhibitor cocktail (PIC, Sigma-Aldrich, #P8340)/500 uL, PMSF (1.0 mM), EDTA pH 8.0 (5 mM).

HL-60 cells were treated with 1 μM RA in cell culture media for 24 h in a 5% CO_2 incubator at 37 °C. Raji cells were not treated with RA. Untreated HL-60 and Raji cells were cultured using the same media except that no RA was used. Cells were harvested by centrifugation at 25 °C, 1500 rpm for 5 min. The cell pellet was washed with 1 mL of PBS. The cells were resuspended in 100 μL PBS and 6-alkyne-F-araNAD was added to a final concentration of 10 μM. Following incubation, the cells were collected at 25 °C, 2000 rpm for 2 min. Then, the reaction mixture was removed. The cell pellet was washed once with PBS to

remove any residual 6-alkyne-F-araNAD. The 6-alkyne-F-araNAD incubation was not done for those samples that only received SR101-F-araNMN labeling. Cells were resuspended in 100 µL of fresh PBS (reaction volume), and SR101-F-araNMN was added to a final concentration of 10 µM and allowed to incubate at RT for 8 min. Following incubation, cells were collected by centrifugation at 25 °C, 2000 rpm for 2 min. The cell pellet was washed twice using 1 mL of PBS. Then, about 30 µL lysis buffer followed by freeze/thaw lysis (the samples were frozen at -80 °C and then removed from -80 °C and thawed on ice for ~30 min while vortexing briefly every 5 min). Once samples were fully thawed on ice, centrifuge at 4 °C, 14,000 rpm for 10 min to collect the supernatant (proteins solubilized by detergent in lysis buffer). Protein concentration in the cell lysate was determined using the Bradford assay, and protein lysate was mixed with 2 µL of 6x SDS-containing protein loading buffer. The samples were heated at 100 °C for 10 min and then resolved by SDS-PAGE. Before staining with Coomassie blue, the fluorescence image of the gel was recorded using a Typhoon 9400 Variable Mode Imager with settings of Green laser at 532 nm and emission collection filter of 610BP30 (sulforhodamine). Data was analyzed using ImageQuant TL v2005.

SR101-F-araNMN labeling of CD38 in live Raji cells followed by fixation with PFA and methanol

Raji cells were kept in cell culture media (GIBCO RPMI Medium 1640 with 10% GIBCO Heat-inactivated Fetal Bovine Serum) in a 5% CO_2 incubator at 37 °C. The cells were harvested from 4 mL cell culture (1×10^6 cells/mL) by centrifugation at 25 °C, 1500 rpm for 5 min. The cell pellet was washed using 1 ml of PBS. Cells were suspended in 100 µL PBS (reaction volume). In one experimental procedure, these cells were directly incubated with 10 µM SR101-F-araNMN at RT for 8 min to label all the CD38 molecules. In another experimental

procedure, the cells were first treated with the non-fluorescent and cell impermeable probe, 6-alkyne-F-araNAD at 10 μM at RT for 8 min, to block the cell surface CD38. Following incubation with 6-alkyne-F-araNAD, cells were collected by centrifugation at 25 °C, 2000 rpm for 2 min. The cell pellet was washed using 1 mL of PBS. Then, cells were suspended in 100 μL fresh PBS (reaction volume), and SR101-F-araNMN was added to a final concentration of 10 μM and allowed to incubate at RT for 8 min. For both experiments, after incubation with SR101-F-araNMN, the cells were washed twice using 1 mL cold PBS (PBS at 4 °C) and then suspended in 1 mL of 2% paraformaldehyde (PFA). Cells suspended in PFA were left on ice for 5 min followed by 10 min at RT. Following PFA fixation, cells were collected by centrifugation at 4 °C, 2000 rpm for 4 min. Cells were washed three times with 1 mL cold PBS (PBS at 4 °C) to wash away PFA. Finally, cells were suspended in 1 mL of cold methanol (methanol stored in -20 °C for at least 1 h prior to use) and held at -20 °C for 2 min. Methanol was removed by centrifugeation at 4 °C, 2500 rpm for 5 min. Cells were then suspended in fresh 1 mL of cold methanol (stored in -20 °C for at least 1 h prior to use) and incubated on ice for 40 min. Methanol was then removed by centrifugation at 4 °C, 2500 rpm for 5 min. Cells were washed once with 1 mL cold PBS (PBS at 4 °C). Finally, cells were suspended in 100 μL of PBS. Then, 10 μL of the cell suspension was applied onto a microscope slide and covered with a micro cover glass. Confocal images (8 line average) of cells were acquired with a Zeiss LSM 710 Confocal Microscope with a 63x/1.4 oil immersion objective. Green 561 nm (DPSS laser) was used for sulforhodamine (SR) fluorescence. Emission signals in the range of 566-717 nm (SR emission) were detected.

Subcellular fractionation of Raji and RA-treated HL-60 cell lysates and detection of CD38 in different subcellular fractions

All buffers were supplemented with 1x protease inhibitor cocktail (PIC, Sigma-Aldrich, #P8340), 1 mM PMSF and 1 mM DTT before use. Recipes for the buffers used within the protocol include: **buffer 1** – Sucrose (250 mM), Tris-HCl pH 7.9 (50 mM), $MgCl_2$ (5 mM); **buffer 2a** – Sucrose (1 M), Tris-HCl pH 7.9 (50 mM), $MgCl_2$ (5 mM); **buffer 2b** – Sucrose (2 M), Tris-HCl pH 7.9 (50 mM), $MgCl_2$ (5 mM); buffer 4 – HEPES (20 mM), $MgCl_2$ (1.5 mM), NaCl (0.5 M), EDTA (0.2 mM), Glycerol (20%), Triton X-100 (1%); **buffer 3** – Tris-HCl pH 7.9 (20 mM), NaCl (0.4 M), Glycerol (15%), Triton X-100 (1.5%).

HL-60 cells were treated with 1 μM RA in cell culture media for 24 h in a 5% CO_2 incubator at 37 °C. Raji cells were not treated with RA. Both Raji and RA treated HL-60 cells (~3.0 x 10^7) were washed twice with PBS and pelleted for 4 min at 500 g. The cell pellet was suspended in 1 ml **buffer 1** and cell lysis was performed by slowly pushing lysate through a 25 gauge needle. To ensure cell lysis has occurred, 10 uL of the lysate was loaded onto a hemocytometer and examined under an optical microscope. The suspension was centrifuged at 800 g for 15 min to obtain supernatant 1 and pellet 1. Supernatant 1 was centrifuged again at 1,000 x g for 15 min to obtain supernatant 2 and pellet 2. Supernatant 2 was saved to isolate the cytosolic and membrane proteins, whereas pellet 2 was discarded. Pellet 1 was dissolved in 1 mL **buffer 1** and centrifuged at 1,000 x g for 15 min to obtain supernatant 3 and pellet 3. Supernatant 3 was added to supernatant 2 for isolating cytosolic and membrane proteins and stored on ice until later use. Pellet 3 (used to isolate nuclei) was suspended in 1 ml **buffer 2a** and layered onto a 3 ml cushion of **buffer 2b** in a 5.0 mL ultracentrifuge tube (thinwall polyallomer tube, Beckman Coulter cat. #: 326819). Afterwards, swing-bucket ultracentrifugation (Beckman

Coulter SW 55 Ti rotor) at 80,000 x g for 35 min was carried out to obtain supernatant 4 and pellet 4. Pellet 4 (the nuclear pellet) was taken up in **buffer 4** and incubated 1 h while on a rotating mixer at 4 °C. Then, the suspension was slowly passaged 20 times through a 25 gauge needle followed by centrifugation at 9,000 x g for 30 min to obtain supernatant 5 and pellet 5. Supernatant 5 contained the nuclear proteins. Pellet 5 was discarded. The pooled supernatants 2 and 3 were centrifuged for 1 h at 100,000 x g in a swing-bucket (SW 55 Ti rotor) ultracentrifuge to obtain supernatant 6 and pellet 6. Supernatant 6 contained the cytosolic proteins. Pellet 6 was dissolved in **buffer 3** and incubated 1 h while on a rotating mixer at 4 °C. The suspension was centrifuged at 9,000 x g for 30 min to obtain supernatant 7 and pellet 7. Supernatant 7 contained the membrane proteins. Pellet 7 was discarded. Then, 2.0% of the total protein from each fraction was resolved by SDS-PAGE analysis and transferred to a PVDF membrane. Membranes were then blocked for 1 h in a solution of 5% dry non-fat milk in TBS-Tween before probing with primary antibody in 5% dry non-fat milk in TBS-Tween for 1 h at RT. Membranes were probed with secondary antibodies in TBS-Tween for 1 h at RT before visualizing with ECL. Antibodies used for the Western blotting include: mouse anti-human CD38 from BD Biosciences (cat. #: 611114) used at 1/2000 dilution (v/v), Histone H3 (nuclear protein marker) antibody from Cell Signaling (cat. #: 9715) used at 1/5000 dilution (v/v), Na+/K+ ATPase (membrane protein marker) antibody from Cell Signaling (cat. #: 3010) used at 1/1000 dilution (v/v), as well as horseradish peroxidase-linked anti-mouse and anti-rabbit antibodies from Santa Cruz (cat. #: sc-2005 and sc-2004, respectively).

REFERENCES

1. Houtkooper, R. H., Cantó, C., Wanders, R. J., and Auwerx, J. (2010) The secret life of NAD^+: An old metabolite controlling new metabolic signaling pathways, *Endocrine Reviews 31*, 194-223.
2. Lin, H. (2007) Nicotinamide adenine dinucleotide: beyond a redox coenzyme, *Org. Biomol. Chem. 5*, 2541-2554.
3. Partida-Sanchez, S., Cockayne, D. A., Monard, S., Jacobson, E. L., Oppenheimer, N., Garvy, B., Kusser, K., Goodrich, S., Howard, M., Harmsen, A., Randall, T. D., and Lund, F. E. (2001) Cyclic ADP-ribose production by CD38 regulates intracellular calcium release, extracellular calcium influx and chemotaxis in neutrophils and is required for bacterial clearance in vivo, *Nat Med 7*, 1209-1216.
4. Jin, D., Liu, H. X., Hirai, H., Torashima, T., Nagai, T., Lopatina, O., Shnayder, N. A., Yamada, K., Noda, M., Seike, T., Fujita, K., Takasawa, S., Yokoyama, S., Koizumi, K., Shiraishi, Y., Tanaka, S., Hashii, M., Yoshihara, T., Higashida, K., Islam, M. S., Yamada, N., Hayashi, K., Noguchi, N., Kato, I., Okamoto, H., Matsushima, A., Salmina, A., Munesue, T., Shimizu, N., Mochida, S., Asano, M., and Higashida, H. (2007) CD38 is critical for social behaviour by regulating oxytocin secretion, *Nature 446*, 41-45.
5. D'Arena, G., Musto, P., Cascavilla, N., Dell'Olio, M., Di Renzo, N., Perla, G., Savino, L., and Carotenuto, M. (2001) CD38 expression correlates with adverse biological features and predicts poor clinical outcome in B-cell chronic lymphocytic leukemia, *Leuk Lymphoma 42*, 109-114.
6. States, D. J., Walseth, T. F., and Lee, H. C. (1992) Similarities in amino acid sequences of Aplysia ADP-ribosyl cyclase and human lymphocyte antigen CD38, *Trends Biochem Sci 17*, 495.
7. Howard, M., Grimaldi, J. C., Bazan, J. F., Lund, F. E., Santos-Argumedo, L., Parkhouse, R. M., Walseth, T. F., and Lee, H. C. (1993) Formation and hydrolysis of cyclic ADP-ribose catalyzed by lymphocyte antigen CD38, *Science 262*, 1056-1059.
8. Kim, H., Jacobson, E. L., and Jacobson, M. K. (1993) Synthesis and degradation of cyclic ADP-ribose by NAD glycohydrolases, *Science 261*, 1330-1333.
9. Lee, H. C., Zocchi, E., Guida, L., Franco, L., Benatti, U., and De Flora, A. (1993) Production and hydrolysis of cyclic ADP-ribose at the outer surface of human erythrocytes, *Biochem Biophys Res Commun 191*, 639-645.
10. Takasawa, S., Tohgo, A., Noguchi, N., Koguma, T., Nata, K., Sugimoto, T., Yonekura, H., and Okamoto, H. (1993) Synthesis and hydrolysis of cyclic ADP-ribose by human leukocyte antigen CD38 and inhibition of the hydrolysis by ATP, *J Biol Chem 268*, 26052-26054.
11. Chini, E. N., Chini, C. C., Kato, I., Takasawa, S., and Okamoto, H. (2002) CD38 is the major enzyme responsible for synthesis of nicotinic acid-adenine dinucleotide phosphate in mammalian tissues, *Biochem J 362*, 125-130.
12. Zubiaur, M., Fernandez, O., Ferrero, E., Salmeron, J., Malissen, B., Malavasi, F., and Sancho, J. (2002) CD38 is associated with lipid rafts and upon receptor stimulation leads to Akt/protein kinase B and Erk activation in the absence of the CD3-zeta immune receptor tyrosine-based activation motifs, *J Biol Chem 277*, 13-22.

13. Khoo, K. M., and Chang, C. F. (2002) Identification and characterization of nuclear CD38 in the rat spleen, *Int J Biochem Cell Biol 34*, 43-54.
14. Yalcintepe, L., Albeniz, I., Adin-Cinar, S., Tiryaki, D., Bermek, E., Graeff, R. M., and Lee, H. C. (2005) Nuclear CD38 in retinoic acid-induced HL-60 cells, *Exp Cell Res 303*, 14-21.
15. Trubiani, O., Guarnieri, S., Eleuterio, E., Di Giuseppe, F., Orciani, M., Angelucci, S., and Di Primio, R. (2008) Insights into nuclear localization and dynamic association of CD38 in Raji and K562 cells, *J Cell Biochem 103*, 1294-1308.
16. Orciani, M., Trubiani, O., Guarnieri, S., Ferrero, E., and Di Primio, R. (2008) CD38 is constitutively expressed in the nucleus of human hematopoietic cells, *J Cell Biochem 105*, 905-912.
17. Ceni, C., Pochon, N., Brun, V., Muller-Steffner, H., Andrieux, A., Grunwald, D., Schuber, F., De Waard, M., Lund, F., Villaz, M., and Moutin, M. J. (2003) CD38-dependent ADP-ribosyl cyclase activity in developing and adult mouse brain, *Biochem J 370*, 175-183.
18. Reinherz, E. L., Kung, P. C., Goldstein, G., Levey, R. H., and Schlossman, S. F. (1980) Discrete stages of human intrathymic differentiation: analysis of normal thymocytes and leukemic lymphoblasts of T-cell lineage, *Proc Natl Acad Sci U S A 77*, 1588-1592.
19. Yamada, M., Mizuguchi, M., Otsuka, N., Ikeda, K., and Takahashi, H. (1997) Ultrastructural localization of CD38 immunoreactivity in rat brain, *Brain Res 756*, 52-60.
20. Adebanjo, O. A., Anandatheerthavarada, H. K., Koval, A. P., Moonga, B. S., Biswas, G., Sun, L., Sodam, B. R., Bevis, P. J., Huang, C. L., Epstein, S., Lai, F. A., Avadhani, N. G., and Zaidi, M. (1999) A new function for CD38/ADP-ribosyl cyclase in nuclear Ca2+ homeostasis, *Nat Cell Biol 1*, 409-414.
21. Zhao, Y. J., Lam, C. M., and Lee, H. C. (2012) The membrane-bound enzyme CD38 exists in two opposing orientations, *Sci Signal 5*, ra67.
22. Moreno-Garcia, M. E., Sumoza-Toledo, A., Lund, F. E., and Santos-Argumedo, L. (2005) Localization of CD38 in murine B lymphocytes to plasma but not intracellular membranes, *Mol Immunol 42*, 703-711.
23. Jiang, H., Congleton, J., Liu, Q., Merchant, P., Malavasi, F., Lee, H. C., Hao, Q., Yen, A., and Lin, H. (2009) Mechanism-based small molecule probes for labeling CD38 on live cells, *J Am Chem Soc 131*, 1658-1659.
24. Kolb, H. C., Finn, M. G., and Sharpless, K. B. (2001) Click Chemistry: Diverse Chemical Function from a Few Good Reactions, *Angew Chem Int Ed Engl 40*, 2004-2021.
25. Lamkin, T. J., Chin, V., Varvayanis, S., Smith, J. L., Sramkoski, R. M., Jacobberger, J. W., and Yen, A. (2006) Retinoic acid-induced CD38 expression in HL-60 myeloblastic leukemia cells regulates cell differentiation or viability depending on expression levels, *J Cell Biochem 97*, 1328-1338.
26. Schnell, U., Dijk, F., Sjollema, K. A., and Giepmans, B. N. (2012) Immunolabeling artifacts and the need for live-cell imaging, *Nat Methods 9*, 152-158.
27. Rockstroh, M., Muller, S., Jende, C., Kerzhner, A., Bergen, M., and Tomm, J. (2011) Cell fractionation - an important tool for compartment proteomics, *Journal of Integrated Omics 1*, 135-143.
28. Cox, B., and Emili, A. (2006) Tissue subcellular fractionation and protein extraction for use in mass-spectrometry-based proteomics, *Nat Protoc 1*, 1872-1878.

29. Khoo, K. M., Han, M. K., Park, J. B., Chae, S. W., Kim, U. H., Lee, H. C., Bay, B. H., and Chang, C. F. (2000) Localization of the cyclic ADP-ribose-dependent calcium signaling pathway in hepatocyte nucleus, *J Biol Chem 275*, 24807-24817.
30. Sauve, A. A., Munshi, C., Lee, H. C., and Schramm, V. L. (1998) The reaction mechanism for CD38. A single intermediate is responsible for cyclization, hydrolysis, and base-exchange chemistries, *Biochemistry 37*, 13239-13249.
31. Marom, H., Miller, K., Bechor-Bar, Y., Tsarfaty, G., Satchi-Fainaro, R., and Gozin, M. (2010) Toward development of targeted nonsteroidal antiandrogen-1,4,7,10-tetraazacyclododecane-1,4,7,10-tetraacetic acid-gadolinium complex for prostate cancer diagnostics, *J Med Chem 53*, 6316-6325.
32. Liu, Q., Kriksunov, I. A., Graeff, R., Munshi, C., Lee, H. C., and Hao, Q. (2005) Crystal structure of human CD38 extracellular domain, *Structure 13*, 1331-1339.
33. Munshi, C., Aarhus, R., Graeff, R., Walseth, T. F., Levitt, D., and Lee, H. C. (2000) Identification of the enzymatic active site of CD38 by site-directed mutagenesis, *J Biol Chem 275*, 21566-21571.

Chapter 3

Evaluating the Contribution from CD38 Dimerization to MAPK Signaling Using Small Molecule Probes of CD38

Abstract

Cells use signaling to adapt to the environment; thus, the role for CD38 as a signaling receptor protein deserves careful investigation. An important biological function can be attributed to the role for CD38 as a receptor in mitogen-activated protein kinase (MAPK) signaling for retinoic acid (RA) induced cell differentiation in the human myeloblastic leukemia cell line (HL-60). CD38 is a type II transmembrane protein that was first identified as a T-cell differentiation marker, but a receptor function was later identified in MAPK signaling. RA is a commonly used treatment, which induces remission in patients with acute promyelocytic leukemia (APL) by activation of MAPK signaling that leads to cell differentiation and G_0 cell cycle arrest. In this process, CD38 is an early expression marker of cell differentiation, and CD38 is a transmembrane protein that is an integral part of sustaining an intracellular signaling complex – c-Cbl and the Raf/MEK/ERK MAPK signaling axis – to drive cellular differentiation. However, it is not clear how CD38 induces MAPK signaling. Here, we report the synthesis and application of dimeric small molecules capable of dimerizing the cell surface CD38 to test whether CD38 dimerization is sufficient to induce MAPK signaling. The dimeric small molecules have two CD38 binding portions – either F-araNMN or F-araNAD – and a linker that controls the induced CD38 dimer conformation. Using these dimeric small molecules, we show that cell surface CD38 dimer formation affects the intracellular phosphorylation levels of key

MAPK signaling proteins, suggesting that CD38 dimerization alone can induce MAPK signaling. Further experiments are required to determine whether increased phosphorylation of MAPK signaling proteins correlates to a sustained MAPK signal that is required for an enhanced and accelerated RA-induced cell differentiation. If so, small molecules such as the ones we synthesized may ultimately be found to be more effective in promoting cell differentiation than the current RA-induced therapy.

Introduction

CD38 was initially identified as a cell surface marker on various hematologic cells (*1*). Subsequent studies on CD38 revealed that binding from the IB4 monoclonal antibody (mAb) caused activation of signaling pathways for proliferation in preparations of human peripheral blood mononuclear cells (PBMC); thus revealing a receptor function (*2*). Presumably, the effects induced by antibody binding would mimic those induced by a putative ligand. Consequently, follow-up studies identified CD31 as the non-substrate putative ligand after observing $CD38^{+}$ human T lymphocytes tended to adhere to endothelial cells having CD31 (*3*). Both the signaling cascade and biological effects seen from mAb binding were recapitulated with CD31 interacting with CD38 and has been analyzed within normal and pathological conditions (*4-6*).

Cellular signaling is critical for cellular adaptation to the environment; thus, the role for CD38 as a signaling receptor deserves careful investigation. In particular, the role for CD38 as a receptor in mitogen-activated protein kinase (MAPK) signaling for retinoic acid (RA) induced cell differentiation in the human myeloblastic leukemia cell line (HL-60) (*7*) is investigated further within this report. Acute promyelocytic leukemia (APL) is a cancer that has a characteristic accumulation of immature (non-differentiating) granulocytes due to the

impairment of cell differentiation mechanisms. Retinoic acid is a metabolite of vitamin A (retinol) that mediates gene transcription, and RA is a frequently used treatment, which induces remission in patients with APL by causing leukemic-cell differentiation (*8*). Therefore, treatment with RA that mediates gene transcription for cell differentiation restores the terminal maturation of leukemia cells resulting in these cells having a limited lifespan rather than continuing to proliferate in the immature state (*9*). RA-mediated gene transcription occurs via RA binding to the retinoid receptors, RAR and RXR, resulting in receptor dimerization. The receptor dimerization is followed by binding of transcription factors to DNA regions (retinoic acid response elements), resulting in transcriptional modulation of the gene through chromatin remodeling and recruitment of other transcription machinery (*10*). The CD38 gene spans more than 62 kilobases (kb) and consists of eight exons and seven introns of heterogenous length with the first and longest intron (>20 kb) containing a retinoic acid response element. Thus, addition of RA is responsible for CD38 up-modulation of expression (*11*). The role of CD38 in RA-induced cell differentiation and cell cycle arrest has been studied in HL-60 cells. HL-60 cells have been an archetype *in vitro* model for studying the mechanism of retinoic acid. The HL-60 cell line is an immature precursor cell line that is uncommitted with respect to differentiation lineage; consequently, it can be induced to undergo myeloid or monocytic differentiation and G_0 cell cycle arrest. During RA-induced differentiation, studies have shown that CD38 is an early receptor expressed, and it contributes to propulsion of RA-induced differentiation and growth arrest that is dependent on its expression levels (*7*). This study showed that decreased CD38 expression reduces downstream differentiation; while enhancing CD38 expression by ectopic expression enhances RA-induced differentiation. Thus, CD38 is needed to propel differentiation. CD38 mediates this response via the MAPK pathway. It has been reported that CD38 causes Raf

activation and can cause tyrosine phosphorylation of key MAPK signaling target molecules, such as extracellular signal-regulated protein kinase (ERK) and c-Cbl (*12-14*). The details of ligand binding to CD38 and CD38 interactions on the plasma membrane in initiating MAPK signaling are still left to be understood. Research that provides understanding of these interactions could lead to enhanced RA-induced differentiation and improved therapy for leukemia.

Here, we investigate whether CD38 dimerization – caused by small molecules – is sufficient to induce MAPK signaling and cause a sustained MAPK signal capable of accelerating and enhancing RA-induced cell differentiation in HL-60 cells. CD38 has only a single transmembrane domain along with a very short 20 amino acid cytoplasmic tail. Therefore, in order to accommodate the initial cytoplasmic MAPK signaling complex, CD38 probably needs to be physically associated with either other cell surface proteins or other cell receptors to modulate intracellular MAPK signaling. A few reports in support of CD38 interacting with other receptors on the cell surface include: the B-cell receptor on B cells (*15*), T-cell receptor on T cells (*16*), and CD32 on myeloid cells (*17, 18*). Then, in support of stereospecific dimerization between two CD38 molecules being required to induce signaling are antibodies – HB7 and OKT10 – that both bind CD38; however, HB7 can induce intracellular signaling while OKT10 cannot. Antibodies are bivalent and should cause dimerization of two CD38 molecules. Structural analysis of CD38 with HB7 and OKT10 revealed that upon binding to CD38, a different CD38 dimer conformation is induced (*19*). Thus, the explanation for this observation is that the antibody inducing the CD38 dimer with the proper distance and orientation produces the CD38 signal.

To further study whether CD38 dimerization induces MAPK signaling and subsequent enhancememnt of RA-induced cell differentiation, we induced dimerization between two CD38

molecules on the cell surface by using dimeric 2'-deoxy-2'-fluoro arabinosyl NAD (F-araNAD) and 2'-deoxy-2'-fluoro arabinosyl nicotinamide mononucleotide (F-araNMN) (Figure 3.1).

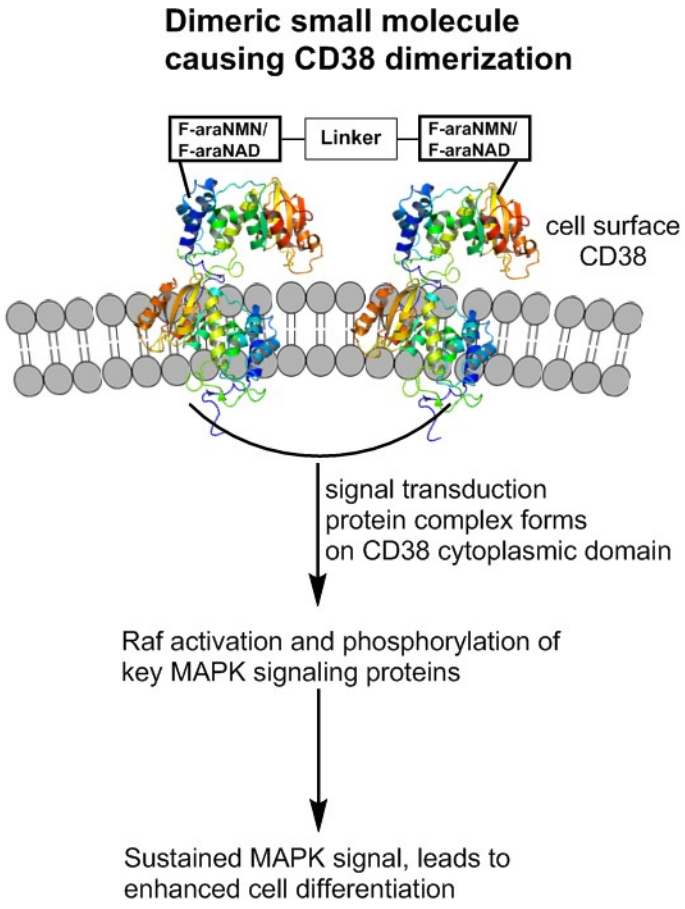

Figure 3.1. Molecular level description for CD38 dimer formation caused by dimeric small molecules to analyze its effect on MAPK signaling and subsequent cell differentiation

Previously, we used the monomeric forms of these molecules to identify CD38 cellular localization (*20*, *21*). These molecules bind to CD38 via mechanism-based labeling through the key catalytic residue, Glu226. The dimeric F-araNAD and dimeric F-araNMN has two CD38 binding portions. Therefore, each dimeric F-araNAD or F-araNMN molecule would bind two cell surface CD38 molecules and bring them into a specific dimer conformation. Then, if the induced CD38 dimerization from the dimeric small molecules enhances MAPK signaling as

detected by phosphorylation on key MAPK signaling proteins, then the dimer orientation induced by the small molecules is the preferred dimer orientation of CD38 for signaling. However, if RA-induced MAPK signaling is decreased, then the induced CD38 dimer is either in the incorrect orientation or induction of CD38 dimerization between two CD38 molecules restricts CD38 from the preferred dimer formation with different cell surface molecules. Using these molecules, we did show that CD38 dimerization increased phosphorylation on a key MAPK signaling protein, Raf. This suggests that MAPK signaling can be affected by CD38 dimerization alone. Ultimately, this study may lead to the development of small molecules that can enhance RA-induced differentiation as a therapy.

Results

Design and Synthesis of Dimeric F-araNAD and F-araNMN molecules

Our strategy for making molecules capable of binding two CD38 molecules to force CD38 dimer formation was to synthesize small molecule dimers of both F-araNAD and F-araNMN. Additionally, the linker portion of the small molecule dimer that links the two F-araNAD or F-araNMN together can be used to either restrict the conformation of the small molecule dimer or allow flexibility. Consequently, the dimer conformation from F-araNAD and dimer F-araNMN would impose upon CD38 either a similar specific dimer conformation or allow flexibility. Thus, we have the potential for stereospecific control of CD38 dimer conformation based upon the small molecule dimer conformation. To conjugate the linker to F-araNMN and F-araNAD, we used the copper-catalyzed Huisgen 1,3-dipolar cycloaddition between alkyne and azide, commonly known as click chemistry (*22*) (Figure 3.2A). The reported synthesis was followed for making F-araNMN alkyne (*20*). The reported synthesis for 6-alkyne-

F-araNAD was followed, with the exception of the coupling reaction between 6-alkyne-AMP and F-araNMN (*21*). Initially, preparation of the magnesium salts of 6-alkyne-AMP and F-araNMN was done in route to coupling the 6-alkyne-AMP to F-araNMN for the synthesis of 6-alkyne-F-araNAD. Subsequently, the coupling reaction proceeded using EDCI in MOPS buffer (1.5 M, pH 7.4) to afford 6-alkyne-F-araNAD (Figure 3.2B). To make either compounds **1** or **3**, we used a molecule containing two free amine groups on opposite sides of the molecule. Then, attached the diamine through amide bond formation to a molecule containing a carboxylic acid and azido groups. Therefore, both free amines form amide bonds which results in two free azido groups that are on opposite ends of the molecule (Figure 3.2B). Finally, either **1** or **3** was conjugated to either F-araNMN alkyne or 6-alkyne-F-araNAD via click chemistry to obtain the desired dimeric small molecules (Figure 3.2C). Two different types of linkers were made in order to either restrict small molecule conformation by using benzene rings or allow flexibility by using ethylene glycol units. Thus, we altered both the CD38 binding portion – F-araNMN and F-araNAD – and linker, either flexible or rigid, in order to investigate whether cell surface CD38 dimerization affected MAPK signaling.

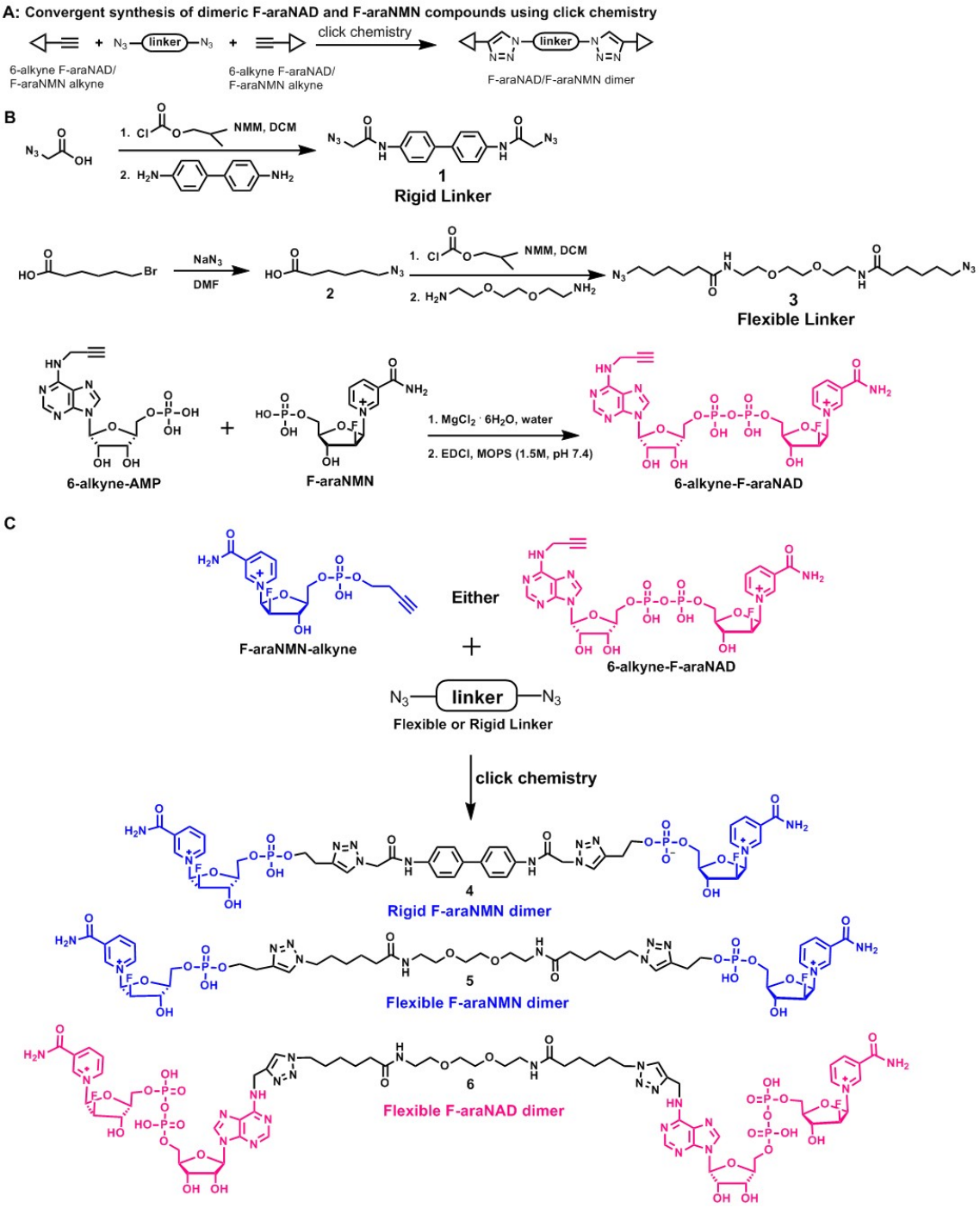

Figure 3.2. (A) The strategy used for the convergent synthesis of dimeric F-araNAD and dimeric F-araNMN compounds using click chemistry. (B) Synthesis of the flexible linker, rigid linker and 6-alkyne-F-araNAD coupling reaction. (C) Synthesis of the three dimeric small molecules using click chemistry, showing molecular structure of the dimeric small molecules.

In Vitro Labeling of Purified CD38 by Dimeric Small Molecules

To test whether the dimeric small molecule can covalently label CD38 and cause CD38 dimer formation, we used purified, wild-type CD38 extracellular catalytic domain. To the wild-type CD38 (1.5 μg, 5 μM) was added various concentrations of the flexible F-araNMN dimer for 20 min. The reaction mixtures were resolved by SDS-PAGE and visualized after staining with Coomassie blue. The most CD38 dimer formation occurred when the flexible F-araNMN dimer concentration equaled the CD38 concentration, but as the flexible F-araNMN dimer concentration increased, the CD38 dimer formation decreased (Figure 3.3). Additionally, as the flexible F-araNMN dimer concentration decreased below equal concentration to the CD38 concentration, the CD38 dimer formation decreased (data not shown). Therefore, dose dependent effects were caused by the flexible F-araNMN dimer, where CD38 dimer formation was at maximum when there were nearly equal amounts of CD38 and flexible F-araNMN dimer, under the reaction conditions tested. Altogether, these results demonstrated CD38 dimer formation can be induced using the small molecule flexible F-araNMN dimer along with revealing dose dependent effects by the flexible F-araNMN dimer on the amount of CD38 dimer formation.

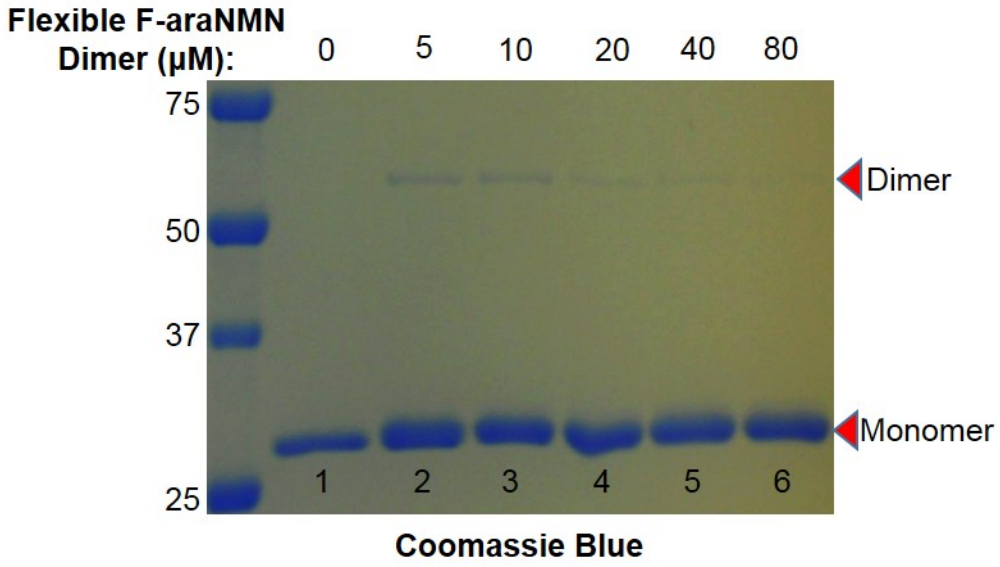

Figure 3.3. *In vitro* labeling of purified CD38 with the flexible F-araNMN dimer molecule. All lanes contain wt CD38 (1.5 μg, 5 μM). Lane 1 has no flexible F-araNMN dimer added to CD38; whereas, Lanes 2 – 6 have increasing concentrations of flexible F-araNMN dimer molecule added. Ladder is on the left, listed first.

Live Cell Labeling of Cell Surface CD38 by Dimeric Small Molecules

The ability for the dimeric small molecules to dimerize cell surface CD38 was next tested using live HL-60 cells. HL-60 cells have a low CD38 expression, but with addition of 1 μM retinoic acid (RA), the level of CD38 expression is increased (*7*). Consequently, within the HL-60 cell line we have cells that express either a high or low amount of CD38 based upon addition of RA. Additionally, we used a stably transfected HL-60 cell line that constitutively expresses a high level of CD38 and GFP (*7*). The higher CD38 protein amount in CD38 overexpressing HL-60 cells allows for detection of the CD38 dimer even in the case that dimer formation is minor. For this experiment, we used Western blotting to analyze the amount of CD38 dimer formation caused by adding the dimeric small molecules, either flexible F-araNMN or flexible F-araNAD, to HL-60 cells and CD38 overexpressing HL-60 cells. The Western blotting results showed a

pronounced increased amount of CD38 dimer formation when using flexible F-araNAD compared to flexible F-araNMN (Figure 3.4). Dimeric small molecules were added to the cells at 1 μM and the incubation time was varied from 1 h to 40 h. Both F-araNMN and F-araNAD labels CD38 within minutes (*20*); however, varying the incubation time revealed that the covalent bond formed between CD38 and the dimeric small molecule is hydrolyzed over an extended time, resulting in decreased CD38 dimer formation as incubation time is increased (Figure 3.4).

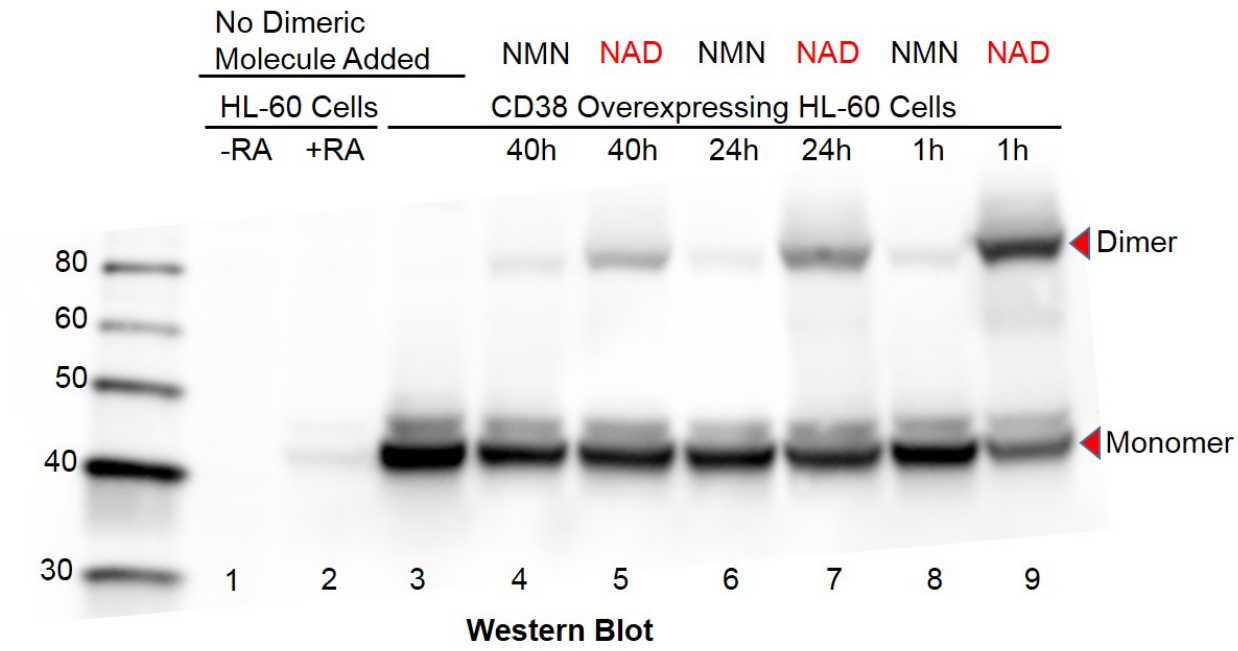

Figure 3.4. Live-cell labeling of cell surface CD38 using either flexible F-araNMN (NMN) or flexible F-araNAD (NAD). Lane 1 – untreated HL-60 cells with no dimeric molecule. Lane 2 – RA-treated HL-60 cells with no dimeric molecule. Lane 3 – CD38 overexpressed in HL-60 cells with no dimeric molecule. Lane 4 – CD38 overexpressed in HL-60 cells with 40 h incubation of flexible F-araNMN. Lane 5 – CD38 overexpressed in HL-60 cells with 40 h incubation of flexible F-araNAD. Lane 6 – CD38 overexpressed in HL-60 cells with 24 h incubation of flexible F-araNMN. Lane 7 – CD38 overexpressed in HL-60 cells with 24 h incubation of flexible F-araNAD. Lane 8 – CD38 overexpressed in HL-60 cells with 1 h incubation of flexible F-araNMN. Lane 9 – CD38 overexpressed in HL-60 cells with 1 h incubation of flexible F-araNAD. Ladder is on the left, listed first. *This data provided by Robert MacDonald from Professor Andrew Yen's lab.

Phosphorylation Effects of MAPK Proteins Caused by Cell-Surface CD38 Dimerization

Next, the intracellular effects caused by cell surface CD38 dimer formation from the flexible F-araNMN and flexible F-araNAD dimeric molecules was investigated. To do this, we performed a Western blot to detect phosphorylation on key serine residues of Raf, MEK and ERK, which are a part of the MAPK signaling pathway. Previous studies have shown CD38 causes Raf activation and tyrosine phosphorylation of key MAPK signaling target molecules, such as ERK and c-Cbl (*12-14*). Consequently, if Raf, MEK or ERK phosphorylation increases

due to increased cell surface CD38 dimer formation, then this may correlate to a sustained MAPK signal required for an accelerated and enhanced cell differentiation. First, using the flexible F-araNMN dimer, the phosphorylation on serine 259 of Raf increased (Figure 3.5A), but this phosphorylation increase was not consistently observed. Additionally, the increase in phosphorylation coincides with the greater amount of cell surface CD38 dimer formation. Therefore, the highest increase in phosphorylation is detected when the flexible F-araNMN dimer is limited to only 1 hour incubation with the cells (Figure 3.5A). Along with this analysis of Raf S259 phosphorylation, MEK (S217 and S221) and ERK phosphorylation also increased upon treatment with dimeric flexible F-araNMN molecule (data not shown); however, the data for MEK and ERK phosphorylation increase was also not consistently observed. Next, using the flexible F-araNAD dimer, the phosphorylation on the serine residue 217 of MEK increased (data from a single trial, Figure 3.5B). However, no increased phosphorylation was seen in Raf and ERK (data not shown). Altogether, this data indicates that the dimeric small molecules by causing cell surface CD38 dimerization, can affect MAPK signaling protein phosphorylation. Although, further experiments will be needed to analyze why there was an increased phosphorylation solely on MEK. Additionally, it will be necessary to investigate whether the cytoplasmic MAPK signaling proteins go into the nucleus to interact with transcription factors, thus initiating gene transcription. Finally, it will be necessary to investigate whether the induced CD38 dimerization causes an enhanced and accelerated cell differentiation and whether this affect operates via the classical MAPK signaling pathway.

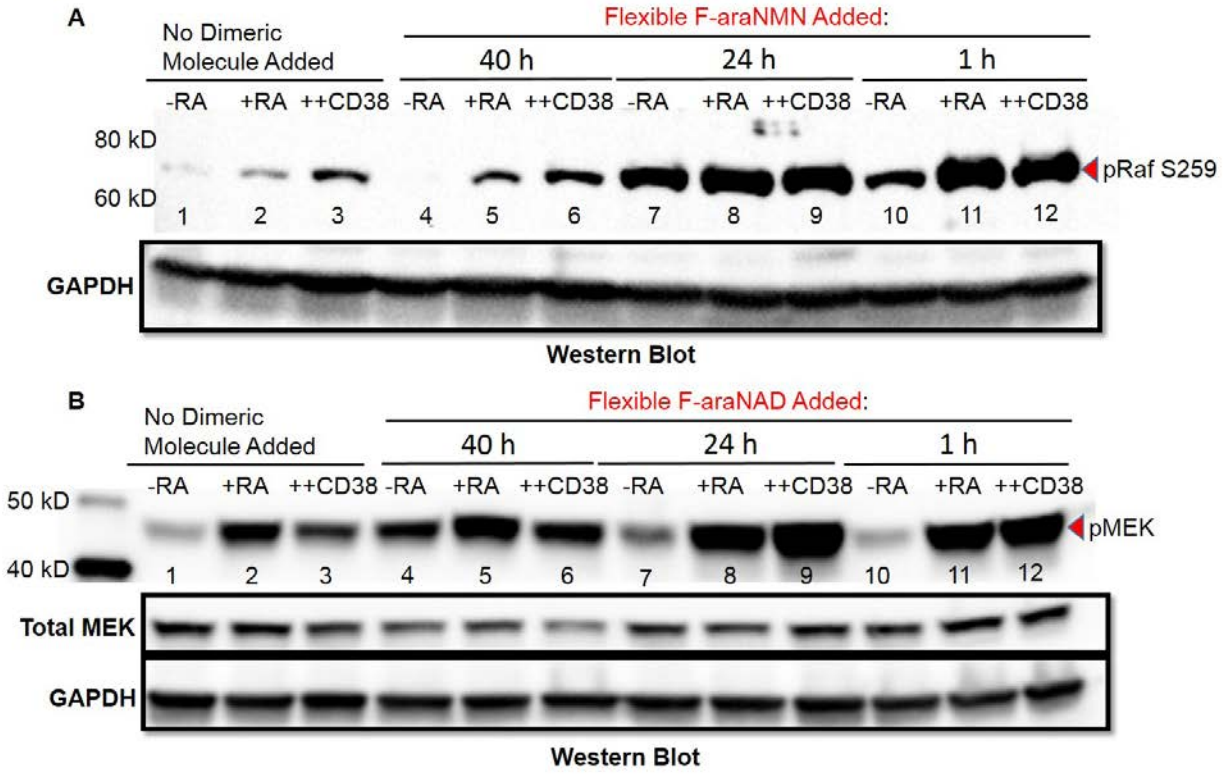

Figure 3.5. (A) Live-cell labeling of cell surface CD38 using flexible F-araNMN to evaluate effects on phosphorylation of Raf S259. (B) Live-cell labeling of cell surface CD38 using flexible F-araNAD to evaluate effects on phosphorylation of MEK. For both A and B: Lane 1 – untreated HL-60 cells with no dimeric molecule. Lane 2 – RA-treated HL-60 cells with no dimeric molecule. Lane 3 – CD38 overexpressed in HL-60 cells with no dimeric molecule. Lane 4 – untreated HL-60 cells with 40 h incubation with flexible dimeric molecule. Lane 5 – RA-treated HL-60 cells with 40 h incubation with flexible dimeric molecule. Lane 6 – CD38 overexpressed in HL-60 cells with 40 h incubation with flexible dimeric molecule. Lane 7 – untreated HL-60 cells with 24 h incubation with flexible dimeric molecule. Lane 8 – RA-treated HL-60 cells with 24 h incubation with flexible dimeric molecule. Lane 9 – CD38 overexpressed in HL-60 cells with 24 h incubation with flexible dimeric molecule. Lane 10 – untreated HL-60 cells with 1 h incubation with flexible dimeric molecule. Lane 11 – RA-treated HL-60 cells with 1 h incubation with flexible dimeric molecule. Lane 12 – CD38 overexpressed in HL-60 cells with 1 h incubation with flexible dimeric molecule. Ladder is on the left, listed first. *This data provided by Robert MacDonald from Professor Andrew Yen's lab.

Discussion

We developed dimeric small molecules capable of causing CD38 dimer formation on the surface of live cells; subsequently, CD38 dimer formation caused an increased phosphorylation

of Raf or MEK, key MAPK signaling proteins. The dimeric small molecules contained either F-araNMN or F-araNAD, which bind CD38 via mechanism-based labeling through the key catalytic residue, Glu226 (*20, 21*). Each dimeric F-araNMN or F-araNAD bind two CD38 molecules and bring them into a specific dimer conformation that is based upon the linker. Conditions for maximal CD38 dimer formation were optimized and include: having nearly equal amounts of dimeric small molecule to CD38 and having a dimeric small molecule incubation time around one hour. Consequently, the effectiveness of CD38 dimer formation by dimeric small molecules is both dose dependent and incubation time dependent. The dimeric F-araNAD molecule caused more CD38 dimer formation on the surface of CD38 overexpressing HL-60 cells than dimeric F-araNMN. Likely, this is due to F-araNAD being more similar to the natural CD38 substrate, NAD; therefore, F-araNAD is a better substrate for labeling CD38. Possibly, the F-araNAD has more favorable interactions within the CD38 binding pocket, thus allowing for a covalent bond with CD38 to be less prone to hydrolysis than the covalent bond between F-araNMN and CD38. Finally, cell surface CD38 dimer formation correlated with an intracellular effect that was revealed by increased S259 phosphorylation on Raf and increased phosphorylation on MEK, which site-specific phosphorylation can influence protein activity (*23*). Increased MAPK signaling protein phosphorylation may correlate to a sustained MAPK signal, which is required for an effect on cell differentiation.

Further experiments are necessary to determine the effect from CD38 dimerization on phosphorylation of other key MAPK signaling proteins and whether this correlates to an enhanced and accelerated cell differentiation via a sustained MAPK signal. The stages of cell differentiation can be analyzed by using a cell surface marker and a functional differentiation marker. First, the cell surface differentiation marker is CD11b, which CD11b expression can be

measured using immunofluorescence. Next, the functional differentiation marker – inducible oxidative metabolism – can be measured using a cell-permeant fluorescent indicator for reactive oxygen species. Inducible oxidative metabolism is the indication of terminally differentiated myeloid cells, which occurs in RA-treated HL-60 cells. An increased and early CD11b expression and inducible oxidative metabolism would indicate an enhanced and accelerated cell differentiation. Therefore, these experiments will be done to determine whether cell surface CD38 dimerization caused by dimeric small molecules can alone or together with RA enhance and accelerate cell differentiation. Ultimately, this may lead to the development of small molecules capable of increased effectiveness or replacement of RA-induced differentiation as a therapy.

Experimental

General Methods

Reagents, unless specified otherwise, were purchased from commercial suppliers in the highest purity available and used as supplied. Antibodies for detection of human CD38 (mouse) were bought from BD Biosciences (San Jose, California, USA, cat. #: 611114), while antibodies for detection of human GAPDH (rabbit), as well as horseradish peroxidase-linked anti-mouse and anti-rabbit antibodies were bought from Cell Signaling (Danvers, MA, USA). The antibody for detection of phosphorylation on S259 of Raf protein was bought from Cell Signaling (cat. # 9421S). Mammalian protein extraction reagent (M-PER) was bought from Pierce (Rockford, IL, USA). All-trans retinoic acid (RA), protease and phosphatase inhibitors were bought from Sigma (St. Louis, MO, USA). ECL was bought from GE Healthcare (Pittsburgh, PA, USA).

^{1}H NMR was performed on INOVA 400/500/600 spectrometers, ^{13}C NMR was performed on INOVA 400 spectrometer, and 2D NMR was performed on INOVA 500/600 spectrometers. NMR data was analyzed by MestReNova (version 8.1.1). ^{1}H NMR chemical shifts are reported in units of ppm relative to tetramethylsilane. ^{1}H NMR data are reported in the following manner: chemical shift (multiplicity, integration). LC-MS experiments were carried out on a Shimadzu HPLC LC20-AD and Thermo Scientific LCQ Fleet with a Sprite TARGA C18 column (40 × 2.1 mm, 5 μm, Higgins Analytical, Inc.) monitoring at 215 and 260 nm with positive mode for mass detection. Solvents for LC-MS were water with 0.1% acetic acid (solvent A) and acetonitrile with 0.1% acetic acid (solvent B). Compounds were eluted at a flow rate of 0.3 mL/min with 0% solvent B for 2 min, followed by a linear gradient of 0% to 10% solvent B over 2 min, followed by a linear gradient of 10% to 100% solvent B over 5 min, and finally 100% solvent B for 1 min before equilibrating the column back to 0% solvent B over 1 min. Preparative HPLC experiments were done on Beckman Coulter System Gold 125p Solvent Module & 168 Detector with a TARGA C18 column (250 × 20 mm, 10 μm, Higgins Analytical, Inc.) monitoring at 215 and 260 nm. Solvents for prep HPLC were water with 0.1% trifluoroacetic acid (solvent A) and acetonitrile with 0.1% trifluoroacetic acid (solvent B). Compounds were eluted at a flow rate of 8.0 mL/min with 0% solvent B for 10 min, followed by first a linear gradient of 0% to X% (X depends on different compounds) solvent B over X min, then a linear gradient of X% to 100% solvent B over 5 min, and finally 100% solvent B for 5 min before equilibrating the column back to 0% solvent B over 5 min.

6-alkyne-F-araNAD

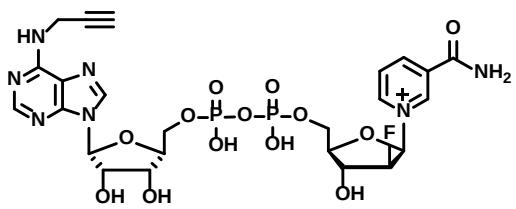

6-alkyne-F-araNAD

Synthesis for F-araNMN and 6-alkyne-AMP were done as previously reported (*20*, *21*) and were coupled to make **6-alkyne-F-araNAD**. First, preparation of the magnesium salt of 6-alkyne-AMP and F-araNMN was done by dissolving 6-alkyne-AMP (4.8 mg, 0.012 mmol, 1.0 eq), F-araNMN (4.2 mg, 0.012 mmol, 1.0 eq) and magnesium chloride hexahydrate (58.6 mg, 0.288 mmol, 24 eq) in water (3 mL) in a round-bottom flask. Subsequently, the water was evaporated using high vacuum. Next, to a solution of F-araNMN and 6-alkyne-AMP magnesium salt in 0.925 mL MOPS buffer (1.5 M, pH 7.4) was added EDCI (460 mg, 2.4 mmol, 200 eq) in an Eppendorf tube. The solution was mixed on a rotating mixer and kept in a 37 °C incubator for approximately 3.5 h. Subsequently, the reaction was lyophilized to obtain dry product. Dry product was washed using acetonitrile (3 x 10 mL washes). The product is insoluble in acetonitrile and thus must be isolated from the acetonitrile washes using filtration. Subsequently, the product was dissolved in water to be purified using preparative HPLC. Prep HPLC purification was done using AG1 anion exchange resin followed by a C18 reverse phase column purification. For the AG1 anion exchange resin purification, water was used as Buffer A and 150 mM trifluoroacetic acid in water as the elution buffer (Buffer B), t_R = 34 min with a gradient of 32 – 64% buffer B from 27 – 32 min followed by 64 – 100% buffer B from 32 – 42 min. For the C18 prep HPLC purification: t_R = 27.5 min with a linear gradient of 0% - 60% solvent B from 10 – 70 min. Solid was obtained (0.47 mg, 5.4% yield). LC-MS (ESI) calcd. for $C_{24}H_{29}FN_7O_{13}P_2^{2+}$ (M^+) 704.13, obsd. 704.17.

Rigid Linker (1)

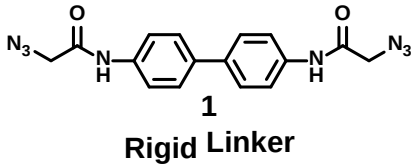

1

Rigid Linker

To a solution of 2-azido acetic acid (380 mg, 3.75 mmol, 4.0 eq) in 19 mL anhydrous DCM in a round-bottom flask fitted with a stir bar was added N-methylmorpholine (0.466 mL, 4.05 mmol, 2.7 eq) and isobutylchloroformate (0.53 mL, 4.05 mmol, 2.7 eq) under nitrogen at 0 °C. This reaction mixture remained heterogeneous even after stirring for 90 min at 0 °C. Therefore, 13 mL of DMF was added to make the reaction homogeneous. Subsequently, benzidine (173 mg, 0.94 mmol, 1.0 eq) was added. The reaction was stirred overnight at rt. The reaction was monitored using LC-MS (260 nm) and upon no detection of the starting material mass, the reaction was quenched by adding water. This caused precipitation of product **1**. Solid product was collected via filtration and used with no further purification. ^{1}H NMR (400 MHz, DMSO): δ 10.21 (s, 1H), 7.64 (d, *J* = 4.47 Hz, 8H), 4.06 (s, 4H).

6-Azido hexanoic acid (2)

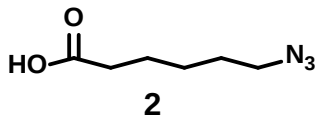

2

To a solution of 6-bromohexanoic acid (1.48 g, 7.59 mmol, 1 eq) in 8.3 mL DMF in a round-bottom flask fitted with a stir bar was added sodium azide (1.0 g, 15.4 mmol, 2.0 eq) with stirring until all solid dissolved. Subsequently, the reaction was put into an 85 °C oil bath and remained stirring. The reaction was monitored by LC-MS (260 nm) to detect product mass formation and by TLC. Even after 7.5 h, a small amount of 6-bromohexanoic acid remained as detected by TLC; however, the reaction was diluted in DCM and washed using 0.1 M HCl (3 x 100 mL). The organic layer was dried over anhydrous Na_2SO_4, and then concentrated on a rotary evaporator and further dried under high vacuum. No further purification was done. Compound **2** was obtained as a colorless liquid (1.167 g, 97%

yield). R_f was 0.63 in 7:3 DCM:EtOAc with 0.5% acetic acid. LC-MS (ESI) calcd. for $C_6H_{10}N_3O_2^-$ [M^-] 156.08, obsd. 156.58.

Flexible Linker (3)

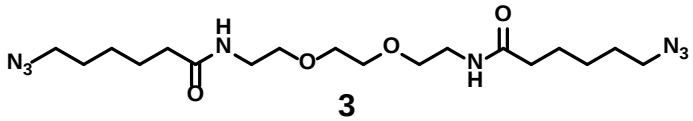

3

Flexible Linker

To a solution of **2** (200 mg, 1.27 mmol, 4.0 eq) in 6.5 mL anhydrous DCM in a round-bottom flask fitted with a stir bar was added N-methylmorpholine (0.094 mL, 0.857 mmol, 2.7 eq) and isobutylchloroformate (0.112 mL, 4.05 mmol, 2.7 eq) under nitrogen at 0 °C. The homogenous solution was stirred for 30 min while at 0 °C. Subsequently, 1,2-Bis(2-aminoethoxy)ethane (47.1 mg, 0.3175 mmol, 1.0 eq) was added. The homogenous solution was stirred for 45 min while under nitrogen at 0 °C after which the reaction was allowed to warm to rt and stirred overnight. Product **3** formation was confirmed by LC-MS. The reaction was diluted in DCM and washed using 0.1 M NaOH (2 x 50 mL) and water (1 x 50 mL) to remove excess 6-azidohexanoic acid (**2**). The organic layer was dried over anhydrous Na_2SO_4, filtered, then concentrated on a rotary evaporator and further dried under high vacuum. Purification was done using silica gel flash chromatography (20:1 DCM:MeOH eluted the product). Compound **3** was obtained as a solid (55 mg, 41% yield). ^{1}H NMR (400 MHz, $CDCl_3$): δ 6.12 (s, 2H), 3.55 (s, 4H), 3.49 (t, J = 5.41 Hz, 5H), 3.38 (q, J = 5.21 Hz, 4H), 3.21 (t, J = 6.65 Hz, 4H), 2.14 (t, J = 7.19 Hz), 1.65 – 1.50 (m, 9H), 1.40 – 1.30 (m, 5H).

Rigid F-araNMN dimer (4)

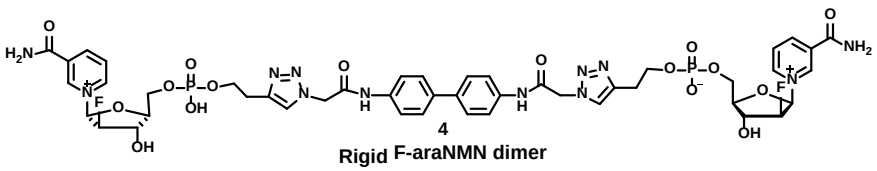

4

Rigid F-araNMN dimer

F-araNMN alkyne (53.6 µL of a 29.5 mM aqueous solution, 1.58 µmol, 2.1 eq., synthesized according to a reported procedure (*20*)), **1** (37.5 µL of a 20 mM DMF solution, 0.75 µmol, 1.0 eq.), Tris[(1-benzyl-1*H*-1,2,3-triazol-4-yl)methyl]amine (as ligand, 45 µL of an 100 mM DMF solution, 4.5 µmol, 6.0 eq.), copper sulfate (45 µL of a 100 mM aqueous solution, 4.5 µmol, 6.0 eq.), sodium ascorbate (96 µL of a 100 mM aqueous solution, 9.6 µmol, 12.8 eq.) were added to DMF (443 µL) in that order to a round-bottom flask fitted with a stir bar. The reaction solution was stirred at rt overnight. Product formation was detected using LC-MS (260 nm). Purification of compound **4** was done by analytical HPLC using water with 0.1% acetic acid as Buffer A and acetonitrile with 0.1% acetic acid as the elution buffer (Buffer B). Analytical HPLC (column 2.5 µm, 100 x 4.6 mm, C18): t_R = ~16 min with a linear gradient of 0% - 40% solvent B from 7 – 20 min, then 40% - 90% solvent B from 20 – 25 min. Solid was obtained (0.509 mg, 60% yield). LC-MS (ESI) calcd. for $C_{46}H_{51}F_2N_{12}O_{16}P_2^+$ (M^+) 1127.30 and [(M^+)/2] 563.65, obsd. 564.33, 1127.5.

Flexible F-araNMN dimer (5)

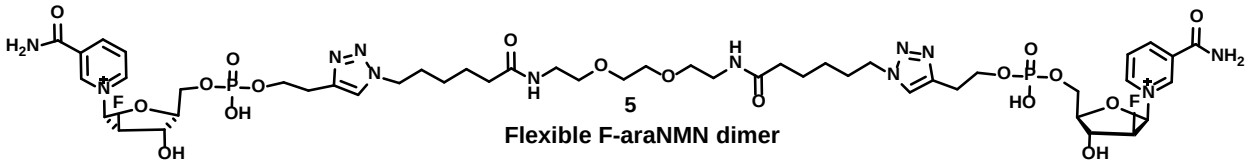

5

Flexible F-araNMN dimer

F-araNMN alkyne (171 µL of a 10.2 mM aqueous solution, 1.74 µmol, 2.1 eq., synthesized according to a reported procedure (*20*)), **3** (41.5 µL of a 20 mM DMF solution, 0.83 µmol, 1.0 eq.), Tris[(1-benzyl-1*H*-1,2,3-triazol-4-yl)methyl]amine (as ligand, 49.8 µL of an 100 mM DMF

solution, 4.98 μmol, 6.0 eq.), copper sulfate (49.8 μL of a 100 mM aqueous solution, 4.98 μmol, 6.0 eq.), sodium ascorbate (79.7 μL of a 100 mM aqueous solution, 7.97 μmol, 9.6 eq.) were added to DMSO (272 μL) in that order to a round-bottom flask fitted with a stir bar. The reaction solution was stirred at rt overnight. Product formation was confirmed using LC-MS (260 nm). Purification by preparative HPLC. Prep HPLC: t_R = 40.5 min with a linear gradient of 0% - 70% solvent B from 10 – 80 min. Solid was obtained (0.422 mg, 42% yield). LC-MS (ESI) calcd. for $C_{48}H_{72}F_2N_{12}O_{18}P_2^{2+}$ (M^{2+}) 602.22, obsd. 602.33.

Flexible F-araNAD dimer (6)

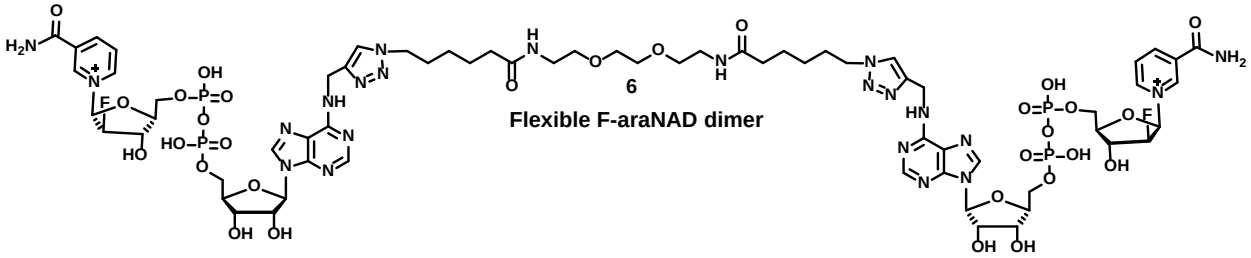

6-alkyne-F-araNAD (2.5 mL of a 0.208 mM aqueous solution, 0.52 μmol, 1.75 eq.), **3** (14.85 μL of a 20 mM DMF solution, 0.30 μmol, 1.0 eq.), Tris[(1-benzyl-1*H*-1,2,3-triazol-4-yl)methyl]amine (as ligand, 17.82 μL of an 100 mM DMF solution, 1.782 μmol, 6.0 eq.), copper sulfate (17.82 μL of a 100 mM aqueous solution, 1.782 μmol, 6.0 eq.), sodium ascorbate (28.5 μL of a 100 mM aqueous solution, 2.85 μmol, 9.6 eq.) were combined in that order to a round-bottom flask fitted with a stir bar. The reaction solution was stirred at rt overnight. Product formation was confirmed using LC-MS (260 nm). Purification by preparative HPLC. Prep HPLC: t_R = 38.5 min with a linear gradient of 0% - 60% solvent B from 10 – 70 min. Solid was obtained (0.154 mg, 28% yield). LC-MS (ESI) calcd. for $C_{66}H_{92}F_2N_{22}O_{30}P_4^{2+}$ (M^{2+}) 917.26, obsd. 917.67.

In vitro Labeling of Purified CD38 using Flexible F-araNMN dimer

CD38 (wt, 5 μM, expressed and purified as reported earlier (*24, 25*)) and flexible F-araNMN dimer (5, 10, 20, 40 and 80 μM) in 10 μL reaction buffer (25 mM HEPES, 50 mM NaCl, pH 7.4) were incubated at RT for 20 min, then mixed with 2 μL 6× protein loading buffer. The samples were heated at 100 °C for 7 min and then resolved by SDS-PAGE. Following staining with Coomassie blue, the gel was visualized (Transillum, Fisher Scientific, model DLT-A), and the image was recorded with a digital camera (Nikon Coolpix L22).

REFERENCES

1. Reinherz, E. L., Kung, P. C., Goldstein, G., Levey, R. H., and Schlossman, S. F. (1980) Discrete stages of human intrathymic differentiation: analysis of normal thymocytes and leukemic lymphoblasts of T-cell lineage, *Proc Natl Acad Sci U S A 77*, 1588-1592.
2. Alessio, M., Roggero, S., Funaro, A., De Monte, L. B., Peruzzi, L., Geuna, M., and Malavasi, F. (1990) CD38 molecule: structural and biochemical analysis on human T lymphocytes, thymocytes, and plasma cells, *J Immunol 145*, 878-884.
3. Dianzani, U., and Malavasi, F. (1995) Lymphocyte adhesion to endothelium, *Crit Rev Immunol 15*, 167-200.
4. Deaglio, S., Dianzani, U., Horenstein, A. L., Fernandez, J. E., van Kooten, C., Bragardo, M., Funaro, A., Garbarino, G., Di Virgilio, F., Banchereau, J., and Malavasi, F. (1996) Human CD38 ligand. A 120-KDA protein predominantly expressed on endothelial cells, *J Immunol 156*, 727-734.
5. Horenstein, A. L., Stockinger, H., Imhof, B. A., and Malavasi, F. (1998) CD38 binding to human myeloid cells is mediated by mouse and human CD31, *Biochem J 330 (Pt 3)*, 1129-1135.
6. Deaglio, S., Mallone, R., Baj, G., Arnulfo, A., Surico, N., Dianzani, U., Mehta, K., and Malavasi, F. (2000) CD38/CD31, a receptor/ligand system ruling adhesion and signaling in human leukocytes, *Chem Immunol 75*, 99-120.
7. Lamkin, T. J., Chin, V., Varvayanis, S., Smith, J. L., Sramkoski, R. M., Jacobberger, J. W., and Yen, A. (2006) Retinoic acid-induced CD38 expression in HL-60 myeloblastic leukemia cells regulates cell differentiation or viability depending on expression levels, *J Cell Biochem 97*, 1328-1338.
8. Warrell, R. P., Jr., Frankel, S. R., Miller, W. H., Jr., Scheinberg, D. A., Itri, L. M., Hittelman, W. N., Vyas, R., Andreeff, M., Tafuri, A., Jakubowski, A., and et al. (1991) Differentiation therapy of acute promyelocytic leukemia with tretinoin (all-trans-retinoic acid), *N Engl J Med 324*, 1385-1393.
9. Brown, G., and Hughes, P. (2012) Retinoid differentiation therapy for common types of acute myeloid leukemia, *Leuk Res Treatment 2012*, 939021.
10. Balmer, J. E., and Blomhoff, R. (2002) Gene expression regulation by retinoic acid, *J Lipid Res 43*, 1773-1808.
11. Kishimoto, H., Hoshino, S., Ohori, M., Kontani, K., Nishina, H., Suzawa, M., Kato, S., and Katada, T. (1998) Molecular mechanism of human CD38 gene expression by retinoic acid. Identification of retinoic acid response element in the first intron, *J Biol Chem 273*, 15429-15434.
12. Lund, F. E. (2006) Signaling properties of CD38 in the mouse immune system: enzyme-dependent and -independent roles in immunity, *Mol Med 12*, 328-333.
13. Kontani, K., Kukimoto, I., Nishina, H., Hoshino, S., Hazeki, O., Kanaho, Y., and Katada, T. (1996) Tyrosine phosphorylation of the c-cbl proto-oncogene product mediated by cell surface antigen CD38 in HL-60 cells, *J Biol Chem 271*, 1534-1537.
14. Munoz, P., Navarro, M. D., Pavon, E. J., Salmeron, J., Malavasi, F., Sancho, J., and Zubiaur, M. (2003) CD38 signaling in T cells is initiated within a subset of membrane rafts containing Lck and the CD3-zeta subunit of the T cell antigen receptor, *J Biol Chem 278*, 50791-50802.

15. Lund, F. E., Yu, N., Kim, K. M., Reth, M., and Howard, M. C. (1996) Signaling through CD38 augments B cell antigen receptor (BCR) responses and is dependent on BCR expression, *J Immunol 157*, 1455-1467.
16. Morra, M., Zubiaur, M., Terhorst, C., Sancho, J., and Malavasi, F. (1998) CD38 is functionally dependent on the TCR/CD3 complex in human T cells, *FASEB J 12*, 581-592.
17. Inove S, K. K., Tsujimoto N. (1997) Protein-tyrosine phosphorylation by IgG_1 subclass CD38 monoclonal antibodies is mediated through stimulation of Fc II receptors in human myeloid cell lines, *J. Immunol.*, 5226-5232.
18. Tsujimoto, N., Kontani, K., Inoue, S., Hoshino, S., Hazeki, O., Malavasi, F., and Katada, T. (1997) Potentiation of chemotactic peptide-induced superoxide generation by CD38 ligation in human myeloid cell lines, *J Biochem 121*, 949-956.
19. Ausiello, C. M., Urbani, F., Lande, R., la Sala, A., Di Carlo, B., Baj, G., Surico, N., Hilgers, J., Deaglio, S., Funaro, A., and Malavasi, F. (2000) Functional topography of discrete domains of human CD38, *Tissue Antigens 56*, 539-547.
20. Shrimp, J. H., Hu, J., Dong, M., Wang, B. S., Macdonald, R., Jiang, H., Hao, Q., Yen, A., and Lin, H. (2014) Revealing CD38 Cellular Localization Using a Cell Permeable, Mechanism-Based Fluorescent Small-Molecule Probe, *J Am Chem Soc*.
21. Jiang, H., Congleton, J., Liu, Q., Merchant, P., Malavasi, F., Lee, H. C., Hao, Q., Yen, A., and Lin, H. (2009) Mechanism-based small molecule probes for labeling CD38 on live cells, *J Am Chem Soc 131*, 1658-1659.
22. Kolb, H. C., Finn, M. G., and Sharpless, K. B. (2001) Click Chemistry: Diverse Chemical Function from a Few Good Reactions, *Angew Chem Int Ed Engl 40*, 2004-2021.
23. Hekman, M., Wiese, S., Metz, R., Albert, S., Troppmair, J., Nickel, J., Sendtner, M., and Rapp, U. R. (2004) Dynamic changes in C-Raf phosphorylation and 14-3-3 protein binding in response to growth factor stimulation: differential roles of 14-3-3 protein binding sites, *J Biol Chem 279*, 14074-14086.
24. Liu, Q., Kriksunov, I. A., Graeff, R., Munshi, C., Lee, H. C., and Hao, Q. (2005) Crystal structure of human CD38 extracellular domain, *Structure 13*, 1331-1339.
25. Munshi, C., Aarhus, R., Graeff, R., Walseth, T. F., Levitt, D., and Lee, H. C. (2000) Identification of the enzymatic active site of CD38 by site-directed mutagenesis, *J Biol Chem 275*, 21566-21571.

Chapter 4

A Bi-functional Small Molecule that Targets CD38 and Recruits Antibodies to Enact Immune Effector Cells for Target Cell Cytotoxicity

Abstract

A vast majority of therapeutic strategies for cancer treatment target cell surface proteins that are either overexpressed or only expressed by the cancer. Thus, CD38 – a type II transmembrane protein – makes for a desirable drug target due to its high expression on many hematologic cancers, particularly in multiple myeloma. Multiple myeloma is a malignant disorder of B cells that has a high CD38 expression on all malignant cells. Here, we report the synthesis and application of a novel, bi-functional antibody-recruiting small molecule (ARM) that targets CD38 and enacts immune effector cells – T-cells, B-cells, monocytes and natural killer cells – for target cell cytotoxicity. The ARM molecular structure has F-araNMN to specifically bind CD38 and 2,4-dinitrophenyl (DNP) to be recognized by endogenous antibodies in humans. Using this molecule, we show the functional formation of a three-body complex between cell surface CD38, ARM and anti-DNP antibody in human cell lines. The three-body complex formed on the cell surface and was seen by using confocal fluorescence microscopy to detect fluorescence from a fluorescent conjugated anti-DNP antibody, a part of the three-body complex. This three-body complex is integral in enacting the immune-effector cells to kill target cells having a high cell surface CD38 expression. Our designed ARM molecule formed the three-body complex that subsequently caused a 2.5 fold increase in overexpressed CD38 target cell cytotoxicity that was shown using a two color flow cytometry experiment. Therefore, this

ARM strategy has potential as a novel therapeutic treatment for hematologic cancers that have abnormally high cell surface CD38 expression on its malignant cells.

Introduction

In the United States, one in every four deaths are caused by cancer; however, cancer death rates have declined by 20% since their peak in 1991 (*1*). Increased efforts within the United States to eradicate cancer as a major cause of death through increased research into cancer biology and treatments was initiated through signing of the National Cancer Act of 1971. Since then, we have seen progress in cancer prevention, early detection with effective treatments and chemotherapeutics that has led to the declining cancer death rates (*2*).

Currently, molecular target-based cancer therapy that includes small molecule protein inhibitors and monoclonal antibodies (mAbs) are areas of promise for effective cancer therapeutics (*3*). Both classes already have Food and Drug Administration (FDA) approved molecules targeting a wide range of cancers. Two examples of effective mAbs are rituximab (Rituxan) that treats B-cell lymphoma by targeting CD20 and trastuzumab (Herceptin) that is a humanized mAb for treatment of breast cancer by targeting ERBB2 (*4, 5*). Mechanisms of action for mAb-based cancer therapy can be direct or indirect. Direct mechanism can involve mAbs that are conjugated with toxins, radioisotopes, cytokines, DNA molecules or small-molecule agents to induce the selective cytotoxicity through various modes of action (*3, 6*). Indirect mechanism is effective through the immune system, which is activated by the Fc portion of the mAb once the mAb binds to its cell surface target. Alternatively, small molecule inhibitors typically exhibit their effects through a direct mechanism by specific binding to target. One mode of action for small molecule inhibitor binding is to block the function of the target signaling receptor. Two

successful examples include those selective for the epidermal growth factor receptor (EGFR), gefitinib (Iressa) and erlotinib (Tarceva). A unique benefit of small molecules compared to mAbs is their capability to translocate through the plasma membrane in order to affect intracellular signaling pathways.

Another approach to designing therapeutic drugs against disease is called synthetic immunology – a rational design and synthesis of molecules that performs an immunological function (*7*). When the body's immune system fails to recognize and treat cells that are evading regulatory growth and proliferation mechanisms, then disease will become worse unless external therapeutics are administered. Therefore, synthetic immunology attempts to cure disease through activation of the immune system. An example of synthetic immunology is an antibody-recruiting small molecule (ARM). Unlike small molecule inhibitors that are effective only through a direct mechanism of action, ARMs are effective through the indirect mechanism of action. These molecules perform this action by first binding to the targeted diseased cell, followed by redirecting antibodies already present in the bloodstream to the surface of the targeted cell (*7*). Once antibodies are recruited to the surface of the targeted diseased cell, the Fc portion of the antibody is recognized by immune-effector cells to enact target cell killing either through complement-dependent cytotoxicity (CDC) and/or antibody-dependent cellular cytotoxicity (ADCC). Though ARMs can be effective via the indirect mechanism similarly to mAb-based therapy, ARMs are less likely to suffer from the mAb-based therapy drawbacks, such as high expense, solely administered by injection and allergic responses to addition of foreign antibodies (*7*). Consequently, CD38 could be used as a target for an ARM due to its high cell surface expression in certain hematologic cancers (*8*).

Here, we report the synthesis and use of a bi-functional ARM that has a target-binding terminus (TBT) to selectively bind CD38 and an antibody-binding terminus (ABT) to associate with anti-hapten antibodies. CD38 has increased cell surface expression in certain hematologic cancers compared to normal cell expression (*8*) and has already been indicated as a target for therapeutic development in the treatment of multiple myeloma (*9*). Therefore, it is an attractive target for the ARM molecule. The TBT is 2'-deoxy-2'-fluoro arabinosyl nicotinamide mononucleotide (F-araNMN) that has previously been shown to be a mechanism-based label specific for CD38 on both the cell surface and intracellular (*10*). The ABT is 2,4-dinitrophenyl that is recognized by endogenous antibodies in most human populations (*11-13*). Initially, we show the ARM molecule is capable of forming the three-body complex – CD38, ARM and antibody – necessary to enact the immune-effector cells by using confocal fluorescence microscopy. Next, we show its effectiveness in targeted cytotoxicity in HL-60 cells overexpressing CD38. The ARM molecule proved to be effective in enacting immune-effector cells for cytotoxicity of the target cells as a 2.5 fold increase in dying cells was observed.

Results

Design and Synthesis of Antibody-Recruiting Small Molecule (ARM) Targeting CD38

Initially, the design of the ARM molecule for targeting CD38 required choices for the TBT and ABT. Consequently, for the TBT we used F-araNMN, because it has previously been shown to be a selective, mechanism-based molecule for labeling CD38 in cells (*10*). For the ABT, we chose 2,4-dinitrophenyl (DNP), because it has previously been shown to be effective as an ABT for other ARM molecules (*14-16*) and there exists anti-DNP antibodies in the human bloodstream in a high percentage of the human population (*11*) that are competent to mediate

target-cell killing (*17, 18*). To conjugate the F-araNMN to the DNP, we used copper-catalyzed Huisgen 1,3-dipolar cycloaddition between alkyne and azide, commonly known as click chemistry (*19*). Synthesis of F-araNMN alkyne was done as reported (*10*). To the DNP moiety was attached a polyethylene glycol (PEG) group that also contained the desired azido group. To make **1**, a nucleophilic aromatic substitution of 1-chloro-2,4-dinitrobenzene was done with an azido PEG amine containing 8 PEG units. The 8 PEG units allows for the ABT of ARM to be at a distance from the cell surface in order to avoid unfavorable steric interactions between the antibody and other cell surface proteins. Finally, the F-araNMN alkyne was conjugated to **1** via click chemistry to obtain the desired **F-araNMN-DNP**, the CD38 targeting ARM molecule (Figure 4.1).

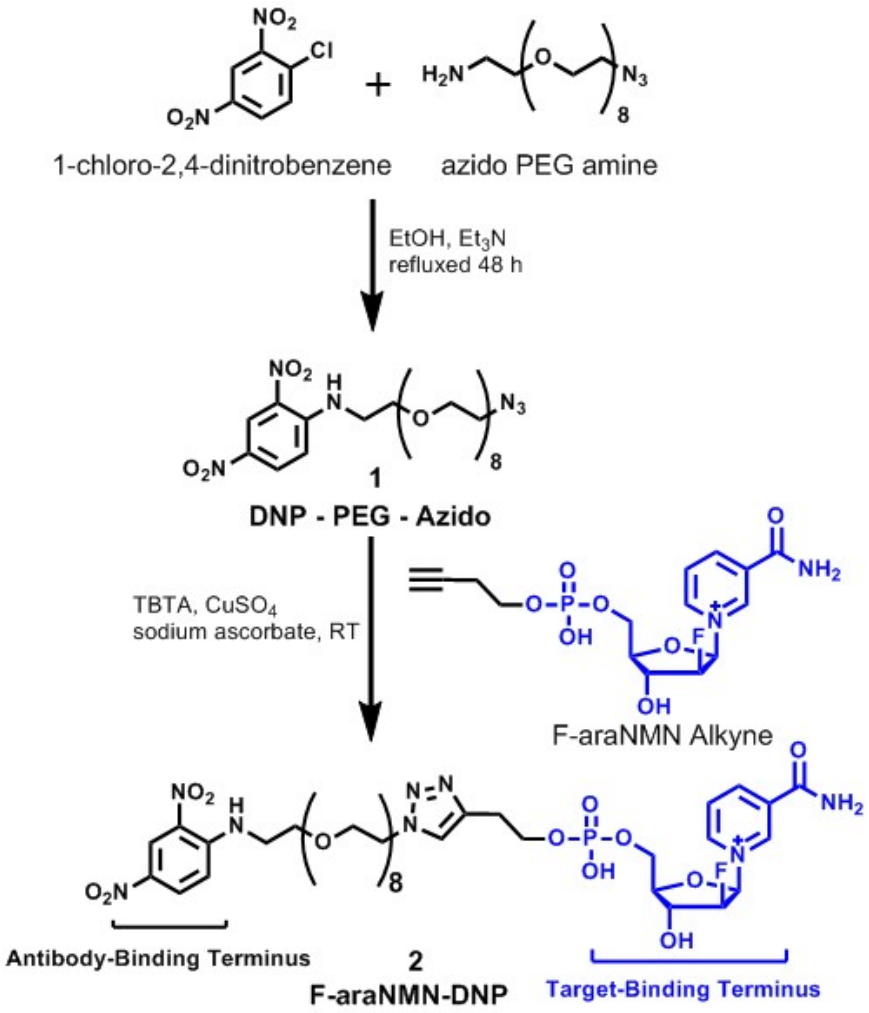

Figure 4.1. Synthesis of F-araNMN-DNP, the bi-functional ARM.

Confocal Microscopy Imaging Reveals Three-Body Complex Formation between CD38, F-araNMN-DNP and Antibody on Live Cells

Next, the capability for F-araNMN-DNP to form a three-body complex – CD38, F-araNMN-DNP and antibody – was tested using HL-60 cells. The experiment was done using HL-60 cells, because it provides a convenient negative control. Untreated HL-60 cells have a low CD38 expression, but retinoic acid (RA)-treated cells have a higher amount of CD38 expression (*20*). In particular, RA-treatment of HL-60 cells causes a pronounced increase of CD38 protein amount on the plasma membrane (*10*). We first incubated RA-treated HL-60 cells with 10 μM F-

araNMN-DNP for 1 hour at 4 °C followed by washing with a buffer to remove unbound F-araNMN-DNP. The incubation time was determined to be sufficient based on previous results using F-araNMN to label CD38 (*10*). Subsequently, AlexaFluor488-labeled rabbit anti-DNP IgG antibody at 15 μg/mL was added to the cells and allowed to incubate for 1 hour at 4 °C. If the antigen-antibody binding occurs between DNP and the anti-DNP antibody, then fluorescence on the exterior of the plasma membrane would be seen (Figure 4.2A). Following antibody staining, a wash with a buffer was performed to remove unbound antibody. Certainly, we found F-araNMN-DNP caused the formation of the three-body complex as strong fluorescence was seen on the plasma membrane of the RA-treated HL-60 cells (Figure 4.2B). When no F-araNMN-DNP was added to the RA-treated HL-60 cells, very little fluorescence was seen from the AlexaFluor488 anti-DNP antibody (Figure 4.2D). Additionally, when untreated HL-60 cells (low CD38 protein amount) were incubated with F-araNMN-DNP and the AlexaFluor488 anti-DNP antibody, very little fluorescence was seen (Figure 4.2C). Thus, F-araNMN-DNP was capable of forming the three-body complex.

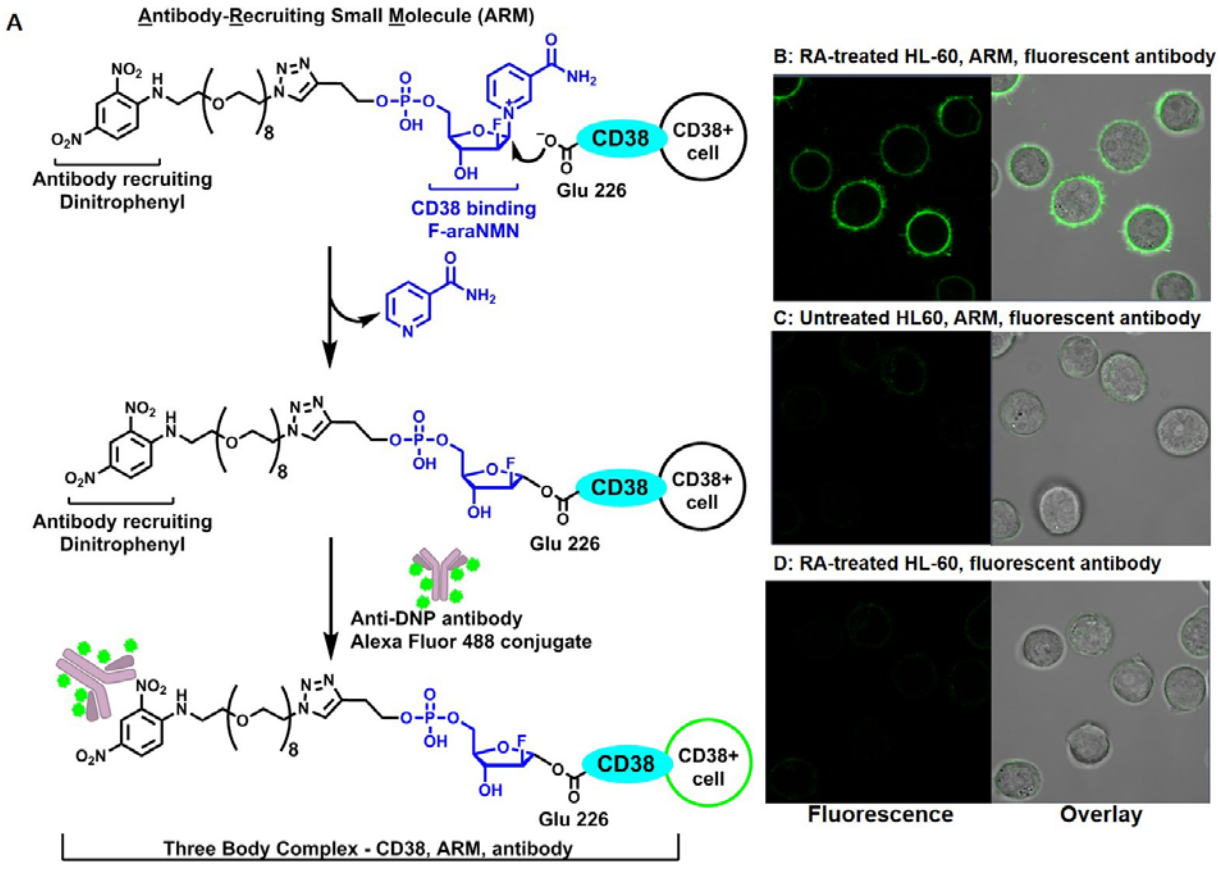

Figure 4.2. Confocal images of HL-60 cells (with or without RA-treatment): (A) Molecular description for the confocal fluorescence microscopy procedure. (B) RA-treated HL-60 cells to induce high CD38 expression, along with addition of both ARM and AlexaFluor488 rabbit anti-DNP IgG antibody. (C) Untreated HL-60 cells (low CD38 expression), along with addition of both ARM and AlexaFluor488 rabbit anti-DNP IgG antibody. (D) RA-treated HL-60 cells to induce high CD38 expression, along with AlexaFluor488 rabbit anti-DNP IgG antibody.

Flow Cytometry Reveals that F-araNMN-DNP Is Able to Induce Cell-Mediated Cytotoxicity

Having established that F-araNMN-DNP is capable of forming the three-body complex, we tested its capability to induce cell-mediated cytotoxicity to HL-60 cells. Cell-mediated cytotoxicity occurs through interactions between the Fc receptors on cytotoxic-effector cells contained in human peripheral blood mononuclear cells (hPBMC) and the Fc portion of the anti-DNP antibody (*18*). Human peripheral blood mononuclear cells are a critical component for the

immune system and consists of T-cells (most abundant), monocytes, B-cells and natural killer (NK) cells. For this experiment we used a stably transfected HL-60 cell line that constitutively expresses a high level of CD38 and green fluorescent protein (GFP), but CD38 and GFP are expressed as separate proteins (*20*). This HL-60 cell line has high CD38 expression allowing binding of F-araNMN-DNP. At the same time, the GFP fluorescence allows us to differentiate the HL-60 cells from the hPBMC during flow cytometry to determine cell killing. Thus, HL-60 cells overexpressing CD38 were combined with F-araNMN-DNP, anti-DNP antibodies and hPBMC in this order, and cell viability was measured using propidium iodide with analysis from a flow cytometer (Figure 4.3). In brief, the cell viability assay used a specific amount of HL-60 cells with sequential addition of 20 μM ARM, 25 μg/mL anti-DNP antibody and 25:1 hPBMC to HL-60 cell ratio. Washes were done after both ARM and anti-DNP incubation periods to ensure removal of unbound ARM and anti-DNP antibodies before addition of hPBMC to the HL-60 cells. The antibody concentration used in this experiment was slightly below reported levels in human serum (*11-13*).

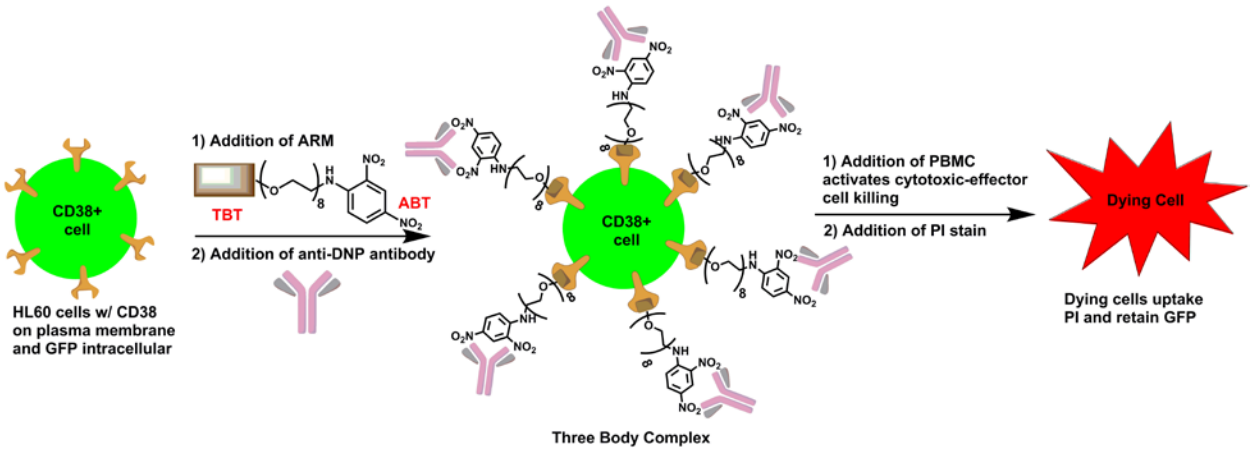

Figure 4.3. Molecular level description of three body complex formation followed by addition of immune effector cells to enact target cell killing.

To evaluate the effect from the three body complex on cell-mediated cytotoxicity, a two color – green from GFP and red from PI – flow cytometry experiment was done. All HL-60 cells have green fluorescence from GFP; however, only those cells with a compromised plasma membrane uptake PI resulting in those cells having red fluorescence, thus indicating the cell is dying. Consequently, gates were set on the flow cytometer to distinguish between four groups of cells; in particular, this was done to distinguish cell death between hPBMCs and HL-60 cells. The four groups of cells included: those with only PI uptake (Q1), those that retained GFP and had PI uptake (Q2), those with either little or no GFP and PI uptake (Q3) and those retaining GFP along with little to no amount of PI uptake (Q4) (Figure 4.4A). An additional gate was set to enclose those cells that retained GFP and shifted upward from PI uptake – these cells were counted as dying HL-60 cells (Figure 4.4A, gate is called “dying”). Subsequently, percentage of dying HL-60 cells was calculated based upon the cell population within the dying gate as part of the total number of HL-60 cells that retained GFP (Figure 4.4B). An approximate 2.5 fold increase in cell-mediated cytotoxicity was observed above the control samples, in which at least one of the components necessary to form the three-body complex was omitted (Figure 4.4B). Currently, replication of these cell-mediated cytotoxicity experiments are underway. In order to determine if similar results occur in cells with a lower CD38 expression than the CD38 overexpressing HL-60 cells, further experiments would be done on Raji cells, which has high CD38 expression, and K562 cells, which has no CD38 expression (*10*).

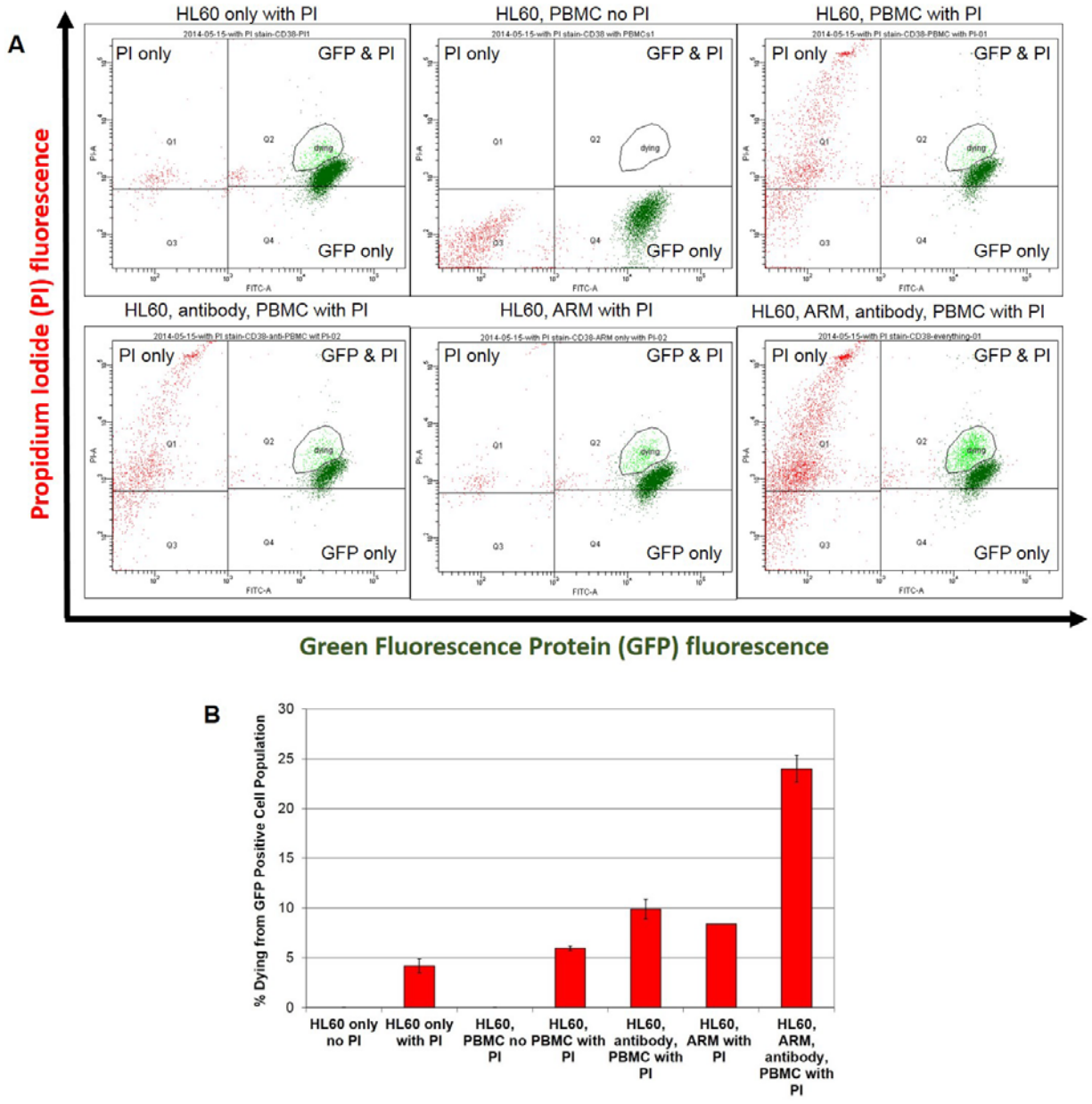

Figure 4.4. Measuring targeted cytotoxicity of HL-60 cells from three-body complex formation. (A) 2D flow cytometry plots placing cells into specific quadrants based on amount of GFP retained and PI uptake. Those with only PI uptake (Q1), those that retained GFP and had PI uptake (Q2), those with either little or no GFP and PI uptake (Q3) and those retaining GFP along with little to no amount of PI uptake (Q4). (B) Graph showing percentage of dying cells, calculated based upon the cell population within the dying gate as part of the total number of cells that retained GFP. *2-color flow cytometry data plots obtained with the assistance of Dr. Rodica Petruta Bunaci from Professor Andrew Yen's lab.

Thus, we made and developed the use of F-araNMN-DNP, a bi-functional ARM, that targets cell surface CD38 and recruits antibodies recognizing 2,4-dinitrophenyl to form a three-body complex – CD38, F-araNMN-DNP and antibody – capable of enacting immune-effector cells for target cell cytotoxicity. Data supporting these conclusions include: 1) immunofluorescence detection on the cell surface of CD38-expressing cells from an anti-DNP fluorescent antibody revealed formation of the necessary three-body complex, and 2) a two-color flow cytometry experiment that revealed the anti-DNP antibodies present in the three-body complex can elicit immune-effector cells for killing of CD38 overexpressing HL-60 cells.

F-araNMN-DNP is unique in that it represents a small-molecule based strategy for both targeting CD38 and eliciting an immunological response, similar to how the mAb-based therapeutic is effective. However, small molecules typically do not suffer from mAb-based therapeutics, which include high expense, administered by injection instead of orally and allergic responses to addition of foreign antibodies (*7*). Consequently, a molecule capable of using CD38 as a drug target has a useful application in certain hematologic cancers, such as multiple myeloma. Multiple myeloma, a malignant disorder of B cells, has a relatively high CD38 expression on all malignant cells (*9, 21*). A future direction for this study will involve elucidation of the molecular details to further describe the effect of immune-effector cells on target cells for cytotoxicity.

Experimental

General Methods

Reagents, unless specified otherwise, were purchased from commercial suppliers in the highest purity available and used as supplied. Antibodies for detection of 2,4-dinitrophenyl were

bought from life technologies and includes: Anti-Dinitrophenyl-KLH Rabbit IgG Fraction, Alexa Fluor® 488 Conjugate (cat. #: A11097) and Dinitrophenyl-KLH Rabbit IgG Antibody (cat. #: A-6430). Human peripheral blood mononuclear cells, frozen (PBMC) were purchased from StemCell Technologies (cat. #: 70025).

^{1}H NMR was performed on INOVA 400/500/600 spectrometers, ^{13}C NMR was performed on INOVA 400 spectrometer, and 2D NMR was performed on INOVA 500/600 spectrometers. NMR data was analyzed by MestReNova (version 8.1.1). ^{1}H NMR chemical shifts are reported in units of ppm relative to tetramethylsilane. ^{1}H NMR data are reported in the following manner: chemical shift (multiplicity, integration). LC-MS experiments were carried out on a Shimadzu HPLC LC20-AD and Thermo Scientific LCQ Fleet with a Sprite TARGA C18 column (40 × 2.1 mm, 5 μm, Higgins Analytical, Inc.) monitoring at 215 and 260 nm with positive mode for mass detection. Solvents for LC-MS were water with 0.1% acetic acid (solvent A) and acetonitrile with 0.1% acetic acid (solvent B). Compounds were eluted at a flow rate of 0.3 mL/min with 0% solvent B for 2 min, followed by a linear gradient of 0% to 10% solvent B over 2 min, followed by a linear gradient of 10% to 100% solvent B over 5 min, and finally 100% solvent B for 1 min before equilibrating the column back to 0% solvent B over 1 min. Preparative HPLC experiments were done on Beckman Coulter System Gold 125p Solvent Module & 168 Detector with a TARGA C18 column (250 × 20 mm, 10 μm, Higgins Analytical, Inc.) monitoring at 215 and 260 nm. Solvents for HPLC were water with 0.1% trifluoroacetic acid (solvent A) and acetonitrile with 0.1% trifluoroacetic acid (solvent B). Compounds were eluted at a flow rate of 8.0 mL/min with 0% solvent B for 10 min, followed by first a linear gradient of 0% to X% (X depends on different compounds) solvent B over X min, then a linear

gradient of X% to 100% solvent B over 5 min, and finally 100% solvent B for 5 min before equilibrating the column back to 0% solvent B over 5 min.

DNP – PEG – Azido (1)

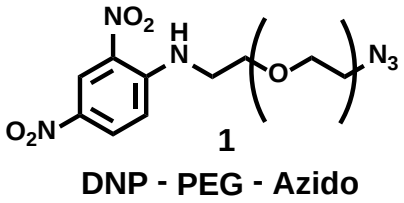

1

DNP - PEG - Azido

To a solution of azido PEG amine (52.8 mg, 0.12 mmol, 1.0 eq) in 7 mL absolute ethanol in a round-bottom flask was added triethylamine (0.034 mL, 0.24 mmol, 2.0 eq) via pipette and 1-chloro-2,4-dinitrobenzene (41 mg, 0.20 mmol, 1.7 eq) under nitrogen. The solution was refluxed for 48 h under nitrogen, and the solution changed from colorless to yellow as product **1** formed. The reaction was monitored by LC-MS (260 nm) and was concentrated on a rotary evaporator. The product was then purified by silica gel flash chromatography (3% MeOH in DCM) yielding an amber semi-solid. ^{1}H NMR (400 MHz, Methanol-d_4): δ = 9.04 (d, *J* = 2.7 Hz, 1H), 8.30 (dd, *J* = 9.58, 2.76 Hz, 1H), 7.24 (d, *J* = 9.69 Hz, 1H), 3.81 (t, *J* = 4.83 Hz, 2H), 3.72 – 3.54 (m, 32H), 3.37 (t, *J* = 5.01 Hz, 2H).

F-araNMN-DNP (2)

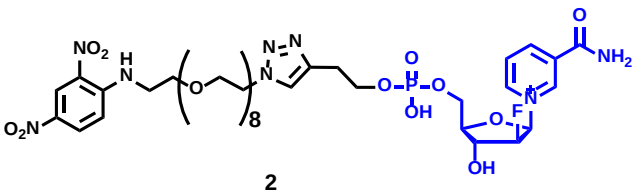

2

F-araNMN-DNP

F-araNMN alkyne (179 µL of a 31 mM aqueous solution, 5.54 µmol, 1.1 eq., synthesized according to a reported procedure (*10*)), **1** (508 µL of a 9.92 mM DMSO solution, 5.04 µmol, 1.0 eq.), Tris[(1-benzyl-1*H*-1,2,3-triazol-4-yl)methyl]amine (as ligand, 201.6 µL of an 100 mM DMF solution, 20.16 µmol, 4.0 eq.), copper sulfate (201.6 µL of a 100 mM aqueous solution, 20.16 µmol, 4.0 eq.), sodium ascorbate (322.6 µL of a 100 mM aqueous solution, 32.26 µmol, 6.4 eq.) were added to DMSO (500 µL) in that order to a round-bottom flask fitted with a stir bar. The reaction solution was stirred at rt overnight. Product

formation was detected using LC-MS (260 nm). Purification by preparative HPLC. Prep HPLC: t_R = 57.5 min with a linear gradient of 0% - 60% solvent B from 10 – 70 min. Solid was obtained (2.8 mg, 56% yield). ^{1}H NMR (400 MHz, Methanol-d_4) δ 9.69 (s, 1H), 9.44 (d, *J* = 6.08 Hz, 1H), 9.07 (d, *J* = 7.97, 1H), 9.01 (d, *J* = 3.04 Hz, 1H), 8.31 (d, *J* = 6.89 Hz, 1H), 8.27 (dd, *J* = 9.41, 2.31 Hz, 1H), 7.90 (s, 1H), 7.22 (d, *J* = 9.89 Hz, 1H), 6.71 (dd, *J* = 10.18, 4.4 Hz, 1H), 5.46 (dt, *J* = 51.7, 4.69 Hz, 1H), 4.50 (m, 3H), 4.32 (m, 1H), 4.13 (m, 4H), 3.81 (dt, *J* = 27.29, 5.49 Hz, 5H), 3.68 – 3.52 (m, 43H). LC-MS (ESI) calcd. for $C_{39}H_{59}FN_8O_{19}P^+$ (M^+) 993.36, obsd. 993.50.

Confocal Microscopy Imaging Showing Three-Body Complex Formation between CD38, ARM and Antibody on Live Cells

Buffer A contains: 50 mM Tris HCl, 100 mM NaCl, 23 mM HEPES, 1 mM $MgCl_2$, 1 mM $CaCl_2$, 1% BSA, pH 7.4.

HL-60 cells were treated with 1 μM RA in cell culture media (GIBCO RPMI Medium 1640 with 10% GIBCO Heat-inactivated Fetal Bovine Serum) for 24 h in a 5% CO_2 incubator at 37 °C. Untreated HL-60 cells were cultured using the same media without RA. Then the cells were harvested from 4 mL cell culture (1×10^6 cells/mL) by centrifugation at 25 °C, 1200 rpm for 5 min. The cells were initially washed once using 1 mL DPBS, then washed a second time using 1 mL Buffer A. Cells were suspended in 100 μL Buffer A (reaction volume) followed by addition of ARM (10 μM) and let sit at 4 °C for 1 h. Subsequently, cells were collected by centrifugation at 4 °C, 1200 rpm for 5 min and washed with Buffer A (2 x 1 mL). Cells were suspended in 70 μL Buffer A followed by addition of AlexaFluor488 rabbit anti-DNP IgG antibody at 15 μg/mL for 1 h at 4 °C. Then, cells were collected by centrifugation at 4 °C, 1200 rpm for 5 min. Cells were washed first using Buffer A (1 mL) then with DPBS (1 mL). Finally, cells were suspended in 100 μL DPBS and 10 μL of the cell suspension was used to put onto a

microscope slide and cover with a micro cover glass. Confocal images (8 line average) of cells were acquired with a Zeiss LSM 710 confocal microscope with a 63×/1.4 oil immersion objective. Blue 488 nm (25mW, laser power at 13.0%) was used for AlexaFluor488 fluorescence. Emission signal in the range of 493 – 630 nm was detected with a pinhole of 49 μm.

Flow Cytometry for Measuring ARM Capability to Induce Cell-Mediated Cytotoxicity

ADCC Media consists of phenol red free RPMI Medium 1640 + 5% FBS

Preparation of frozen human peripheral blood mononuclear cells (hPBMC): Frozen hPBMC at 100 x 10^6 cells/vial were purchased from StemCell Technologies (Cat. #: 70025). Frozen hPBMC were thawed upon arrival and aseptically transferred to a 50 mL conical tube. Warm RPMI medium 1640 + 10% FBS was added drop wise to the cells in the 50 mL tube while swirling the tube until the volume reached 20 mL. Cells were collected by centrifugation at 300 x g, rt for 10 min. Supernatant was removed, leaving behind 1 mL so as to not disturb the cell pellet. Again, the cells were gently suspended by adding warm RPMI medium 1640 + 10% FBS drop wise to the cells in the 50 mL tube while swirling the tube until the volume reached 20 mL. Cells were collected by centrifugation at 300 x g, rt for 10 min. Supernatant was removed, and leaving behind 1 mL in order to not disturb the cell pellet. The cells were counted and viability was analyzed using 0.4% trypan blue exclusion dye. From the 100 million hPBMC, the required amount for the current experiment was plated at approximately 2.5 x 10^6 cells per plate and incubated overnight at 37 C, 5% CO_2. Those hPBMC not used in the current experiment were collected and suspended in cold cryo media (50% RPMI Medium 1640, 40% FBS, 10% DMSO, kept at 4 °C). Cells were then cryopreserved in liquid nitrogen.

Procedure for Antibody Dependent Cell-Mediated Cytotoxicity (ADCC) Experiment: A stably transfected HL-60 cell line that constitutively expresses a high level of CD38 and GFP was kept

in cell culture media (GIBCO RPMI Medium 1640 with 10% GIBCO HI FBS) in a 5% CO_2 incubator at 37 °C. Then, 1.0 x 10^6 cells were collected by centrifugation at 25 °C, 700 rpm for 5 min. The cells were washed using PBS (1 x 1mL). Then, 2 mL of PBS were added to the cells giving a cell density of 5.0 x 10^5 cells/mL. To a falcon tube was added 50 µL of cell suspension (0.25 x 10^5 cells used per sample). To each tube containing the stably transfected HL-60 cells was added 50 µL of 80 µM F-araNMN-DNP, giving a final F-araNMN-DNP concentration of 40 µM and total sample volume of 100 µL. Incubated the samples in a 5% CO_2 incubator at 37 °C for 15 minutes. Subsequently, collected the cells by centrifugation at 25 °C, 700 rpm for 5 min, then washed cells using PBS (1 x 1mL), leaving 100 uL to remain in the tube with the cells pelleted. Then, anti-dinitrophenyl-KLH Rabbit IgG antibody was added at 25 µg/mL to the cells in PBS and suspended the cells. Incubated samples in a 5% CO_2 incubator at 37 °C for 1 h. Next, collected cells by centrifugation at 25 °C, 700 rpm for 5 min, followed by washing cells using PBS (1 x 1mL), leaving 100 µL to remain in the tube with the cells pelleted. Preparation of human peripheral blood mononuclear cells (hPBMC) was done by collecting the hPBMC from culture using centrifugation at 25 °C, 700 rpm for 5 min, followed by suspension in ADCC media that gives a cell density of 12.5 x 10^6 cells/mL. Then, 50 µL of hPBMC cell suspension (6.25 x 10^5 cells per sample, a 25:1 ratio of hPBMC to HL-60 cells) was added to each stably transfected HL-60 cell sample giving a total sample volume of 150 µL. Incubated samples at 37 °C, 5% CO_2 for 4 hours. Next, added 150 µL of propidium iodide stock solution (30 µg/mL) giving a final propidium iodide concentration of 15 µg/mL. Finally, samples were incubated at 37 °C, 5% CO_2 for 25 min. followed by performing flow cytometry analysis. Controls included both a positive killing by heating the cells in 95 °C water bath for 15 seconds and a negative control where a combination of one or more components (F-araNMN-DNP, anti-DNP antibody

or hPBMC) was missing. Additionally, one control involved first labeling CD38 with 6-alkyne-F-araNAD prior to addition of F-araNMN-DNP, antibody and hPBMC. This sample should have no F-araNMN-DNP binding to CD38 due to prior labeling of CD38 by 6-alkyne-F-araNAD; thus, little to no killing caused by the cytotoxic-effector cells.

REFERENCES

1. Siegel, R., Naishadham, D., and Jemal, A. (2013) Cancer statistics, 2013, *CA Cancer J Clin 63*, 11-30.
2. Jemal, A., Ward, E., and Thun, M. (2010) Declining death rates reflect progress against cancer, *PLoS One 5*, e9584.
3. Imai, K., and Takaoka, A. (2006) Comparing antibody and small-molecule therapies for cancer, *Nat Rev Cancer 6*, 714-727.
4. Maloney, D. G., Grillo-Lopez, A. J., White, C. A., Bodkin, D., Schilder, R. J., Neidhart, J. A., Janakiraman, N., Foon, K. A., Liles, T. M., Dallaire, B. K., Wey, K., Royston, I., Davis, T., and Levy, R. (1997) IDEC-C2B8 (Rituximab) anti-CD20 monoclonal antibody therapy in patients with relapsed low-grade non-Hodgkin's lymphoma, *Blood 90*, 2188-2195.
5. Carter, P., Presta, L., Gorman, C. M., Ridgway, J. B., Henner, D., Wong, W. L., Rowland, A. M., Kotts, C., Carver, M. E., and Shepard, H. M. (1992) Humanization of an anti-p185HER2 antibody for human cancer therapy, *Proc Natl Acad Sci U S A 89*, 4285-4289.
6. Brekke, O. H. S., I. (2003) Therapeutic antibodies for human diseases at the dawn of the twenty-first century, *Nature Rev. Drug Discov. 2*, 52-62.
7. Spiegel, D. A. (2010) Grand challenge commentary: Synthetic immunology to engineer human immunity, *Nat Chem Biol 6*, 871-872.
8. Chillemi, A., Zaccarello, G., Quarona, V., Ferracin, M., Ghimenti, C., Massaia, M., Horenstein, A. L., and Malavasi, F. (2013) Anti-CD38 antibody therapy: windows of opportunity yielded by the functional characteristics of the target molecule, *Mol Med 19*, 99-108.
9. Lin, P., Owens, R., Tricot, G., and Wilson, C. S. (2004) Flow cytometric immunophenotypic analysis of 306 cases of multiple myeloma, *Am J Clin Pathol 121*, 482-488.
10. Shrimp, J. H., Hu, J., Dong, M., Wang, B. S., Macdonald, R., Jiang, H., Hao, Q., Yen, A., and Lin, H. (2014) Revealing CD38 Cellular Localization Using a Cell Permeable, Mechanism-Based Fluorescent Small-Molecule Probe, *J Am Chem Soc*.
11. Ortega, E., Kostovetzky, M., and Larralde, C. (1984) Natural DNP-binding immunoglobulins and antibody multispecificity, *Mol Immunol 21*, 883-888.
12. Farah, F. S. (1973) Natural antibodies specific to the 2,4-dinitrophenyl group, *Immunology 25*, 217-226.
13. Jormalainen, S., and Makela, O. (1971) Anti-hapten antibodies in normal sera, *Eur J Immunol 1*, 471-478.
14. Parker, C. G., Domaoal, R. A., Anderson, K. S., and Spiegel, D. A. (2009) An antibody-recruiting small molecule that targets HIV gp120, *J Am Chem Soc 131*, 16392-16394.
15. Jakobsche, C. E., McEnaney, P. J., Zhang, A. X., and Spiegel, D. A. (2012) Reprogramming urokinase into an antibody-recruiting anticancer agent, *ACS Chem Biol 7*, 316-321.
16. Murelli, R. P., Zhang, A. X., Michel, J., Jorgensen, W. L., and Spiegel, D. A. (2009) Chemical control over immune recognition: a class of antibody-recruiting small molecules that target prostate cancer, *J Am Chem Soc 131*, 17090-17092.

17. Muller-Eberhard, H. J. (1988) Molecular organization and function of the complement system, *Annu Rev Biochem 57*, 321-347.
18. Hale, G., Clark, M., and Waldmann, H. (1985) Therapeutic potential of rat monoclonal antibodies: isotype specificity of antibody-dependent cell-mediated cytotoxicity with human lymphocytes, *J Immunol 134*, 3056-3061.
19. Kolb, H. C., Finn, M. G., and Sharpless, K. B. (2001) Click Chemistry: Diverse Chemical Function from a Few Good Reactions, *Angew Chem Int Ed Engl 40*, 2004-2021.
20. Lamkin, T. J., Chin, V., Varvayanis, S., Smith, J. L., Sramkoski, R. M., Jacobberger, J. W., and Yen, A. (2006) Retinoic acid-induced CD38 expression in HL-60 myeloblastic leukemia cells regulates cell differentiation or viability depending on expression levels, *J Cell Biochem 97*, 1328-1338.
21. Aggarwal, S. R. (2014) A survey of breakthrough therapy designations, *Nat Biotechnol 32*, 323-330.

APPENDIX A

LC-MS and NMR Data for Synthesized Molecules

Chapter 2: LC-MS and NMR Data

^{1}H NMR: Compound 2

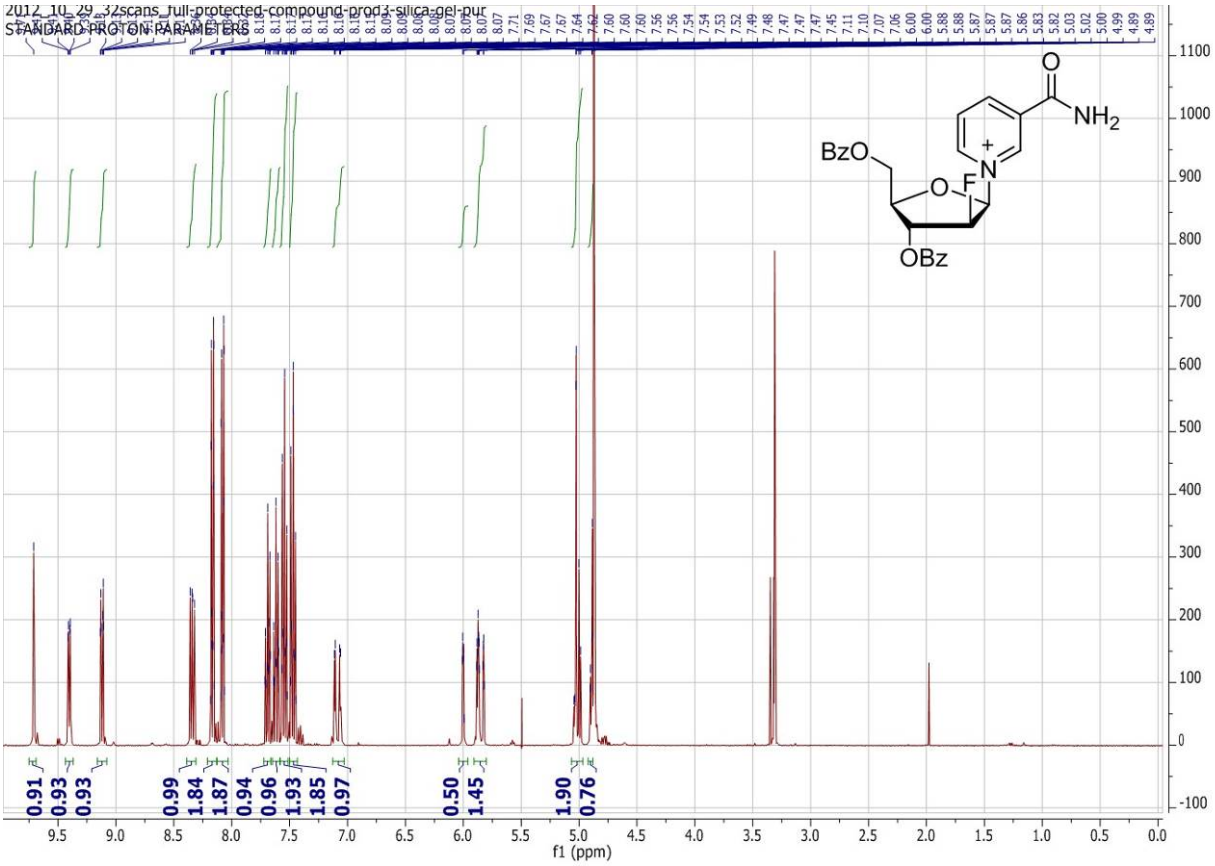

LC-MS: Compound 2

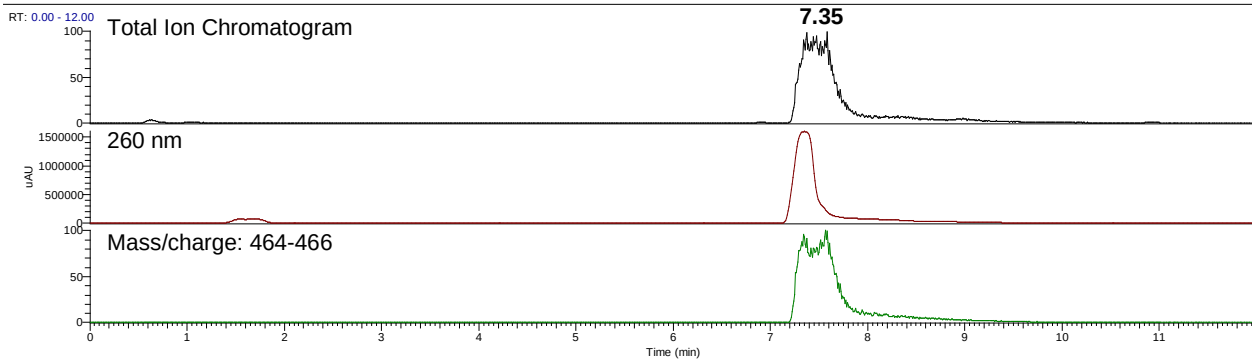

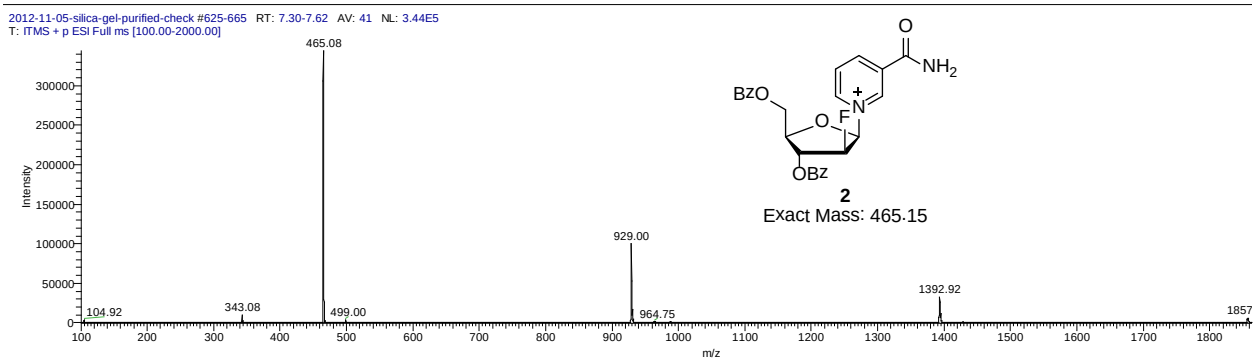

2

Exact Mass: 465.15

^{1}H NMR: Compound 3

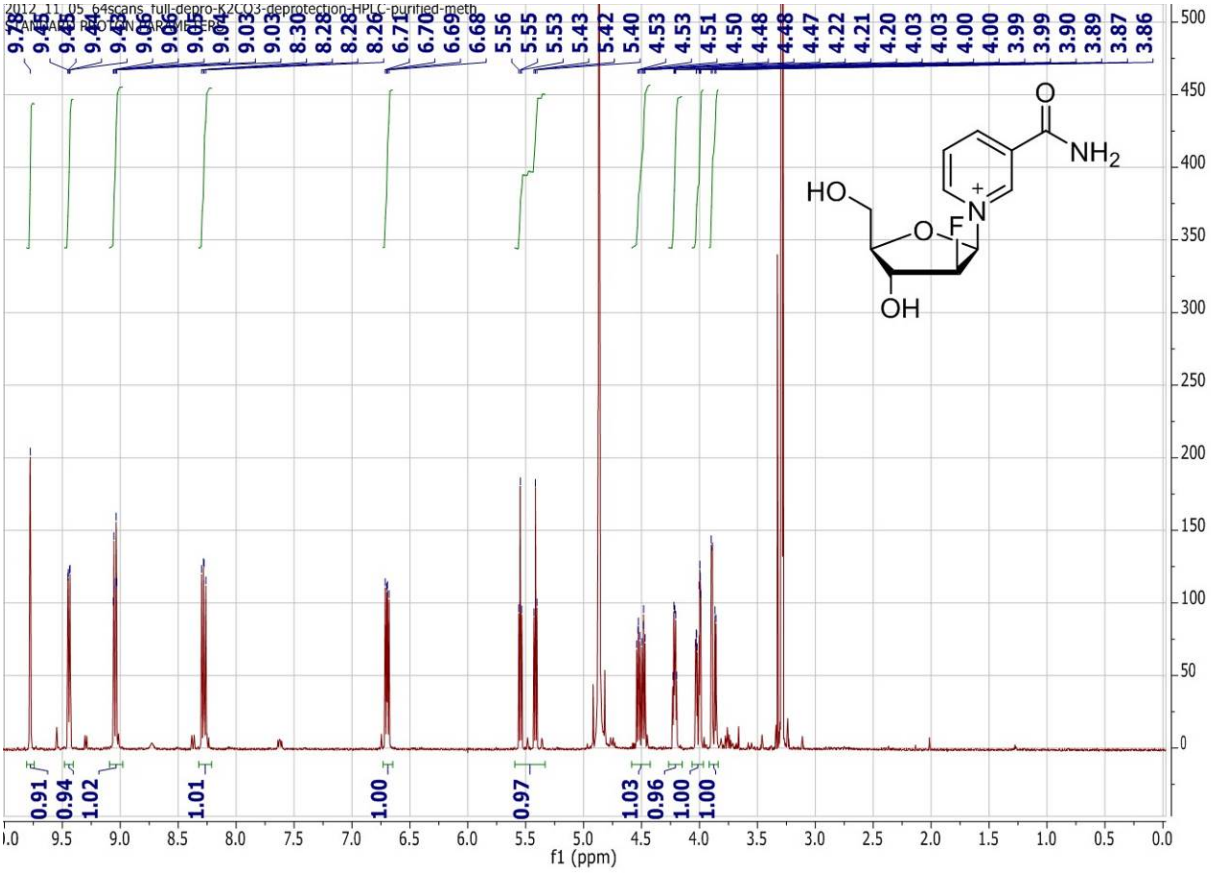

LC-MS: Compound 3

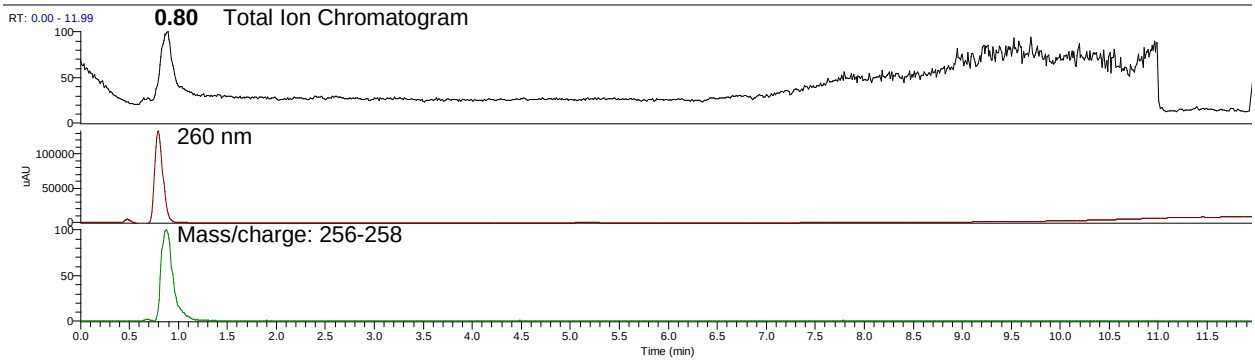

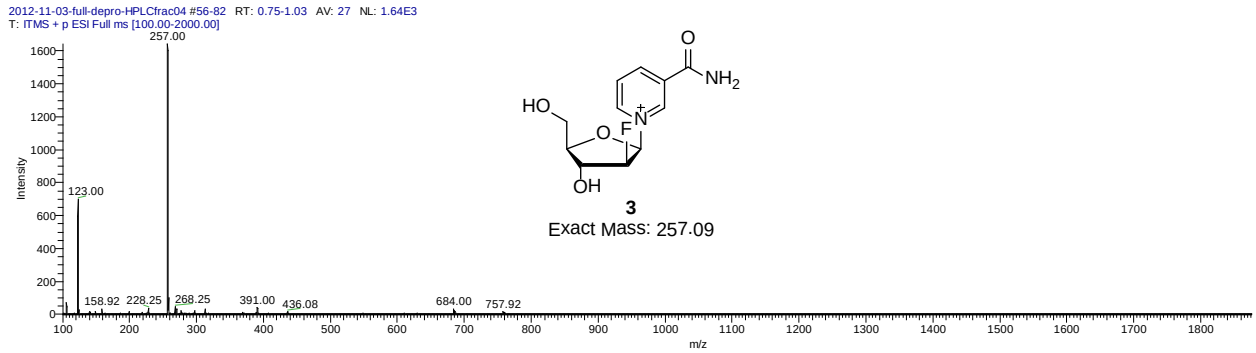

3

Exact Mass: 257.09

^{1}H NMR: F-araNMN alkyne (4)

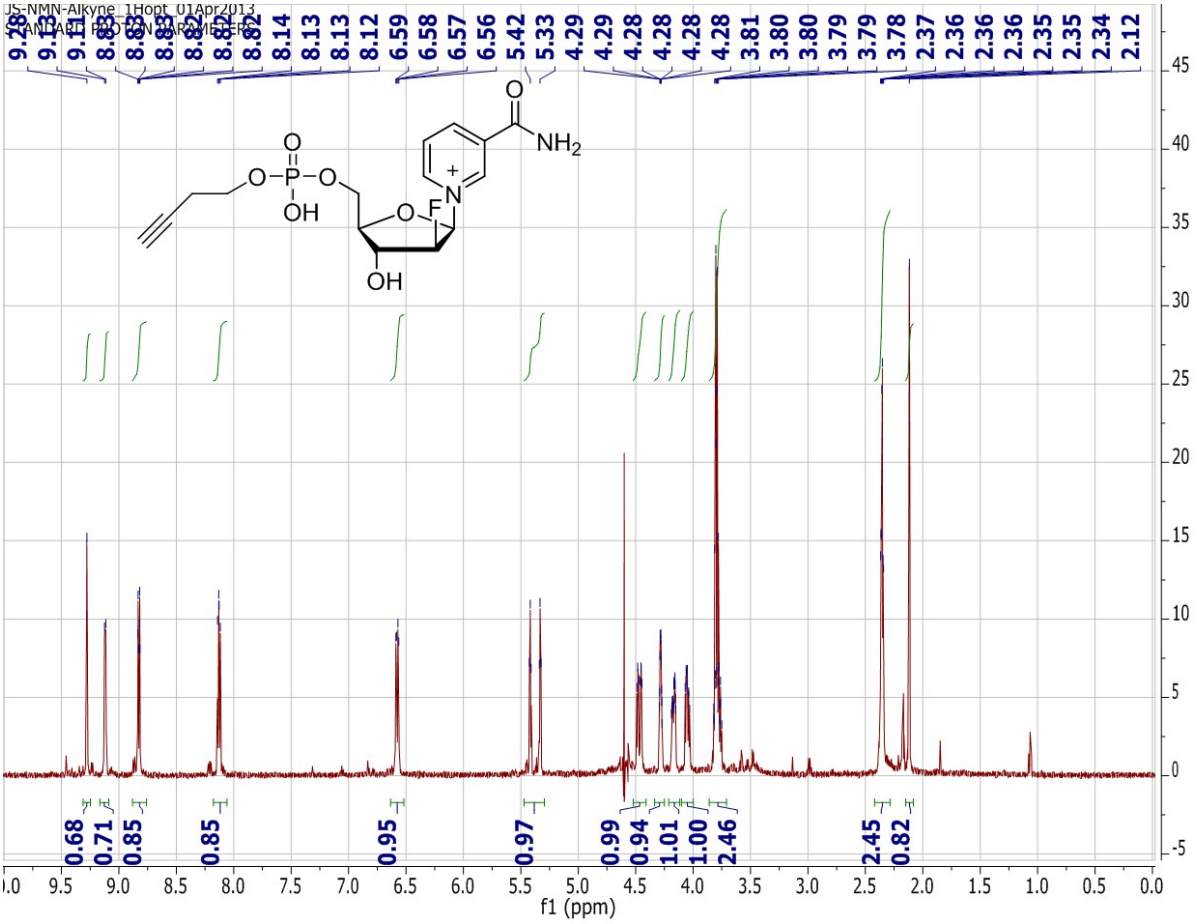

LC-MS: F-araNMN alkyne (4)

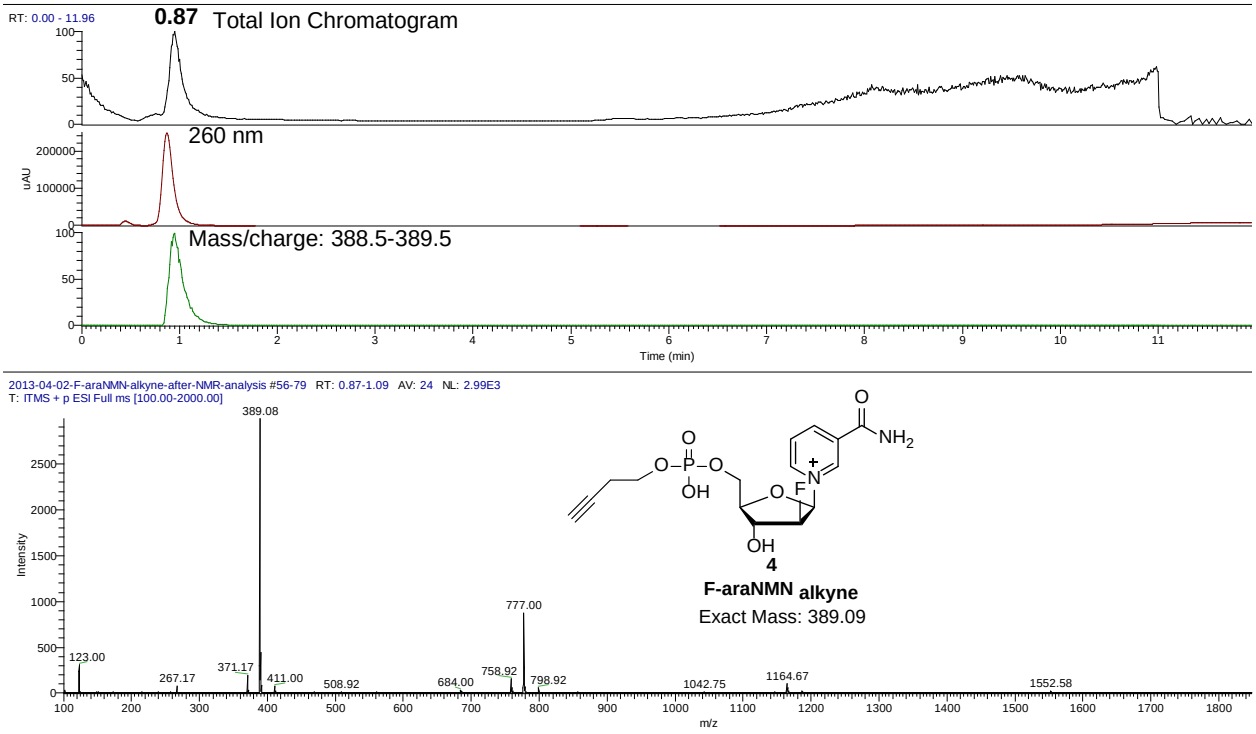

^{1}H NMR: 2-azidoacetic acid (5)

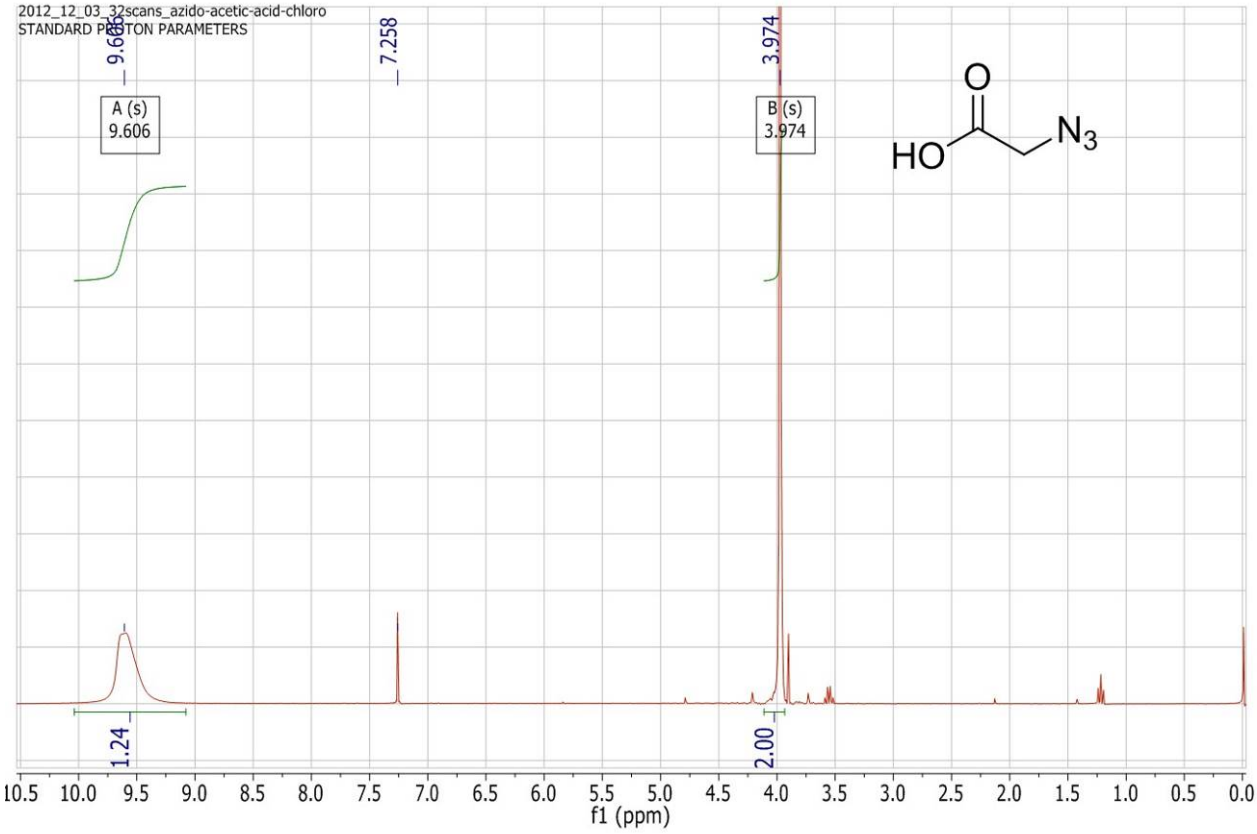

LC-MS: Compound 7

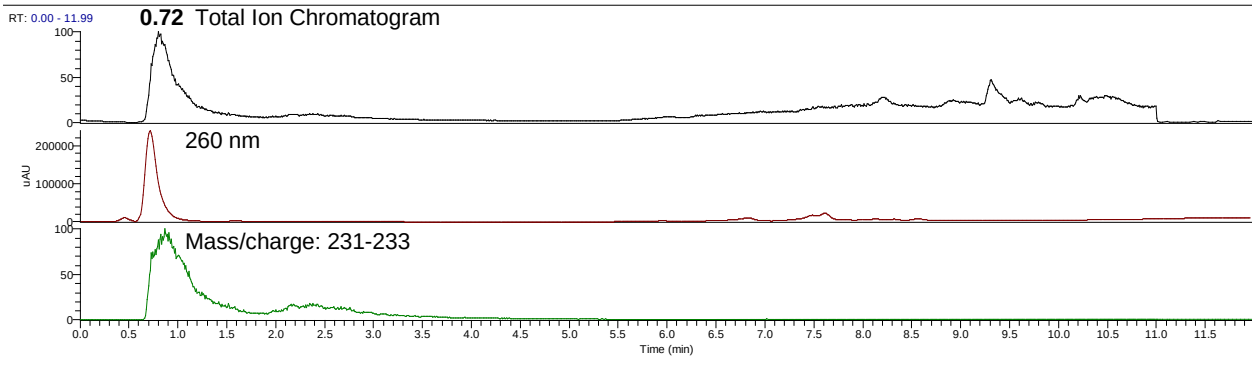

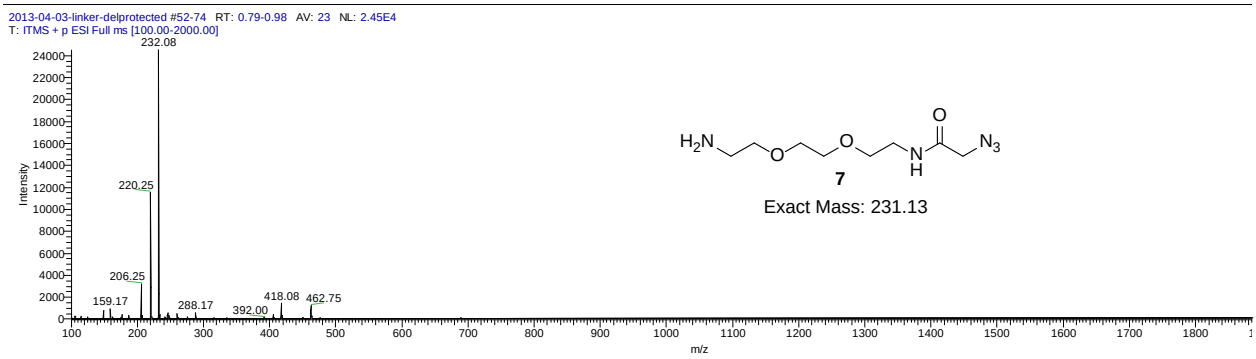

7

Exact Mass: 231.13

^{1}H NMR: SR101-azide (9)

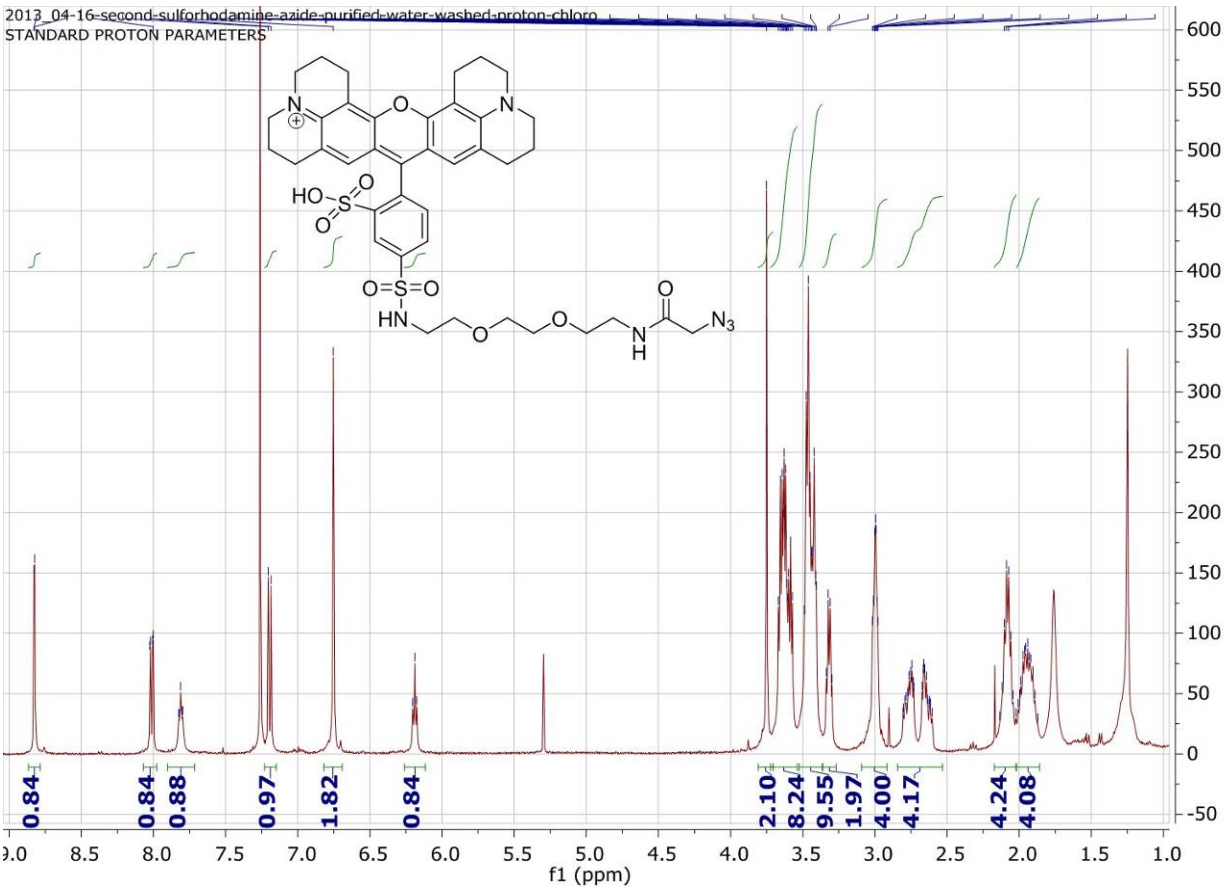

LC-MS: SR101-azide (9)

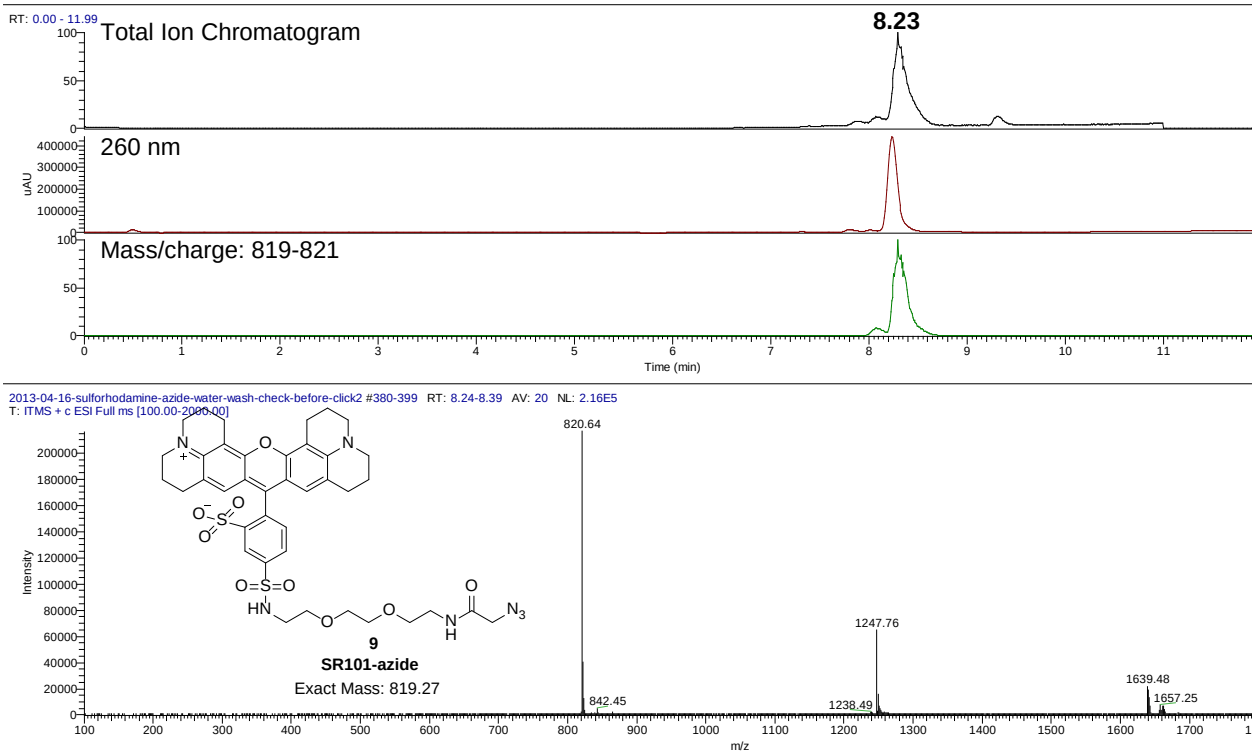

^{1}H NMR: SR101-F-araNMN (10)

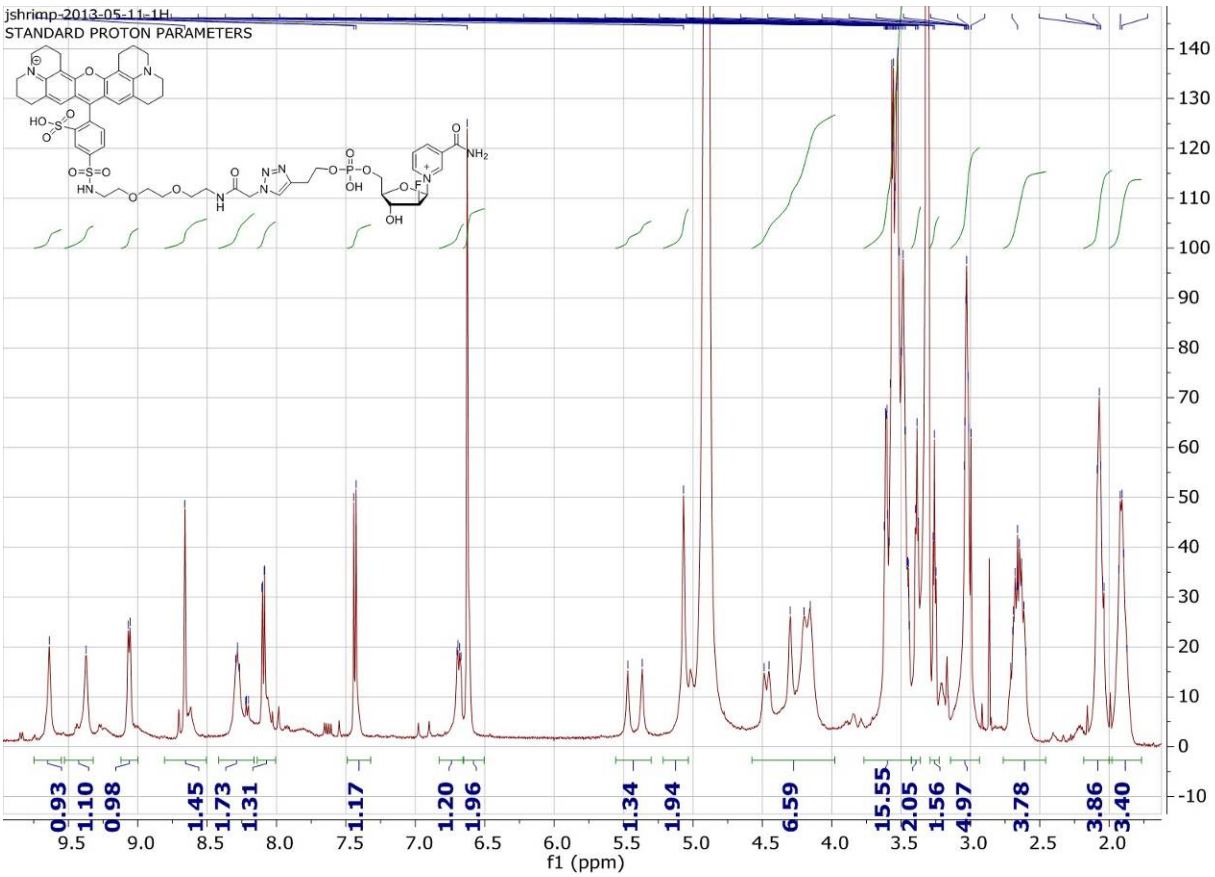

LC-MS: SR101-F-araNMN (10)

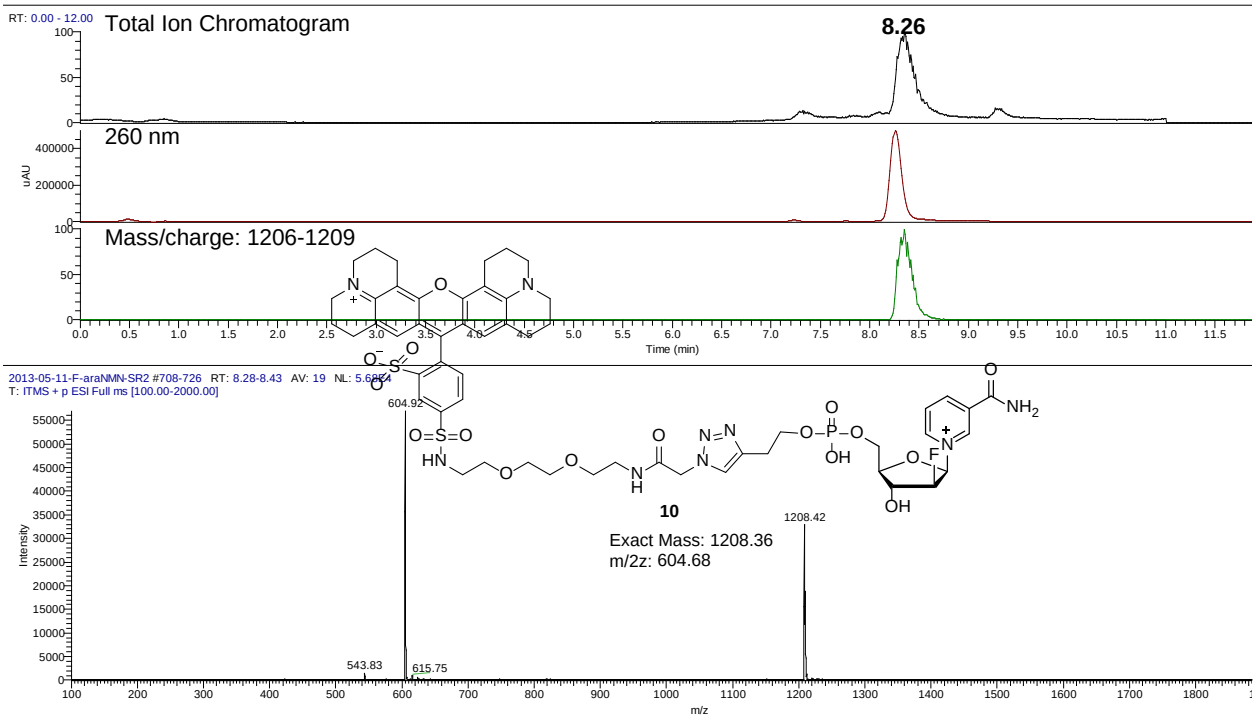

Chapter 3: LC-MS and NMR Data

LC-MS: 6-alkyne-F-araNAD

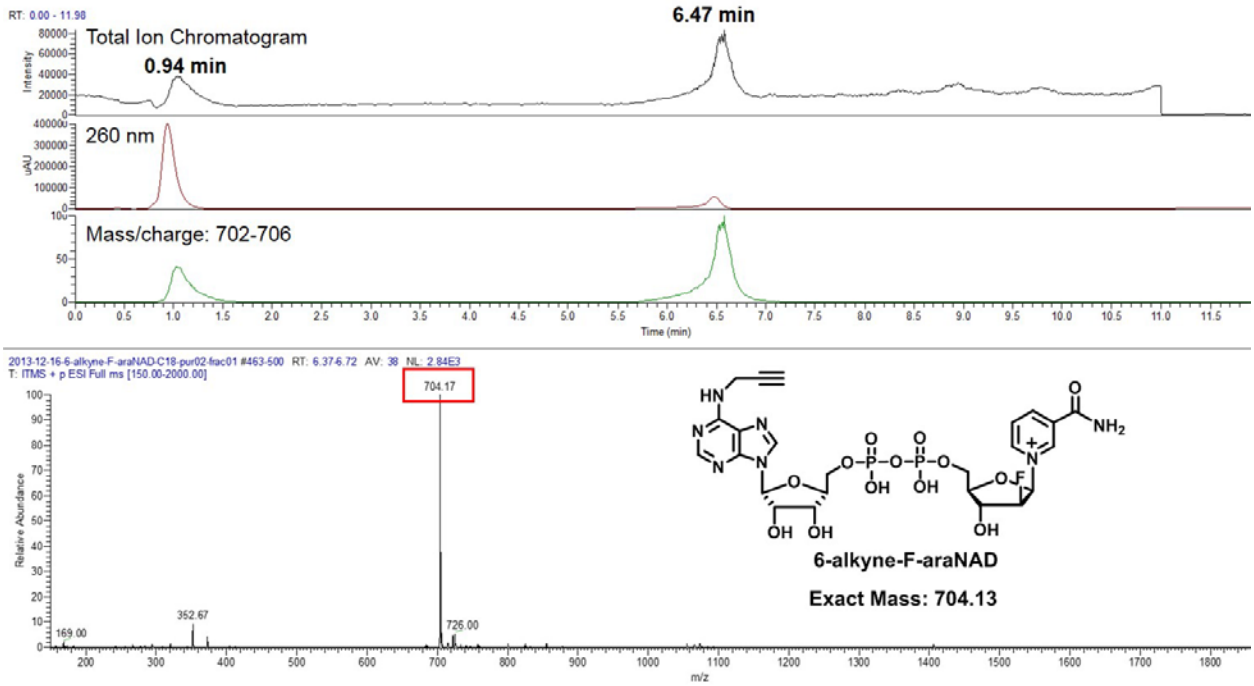

^{1}H NMR: Rigid Linker (**1**)

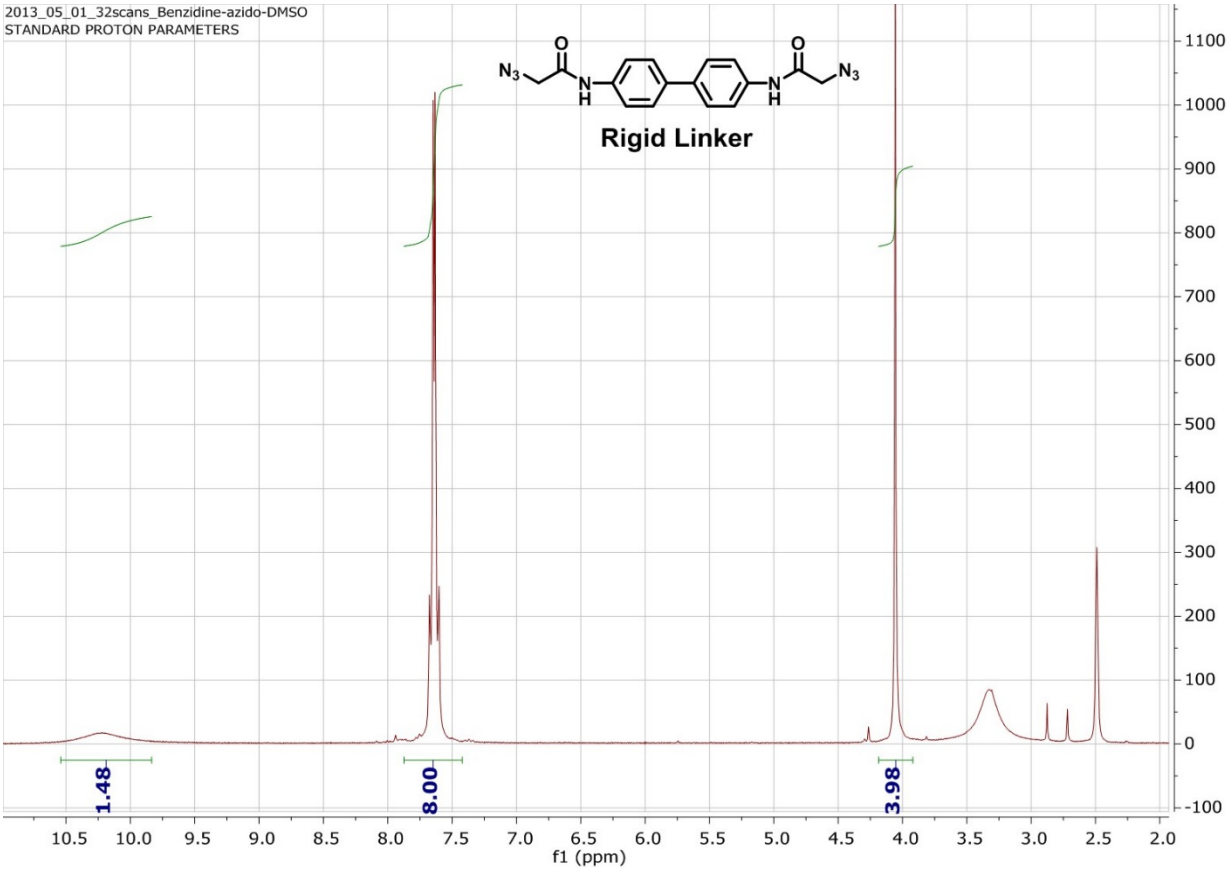

LC-MS: Rigid Linker (**1**)

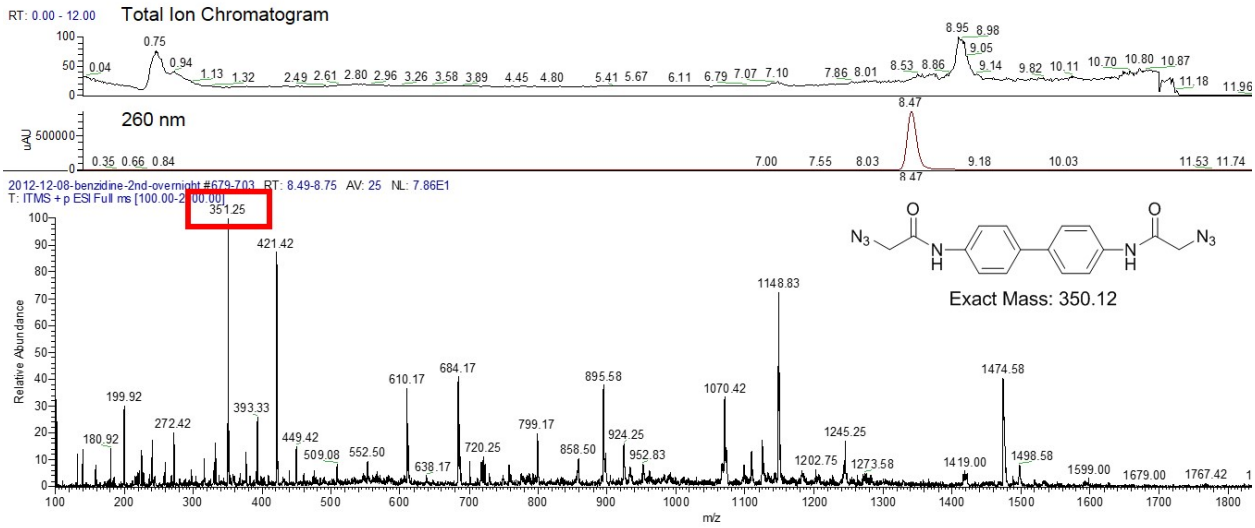

LC-MS: 6-azidohexanoic acid (**2**)

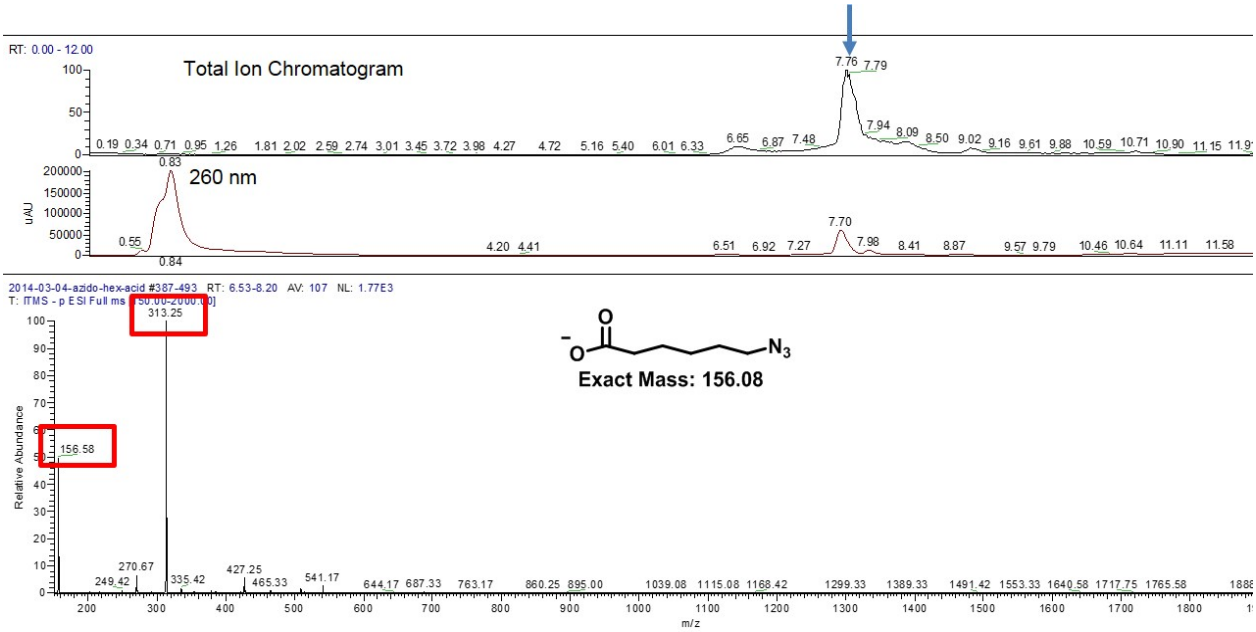

^{1}H NMR: Flexible Linker (**3**)

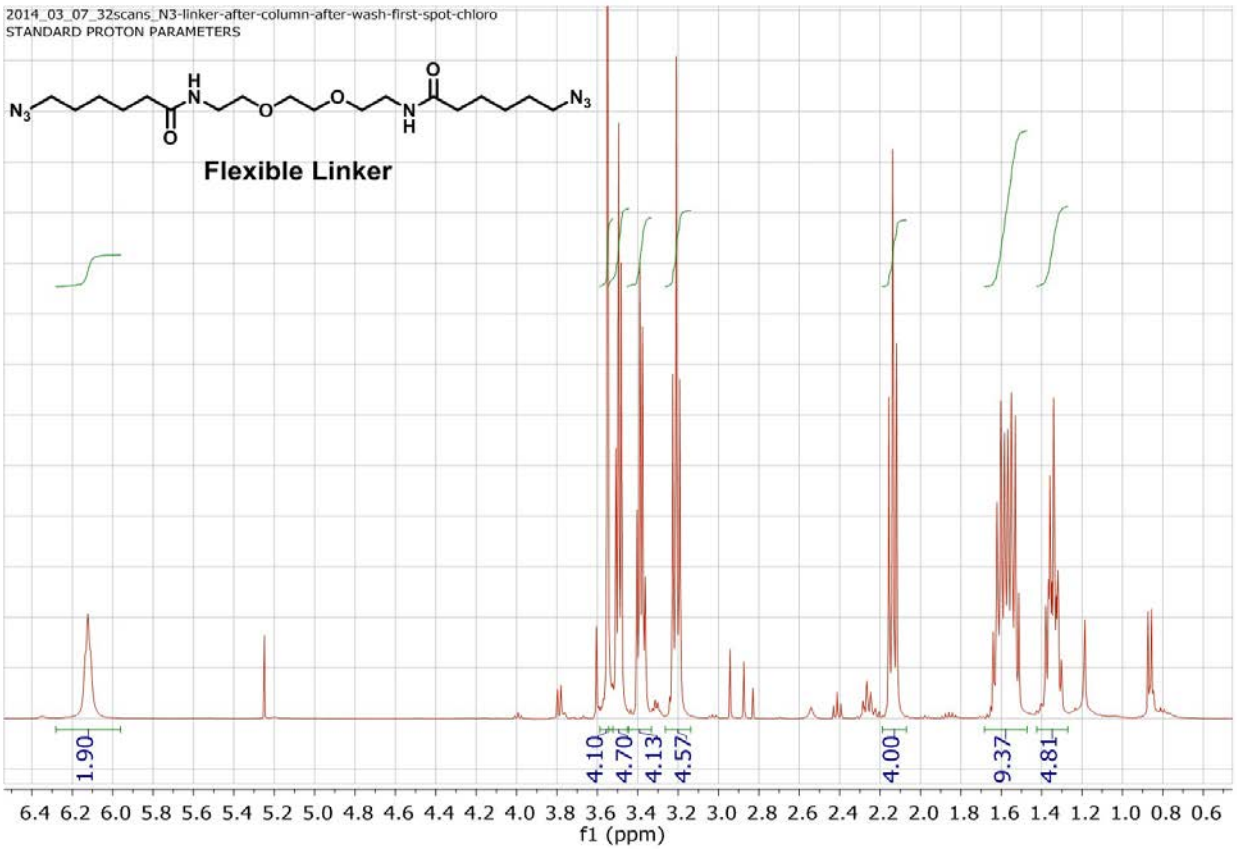

LC-MS: Flexible Linker (**3**)

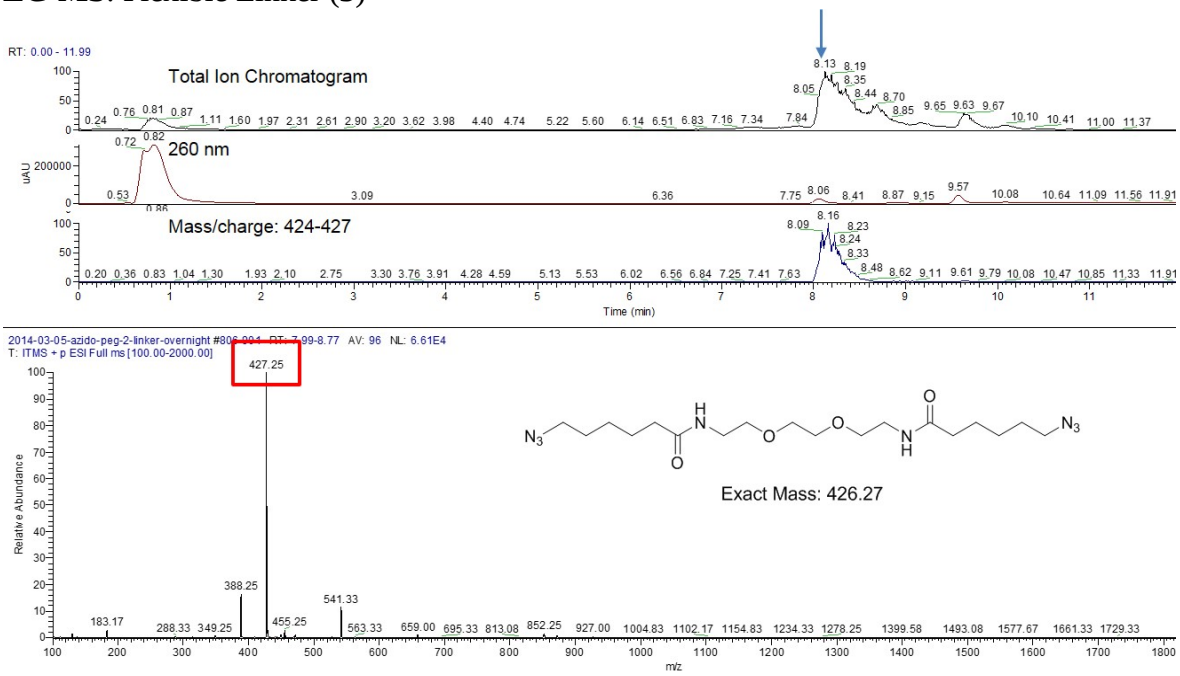

LC-MS: Rigid F-araNMN dimer (**4**)

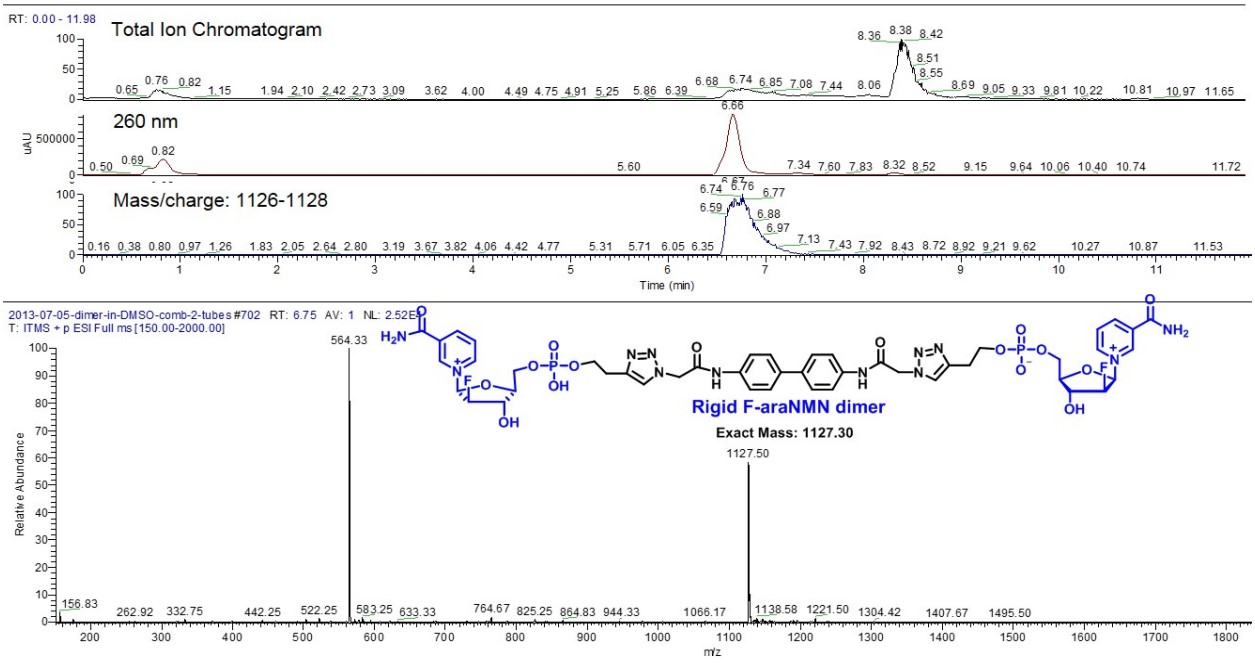

LC-MS: Flexible F-araNMN dimer (**5**)

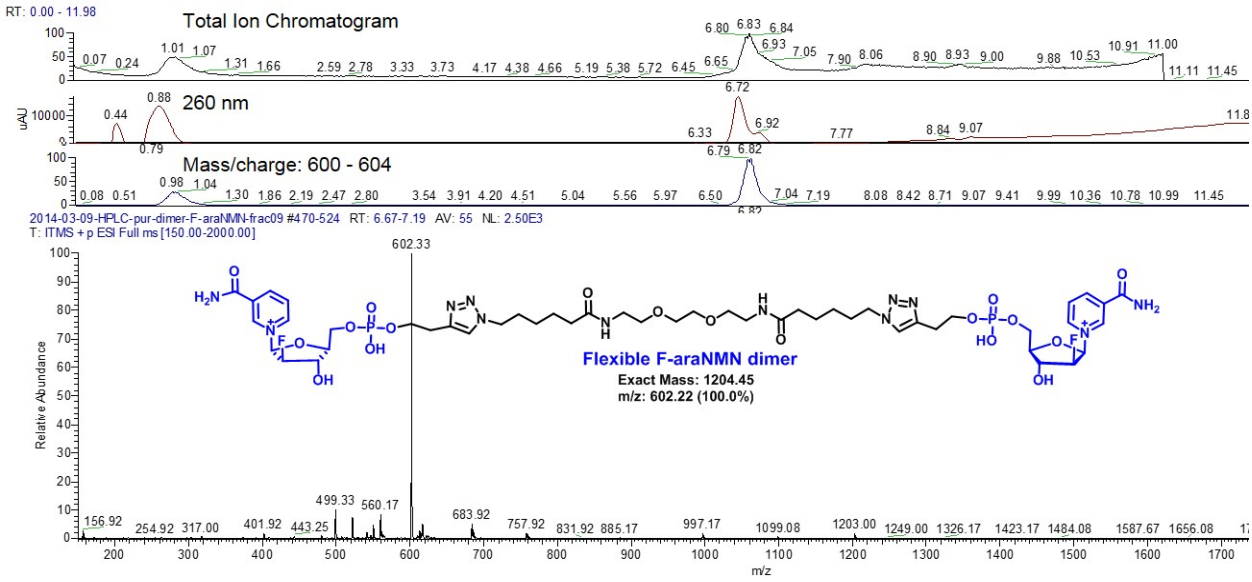

LC-MS: Flexible F-araNAD dimer (**6**)

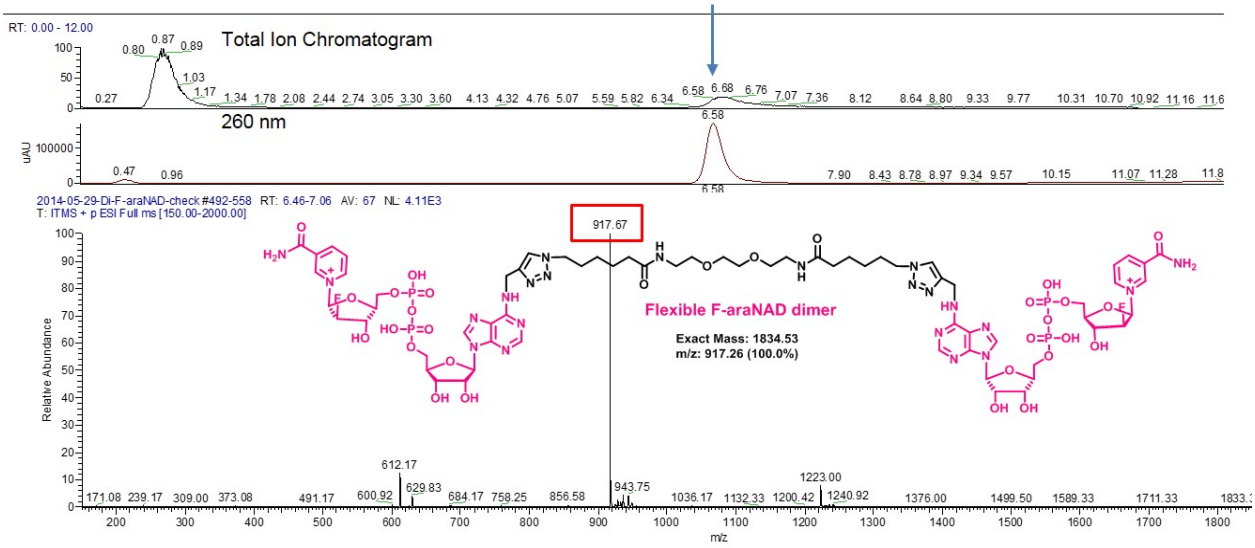

Chapter 4: LC-MS and NMR Data

^{1}H NMR: DNP-PEG-azido (**1**)

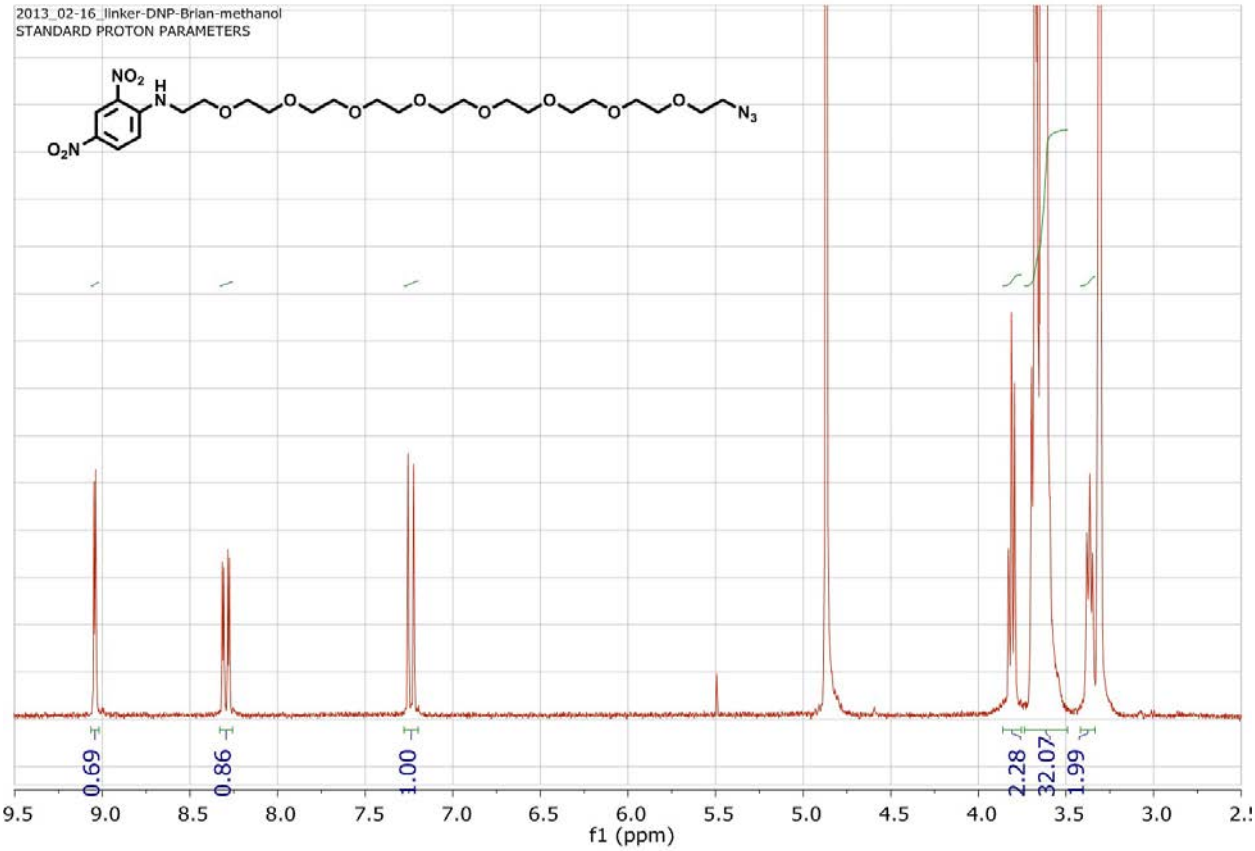

LC-MS: F-araNMN-DNP (**2**)

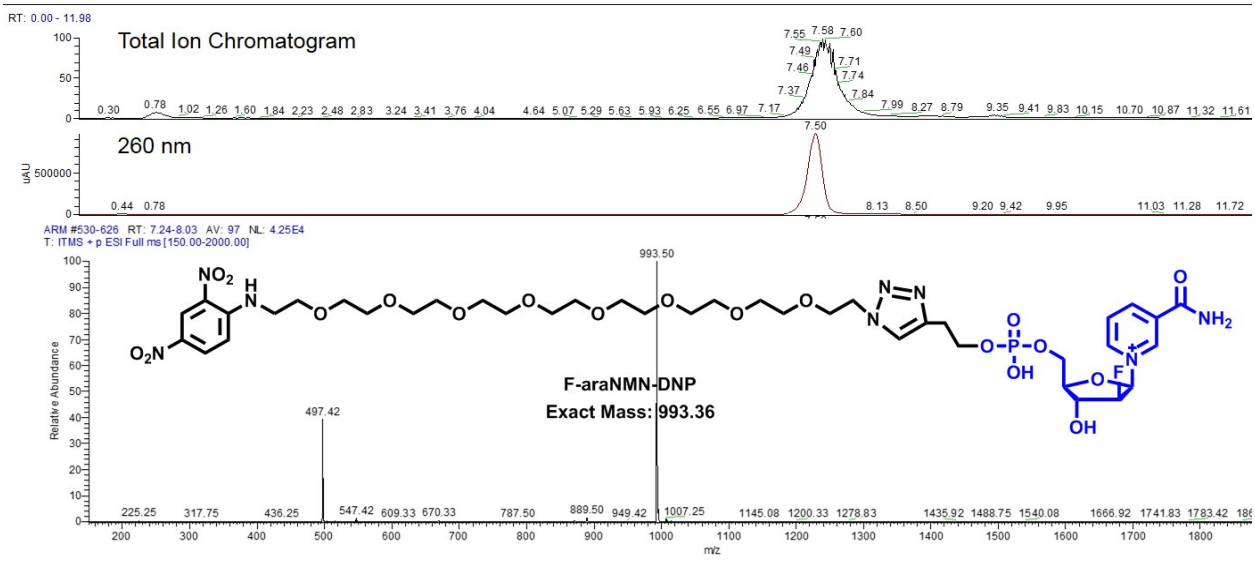

^{1}H NMR: F-araNMN-DNP (**2**)

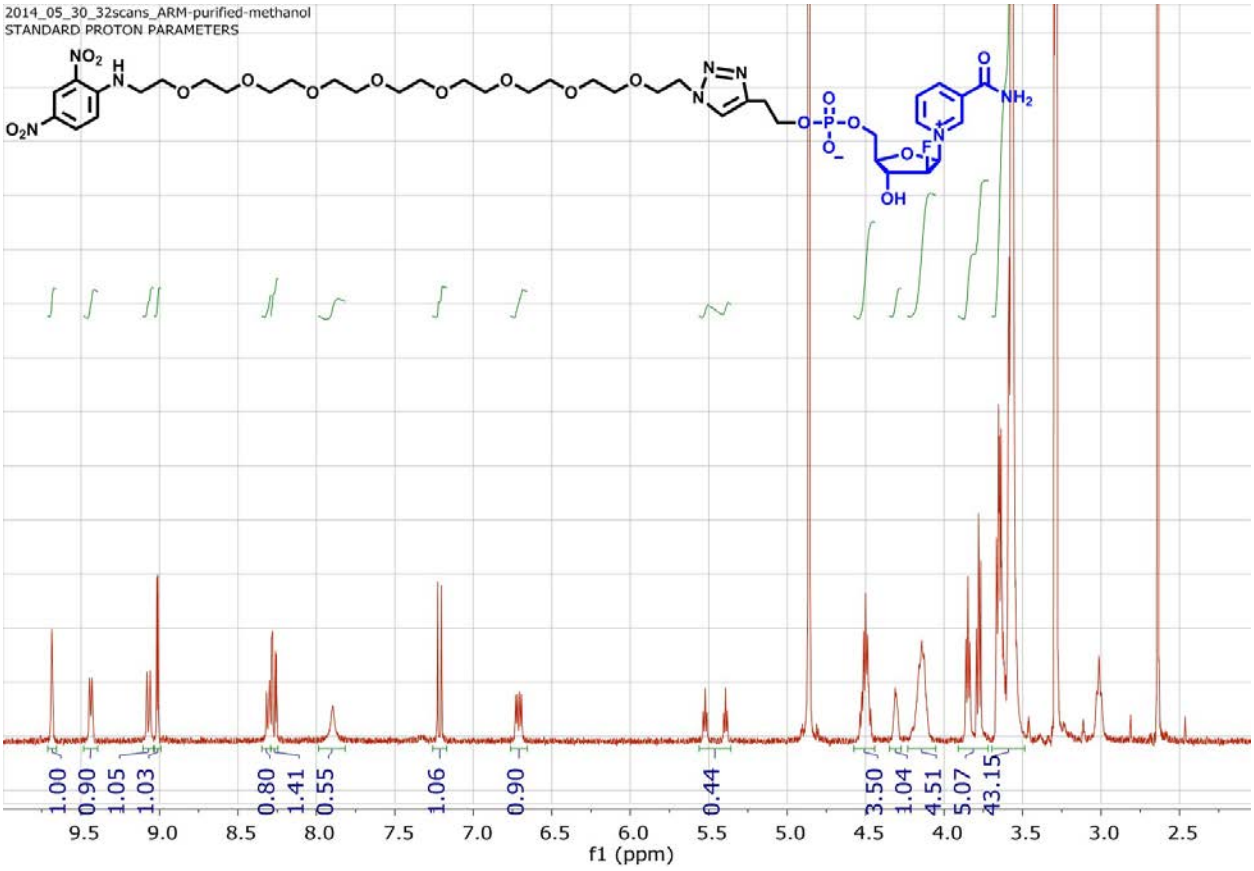

APPENDIX B

PERMISSION FOR REPRODUCTION

Chapter 2: Reproduced with permission from Shrimp, J. H. et al. *J. Am. Chem. Soc.* **2014**, *136*, 5656−5663.

Title: Revealing CD38 Cellular Localization Using a Cell Permeable, Mechanism-Based Fluorescent Small-Molecule Probe

Author: Jonathan H. Shrimp, Jing Hu, Min Dong, Brian S. Wang, Robert MacDonald, Hong Jiang, Quan Hao, Andrew Yen, and Hening Lin

Publication: Journal of the American Chemical Society

Publisher: American Chemical Society

Date: Apr 1, 2014

PERMISSION/LICENSE IS GRANTED FOR YOUR ORDER AT NO CHARGE

This type of permission/license, instead of the standard Terms & Conditions, is sent to you because no fee is being charged for your order. Please note the following:

- Permission is granted for your request in both print and electronic formats, and translations.
- If figures and/or tables were requested, they may be adapted or used in part.
- Please print this page for your records and send a copy of it to your publisher/graduate school.
- Appropriate credit for the requested material should be given as follows: "Reprinted (adapted) with permission from (COMPLETE REFERENCE CITATION). Copyright (YEAR) American Chemical Society." Insert appropriate information in place of the capitalized words.
- One-time permission is granted only for the use specified in your request. No additional uses are granted (such as derivative works or other editions). For any other uses, please submit a new request.